Active Filter Current Compensation for Transmission Optimisation

Prepared by: **Paul Andrew Carpenter**
Supervisor/s: **Dr CT. Gaunt**
and Dr M. Malengret
August 2015

Dissertation presented for the degree of
Master of Science in Engineering
Department of Electrical Engineering
University of Cape Town

Faculty of Engineering & the Built Environment
ISebe leeNjineli kunye neZakhiwo eziSingqongileyo — Fakulteit Ingenieurswese en die Bou-omgewing

DECLARATION

I declare that this dissertation is my own work and that apart from the normal guidance of my supervisor *(supervisors, if more than one)* I have received no assista ce apart from that which has been stated.

Signed by candidate

Department of Electrical Engineering,
University of Cape Town,
South Africa

Abstract

This dissertation is based on the fact that any m-wire electrical system can be modelled as m-equivalent Thévenin voltages and impedances when viewed from any node. The dissertation describes how to calculate the optimal distribution of currents, so a specific amount of power can flow through and reach the network equivalent Thévenin voltages with minimal losses.

The optimal current distribution method uses a recently patented method which calculates the optimal currents for each of the wires which are shown to be obtained from the Thévenin parameters and power flow at any instant in time at any node.

Once the ideal currents are found, these can be obtained by active and passive devices to inject a specific amount of power (positive and negative) as to compensate existing currents.

The focus is particularly on the proof of concept by simulations and physical experiments with work not specifically described in the patent with more emphasis on the optimisation to active compensation. It is explained and shown how this can be implemented using the Malengret and Gaunt method. This method reduces the cost in application where not all the currents need to be processed through a converter (e.g. inverter) but only the difference between the existing and desired optimal currents.

A smaller shunt parallel converter can result with ideal current flow without the need for interrupting the currents as described in the present patent. The methodology is explained and demonstrated by simulation.

Acknowledgments

Although I do my best to survive on my own, throughout my university career I have been supported, loved and looked after by my parents. I have learnt so many lifelong qualities and have been shaped into the person I have become today. I would like to say an epic thanks to my parents, for without them this would all not be possible.

I would also like to thank my supervisors CT. Gaunt and Michel Malengret, for they have been amazing. Michel was always there to give me advice and to push me in the right direction. Both were always enthusiastic when we met and were truly excited by the topic. I received great constructive feedback from Trevor.

Finally I would like to thank my girlfriend, Leanne Slack, for all the support she has provided me, not only for the duration of this dissertation but throughout my learning career.

Glossary of Terms

RMS:	**Root Mean Squared**: the DC equivalent of a varying waveform. It is calculated by squaring it then calculating the mean and finally the answer is the root.
PCC:	**Point of Common Coupling**: is often the place where metering takes place in a power network or where a power electronic converter such as a three-phase inverter that supplies renewable energy power is connected. It
Grid connected Inverter:	A power electronic device that converts electrical DC electrical power into AC power electrical which then can be injected onto the network.
KCL:	**Kirchoffs Current Law**: It is the conservation of charge, charge cannot be destroyed or created. Therefore all the currents going into a point add up to zero.
TR_Probe:	Time probe in Simplorer, which inputs a signal and outputs the time parameters from it.
MGCC	**Malengret and Gaunt Current Compensation**: is a method which is described and applied throughout this dissertation. It finds the desired currents as to remove the reactive component, using the voltage and resistance parameters.
OPF	**Optimal Power Flow**: is the process of studying the load profile of a system and controlling the flow of power in reaction to the requirements by the load.
SMART grid	A **SMART grid**: is a modern grid that uses information to act on complex system before the actions happen.

Key Words: Thévenin equivalent, Current Compensation, active filter, optimal real power, impedance calculator, optimal current flow.

Table of Contents

List of Illustrations

List of Tables

Chapter 1: Introduction

This dissertation is based on the fact that any m-wire electrical system can be modelled as m-equivalent Thévenin voltages and impedances when viewed from any node. How current flows in the Thévenin model is looked at; if the Thévenin models optimal has been found, how closely would this relate to the physical networks optimal. The dissertation describes how to calculate the optimal distribution of currents so a specific amount of power can flow through and reach the network equivalent Thévenin voltages with minimal losses.

In terms of optimisation we look at maximising the active power component which gives energy to the load and to remove the reactive components which contribute to only losses, providing no energy to the load. The definition of reactive power is looked at where Malengret and Gaunt show the power triangle concept can still be applied but must include the voltage imbalance and distortion components. Recently their research showed if the line resistances are unequal, the components must be taken in the weighted domain.

The Malengret and Gaunt Current Compensation (MGCC), a recently patented method, calculates the optimal currents for a set of wires with unequal line resistances. These are shown to be obtained from the Thévenin parameters and power flow at any instant in time at any node. It finds the weighted currents by looking at the present state of the system. The present state is found by weighting the voltages at the correct reference according to the line resistances. The Thévenin parameters will be constantly changing with the dynamic behaviour of the network. These parameters need to be constantly found for any device in the network to compute the currents for optimal current flow.

A method developed in my previous paper was required to enable a device to compute the dynamic system parameters. This method injects a current in-phase with a specific magnitude and within a short period of time injects another current with the *same* magnitude, in-antiphase. The voltages are recorded at both instances and applying a formula, the impedance parameters are easily found.

This method of distributing the current can be applied in a few different ways: the first way is described in my previous paper where a device at any node in the network is able to inject/extract power optimally; another three methods are studied, where a device intercepts a transmission network and redistributes the current so as to remove the reactive current components. Once the ideal currents are found, active and passive devices can redistribute the currents accordingly to compensate existing currents to remove the reactive power with zero power at the device.

The focus is particularly on the proof of concept by simulations and physical experiments with work not specifically described in the patent and with more emphasis on the optimisation to active power compensation. It was shown that any inverter can measure the dynamic behaviour of the network by toggling a known resistance in series with the grid and comparing the inverter-found values with the previous grid values plus the known resistance.

It is explained and shown how this can be implemented using the Malengret and Gaunt method. Both a six-wire and three-wire case is looked at. Where the six-wire device interrupts the transmission network, having two sides to it, each side is looked at independently and the reactive components are removed for both sides. The three-wire device rearranges the currents in the system by applying Kirchhoff's Current

Law. Each side of the node needs to be looked at independently, while treating the other side as a constant current source, enabling the device to change the currents to the desired components.

The three-wire method reduces the cost in application where not all the currents need to be processed through a converter (e.g. inverter) but only the difference between the existing and desired optimal currents. A smaller shunt parallel converter can result in ideal current flow without the need for interrupting the currents as described in the present patent. The methodology is explained and demonstrated by simulation.

1.1 Hypothesis

Based on the present technologies of inverters and the developments by Malengret and Gaunt, the following hypothesis is believed to be valid and, if so, useful:
A device at any PCC can measure the dynamic parameters of any power network and find the currents removing the reactive current component in the system, therefore reducing the resistive losses while maintaining the energy at the loads.

1.2 Guiding questions

The following research (guiding) questions can be identified to guide the investigation into the validity of the hypothesis:
What techniques are suitable/practical for measuring the dynamic parameters of the network?
How accurate are the measurements and the derived dynamic parameters?
Does a single optimum solution of 'power loss reduction' exist?
What components contribute to energy at the load?
How has the definition of reactive power changed over time?
Does the measurement, derivation and optimisation suffer from interference from other similar sources in the network?
What limits the adoption of such a solution for all inverters on power systems – at any PCC?

1.3 Plan of development

The following chapters were written to answer the guiding questions of this dissertation:

- **Chapter 1: Introduction** – develop a hypothesis and introduce the reader to what this dissertation is looking at.
- **Chapter 2: Literature Review** - is a research section where information and research previously done on optimal power is compiled and explained. It is used to demonstrate and define what optimal power in this context is. Also focusses on the history of the work of others on this topic.
- **Chapter 3: Computation of Thévenin Resistance for Network Changes** demonstrates an experiment where a power inverter is coded to calculate the Thévenin Equivalent Resistance of the grid. The accuracy of this process is investigated in this chapter by performing known network changes.
- **Chapter 4: Thévenin Equivalent Model Power for Optimal Power Flow** develops the theory of Superposition with regard to power. It explains the power is only optimised with regard to the power we have available and doesn't change the present state of power flow.

- **Chapter 5: Current Compensation Sweep Analysis** proves there is a single optimal solution and the current ratios are found by the Current Compensation method by Malengret and Gaunt.
- **Chapter 6: Weighted Voltage Vector Normal** gives the reader the definition of the normal of the voltage vector and what happens when we weight the voltages with resistance. To show the norm describes the state of the system.
- **Chapter 7: Instantaneous vs Average Power over a Cycle** investigated using the average norm of the weighted voltages over a cycle, assuming a small amount of storage is available, will provide a better solution than using it in an instantaneous domain. Then goes on to prove it will find the optimal for a period of a waveform.
- **Chapter 8: Active Filter** is a chapter introducing the concept of applying the MGCC method with the ability to compute the parameters to an inverter in a transmission network. Three different methods of applying this device are shown.
- **Chapter 9: Current Compensation for Power Devices** is a chapter showing the magnitude of the MGCC method being applied inside a power device injecting/taking power in a power network.
- **Chapter 10: Current Compensation Active Filter** is a chapter showing the magnitude of an Active Filter device working in typical networks.
- **Chapter 11: Conclusion** is a chapter which brings everything together showing what points have come from this dissertation.

Chapter 2: Literature Review

2.1 Review of Optimal Power Flow

Economic dispatch for AC power systems was first introduced by Carpentier and then Optimal Power Flow (OPF) was defined in Dommel and Tinney's paper (Dommel & Tinney, 1968). Since then the definition has been refined throughout the years. In the early days optimal power flow was defined as minimising the amount of power required by generators by reducing transmission losses (Noroozian, 1997) (Liang & Duncan Glover, 1992) (Alsac, 1990) (Yuryevich, 1999), so the devices controlling the amount of fuel into the generators (governors) can release less fuel to generate the electricity required by the loads (Lee, et al., 1984). This has a direct influence on reducing the cost of power generation and therefore focusing purely on economic optimisation. In the case of a generating unit using a cheaper fuel but at a location where more transmission losses occur, it could be still cheaper to generate more at its location. Lee, et al.'s later paper (Lee, et al., 1985) suggests optimisation should be a function of the fuel costs and transmission losses. This paper also suggests lumping real and reactive power together into an objective function for optimisation, where previously each optimisation method had been decomposed individually. It is said that the variables of each individual function is dependent on the other and therefore they are performed iteratively until an optimum is found.

Squires' paper explains how a power network is made up of several power source generators all of which have their own cost function. Initially the method of optimisation was used as if the transmission losses were neglected and the function was made up of the incremental cost. Subsequently the transmission losses were then included into the cost function of each generation's incremental cost function. This method had been refined by many authors since but was initially started by George, Page, and Ward (1961). In this new cost function, partial derivative is found with respect to the power generation unit but since the losses are not always known, this solution is not exact. This loss formula applies a number of assumptions which further makes it an approximation instead of an exact solution. In Squires' method of economic dispatch, a fuel cost function is shown which is a function of the loads' voltages. Huge simplifications are made by using constant in-phase voltages instead of constant scalar voltages. To minimise the overall fuel cost, the rate of change of the cost is equated to zero. These result in a set of non-linear algebraic equations. The method chosen to solve these is the Newton-Raphson iterative method, ignoring terms greater than first order. This method is explained again later.

Reactive power generation needs to be located and studied in such a way as to improve voltage profiles and reduce real power lost on transmission lines (Mamandur & Chenoweth, 1981). This correlates to Lee, et al. (1985)'s theory which says that both reactive and real power optimisation needs to take place.

The control variables are real power generation outputs (watts) for real power optimisation and shunt capacitor and transformer tap settings for reactive power optimisation (Lee, et al., 1985) (Lai, et al., 1997). The problem consists of a non-linear program with a non-linear objective function controlled by non-linear functional equalities. Large amounts of electrical power cannot be stored effectively therefore the generation of power should be well balanced with the amount of power required by the customers (Kothari, 2012).

Reducing the transmission losses and having the power generated in an optimal location, i.e. where it is being used at the load, will also improve the efficiency. With today's environment and the ever need for focus on a greener solution, another factor that could be required when optimising power flow is the reduction of carbon emissions by reducing peak power generation, as this emits more carbon emissions (Geidl, et al., 2007) (Lai, et al., 1997). At first thought you would think a pumped storage, being the typical peak power source, doesn't emit any carbon emissions but the pumped storage is not generating power, it is taking power previously generated and storing it. The efficiencies of both processes influence the same power transfer. The first paper by Lee, et al (Lee, et al., 1984), having been written before the focus on the environment, has a more narrow definition of optimal power flow, whereas the second paper deals with cost and environmental influences. A problem is observed between Lee's (Lee, et al., 1985) theories of reducing fuel costs and between the environmental impact of different fuels and assigning them a cost function. In modern times the cost function has included environmental impacts, as we look to become a cleaner and more efficient planet.

The system's optimal current flow can only be looked at once the system is stable, forming a hierarchy in Grigby's definition. Being within limits, reliability is more important than economic supply. As soon as the system is seen as stable (Grigby & Leonard, 2012), it can move its focus onto economic optimisation.

Linear reactive power optimisation will improve the system voltage and minimize real power losses (Deeb, et al., 1990). Deeb's (Deeb, et al., 1990) paper also says reactive power distribution is optimized by varying the transformer taps, generator voltages and shunt capacitors and inductors. However, the analysis of the system is the main objective. Decomposition methods are used to simplify and reduce computational times. Linear programming is generally used to analyse a network.

Savulescu (1976) presents an approach to determine the power system's loss sensitivity, reactive power transmission and steady-state stability functions and from there developed search procedures to find the optimal system parameters. Narita and Hammam (1971) use the sensitivity of the system and the Method of Box to minimise the voltage derivations from their desired results. This indirectly minimises the system losses.

2.2 Reviewing Optimisation of micro-grids and small injection nodes.

A whole new process of optimising is formed when we start using a PV-hybrid system, a system having intermittent solar energy generation with storage elements (batteries). Optimising a hybrid system as mentioned means the main focus is the highest power output with least degradation and aging of the batteries and managing the grid so that the customers incur the least cost. Some of the ways of achieving this is by peak load shaving, limiting the peak power exchange between the grid and the user thereby reducing the utility cost (Riffonneau, et al., 2011) but doesn't mention the resistance parameters of the wires. Peak shaving also has other advantages for the grid, for example being able to emit less carbon emissions as the peak load generation units are used which decrease in efficiency and the system design can be made with lower specifications (smaller transformers and transmissions lines). Therefore the definition of optimisation with regard to real power changes depending on, if you are the system operator or a small de-regulated generating unit operator, according to Riffonneau however there are still links.
For Injection into a grid Grigby (Grigby & Leonard, 2012) defines:

- Voltage regulation, the voltage level should remain within the ±10% of the nominal voltage range at the Point of Common Coupling (PCC) so as not to damage equipment connected to the network.
- System frequency, again the frequency should not be moved out of the specified range (47.5Hz-52Hz).
- Synchronisation, while the unit is synchronising to the grid, the voltage fluctuations must remain within the 5 percent specified range.
- Monitor surrounding parameters, systems of 250kW and greater must have connection status and real and reactive power output at the PCC.
- Isolation, the unit must be able to isolate from the grid under all necessary conditions. In a grid fault state, the device must be able to detect this and thereafter no longer inject power into the grid.
- Grounding, the unit must be properly grounded with protection.
- Voltage disturbances, during any abnormal voltage or frequency conditions the unit shall cease to energise the grid.
- Loss of synchronisation, loss of synchronisation needs to be on all units greater than 250kW.
- Reconnection, after an out-of-bound disturbance has been detected the unit must stop all current injections into the grid.
- Anti-islanding, a unit must be able to detect an island condition and cease to energise the grid when a condition has been detected.
- Harmonics, the unit cannot inject current harmonics into the grid greater than a specified amount.
- DC current injection, a unit shall not inject a DC current of greater than 0.5% of its rated.
- Flicker, the utility's customers nearby may not experience a large amount of voltage flicker.

These constraints act as limits on the optimising function. Once safety and reliability constraints are met, optimising the system can be looked at. These limits are defined generally, where at different locations around the world, the limits can be defined differently.

A method of optimising is explained by Baran (1989) where two functions are created, one for the system transmission losses and another for the load balance of the system. Also noted though is that though they are different, they depend on similar variables such as reactive and real power and voltages (Mesut & Wu, 1989). Reactive power doesn't influence the fuel cost for generation as the power is never used. It may however damage equipment in the power system and make the power system require large power ratings on the system's equipment (Akagi, et al., 1984). As reactive power has an influence on the cost of a network, it would also want to be optimised or kept within the limits concerned because it would increase the size of the power carriers in the network.

Subsequent to the blackouts in the United States of America, Amin, et al (2005) present an article about a method for enabling a grid to be self-healing. They compare the desired result of the method to the control designed in an F15 fighter jet. This method doesn't only protect the power network from outages and faults, it is also used to compute an optimal power flow for any network. The necessary variables can be computed before any action has happened as each node in the network is communicating with a central operator.

Power system operators maintain system reliability and quality by controlling the system bus voltages (Mamandur & Chenoweth, 1981). The network operator is compared to the pilot of a F15 fighter jet (Amin & Massoud and Bruce F., 2005), since the power generated must be moved to where it is used optimally. One of the problems is that any network additions need to be described at the central control of a sub-station or power plant. This can only be done after the action in question has been completed, but what is often required is the information before the occurrence so that the necessary computations can be compiled (Amin & Massoud and Bruce F., 2005). In this method, known as the SMART grid, each node can communicate back and forth with the central control and therefore what is required can be known before the action is performed. The central control can also control the end nodes.

The SMART grid's objectives are to provide operators with the ability to observe the grid in real-time as well as a well-defined prediction to enhance grid stability and reliability and provide an easy optimal power flow solution. It is also supposed to fully accommodate the use of grid energy markets, where supply providers can be allocated with more ease (Momoh, 2009).

The increasing use of solid state switching devices, nonlinear and power electronically switched loads, unbalanced power systems, lighting controls, computer and data processing equipment, as well as industrial plant rectifiers and inverters has created power supply quality issues leading to resultant problems. These devices cause harmonic distortions in the current waveforms in the system in which the system equipment is not designed to operate and therefore can cause expensive damage (Dash, et al., 2003). However, in more recent literature (Grigby & Leonard, 2012) the focus on a system's quality being dependent on safety, reliability and economic supply is broadened. The first definition could be thought of as a deeper definition of economic supply. As damaging the equipment will might be costly and therefore add to the cost function of the system.

As power system quality can influence the performance and life of equipment connected to it (Dash, et al., 2003), methods are often applied to improve network quality, e.g. voltage balancing, where the dirty signal is rectified into dc then fed straight into an inverter for a clean output (Pan & Zhiguo, 2005). Capacitors are used to change and improve the power factor.

A few authors, including Kirschen and Hand (Kirschen & Hans, 1988), separate the optimisation problem into active power control and optimisation and reactive power control and optimisation. This is shown in the Figure 1 below, demonstrating how each has its own respective control variables and constraints. A global optimisation is therefore done in 3 steps: power flow of the system; real optimal power flow; and finally reactive optimal power flow.
The optimal current distribution method uses a recently patented method which calculates the optimal distribution of currents. These are shown to be obtained from the Thévenin parameters and power flow at any instant in time at any node. It finds the weighted currents by looking at the present state of the system and by weighting the voltages at the correct reference according to the line resistances.

	CONSTRAINTS	CONTROL
ACTIVE O.P.F.	POWER BALANCE	MW GENERATION
	MW LINE FLOWS	PHASE SHIFTERS
	RESERVE MARGINS	DC LINES
	AREA INTERCHANGES	LOAD SHEDDING
	VOLTAGE MAGNITUDE	ECONOMY INTERCHANGES
REACTIVE O.P.F.	VOLTAGE MAGNITUDES	GENERATOR VOLTAGES
	MVAR GENERATIONS	TRANSFORMER TAPS
	MVAR LINE FLOWS	SHUNT BANKS

Figure 1: Constraints and control variables for real and reactive power (Kirschen & Hans, 1988)

2.2.1 *Review of Reactive Power definition*

Eliminating non-active current using various methods with active and passive components has been the subject of many publications (Akagi, et al., 1984), (Filipski, 1980). Under distortion of voltage and current conditions the definition of reactive power has been complex and still the subject of much debate.

Malengret and Gaunt (Malengret & Gaunt., 2008) detailed in a distorted system that the currents be analysed as the classical power triangle for sinusiodal systems, provided the reference of the voltages is correctly chosen for every instant in time.

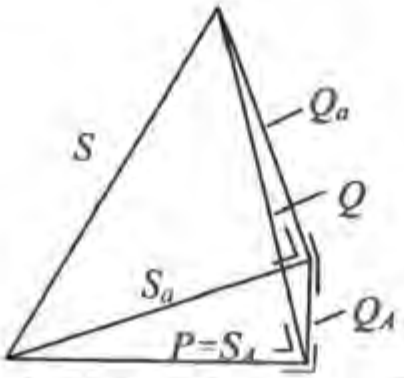

Figure 2: The power triangle with its added components (Malengret & Gaunt, 2012)

In Malengret and Gaunt's paper (Malengret & Gaunt., 2008) the concept of the removal of non-active current is discussed. Where Q is the non-active power component in Figure 2 and Q_a is the power component which can be achieved without energy storage at the compenstator. Q_A represents the power which can be eliminated with a compensator with energy storage. In Figure 2 above, these components are orthogonal.

Later work (Malengret & Gaunt., 2012), continues this objective of reactive power compensation but now includes the case of the wires resistance no longer being equal. It was also shown that the power triangle

concept is still valid and orthogonal if the voltage and current components are weighted with the resistance of the wires.

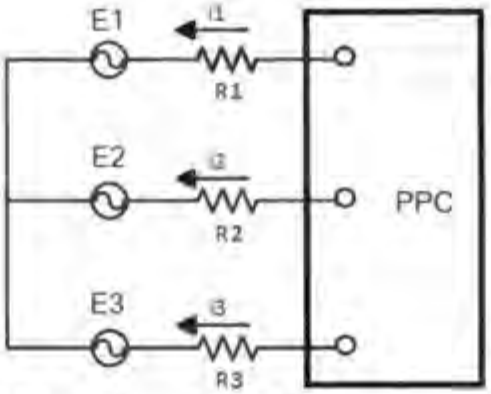

Figure 3: Power network for current compensation

The objective for current compensation in the network above in Figure 3 is to get power from the PCC to the Thévenin Equivalent voltages (e_{th} in Eq.1) optimally.

Bold lettering, denotes it as a vector

$$\boldsymbol{e_{th}} = (\boldsymbol{e_1}, \boldsymbol{e_2}, \boldsymbol{e_3}) \qquad \textbf{Eq. 1}$$

Where the lower case symbol indicates the instantaneous value for upper case symbol in Figure 3 above.

Firstly, the correct reference for e_{th} has to be found from Eq. 2, taking into account the resistance of each wire. The amount of power lost in a wire is dependent on its resistance. This is why the system is looked at in a weighted domain, where the voltages (at their correct reference) are weighted with respect to the wire's resistance, as shown in Eq. 3 below:

$$\boldsymbol{v_{ref}} = \frac{\frac{e_1}{r_1}+\frac{e_2}{r_2}+\frac{e_3}{r_3}}{R_1^{-1}+R_2^{-1}+R_3^{-1}} \qquad \textbf{Eq. 2}$$

$$\boldsymbol{v'} = \left(\frac{e_1-v_{ref}}{\sqrt{R_1}}, \frac{e_2-v_{ref}}{\sqrt{R_2}}, \frac{e_3-v_{ref}}{\sqrt{R_3}}\right) \textbf{ Eq. 3}$$

The voltage norm is found by squaring and summing each component of the weighted voltage vector, as shown in Eq. 4 below:

$$||v|| = (v_1')^2 + (v_2')^2 + (v_3')^2 \textbf{ Eq. 4}$$

The next was given as:

$$k = \frac{p_{Th}}{||v||^2} \qquad \textbf{Eq. 5}$$

Where p_{Th} is power on the e_{th} side and calculated below in Eq.6. p is the available/required power at the Point of Common Coupling.

$$p_{Th} = \frac{-||v|| \pm \sqrt{||v||^2 - 4p||v||}}{2} \qquad \textbf{Eq. 6}$$

Finally by multiplying the weighted voltage vector (v') by k (the current scaler, found in Eq. 5) we find **i'** (the weighted currents vector), as in Eq. 7 below:

$$i' = kv' \qquad \textbf{Eq. 7}$$

This is the Current Compensation method used throughout this paper which was developed by Malengret (Malengret & Gaunt., 2012).

2.3 Review of the Development of Optimal Power Flow Methods

Depending on what is defined as the optimal power flow and the objective, there are different methods for the OPF problem. The different mathematical functions can be classified as linear, non-linear or mixed-integer linear problems. Jizhong (Jizhong, 2009) classified three methods for the OPF problem: conventional optimization methods, intelligence search methods, and non-quantity approach to address uncertainties in objectives and constraints.

At first conventional calculus-based optimisation algorithms were used for OPF. These methods linearise the functions and use the first and second derivatives of objective function and their constraint equations as their search directions (Lai, et al., 1997). The optimal power flow of any network can be computed, but the time it takes to compute is of great importance. If the computation takes a longer period of time than the general dynamic changes of the network it can become useless. This is because the system changes back in the time it took to read the change and, therefore, can result in an adverse effect.

1.1. Linear Programming OPF

The Linear Programming (LP) OPF, one of the first optimisation methods, is reliable and finds regions of infeasibility quickly and easily. It, therefore, finds the operation limits for contingency constraints. The convergence is also fast even with small changes (Jizhong, 2009).

The problem arises when simplifications are done to the systems equations and because systems are so big, generally, this is often required (Sun, 1984). Traditionally the calculations have been based on the sum of both the convex cost curves of real and reactive power dispatch. Piecewise LP based OPF fixes these problems but introduces the problem of storage.

1.2. Newton Method

The algorithm to find the OPF by the Newton Method is defined in (Tinney & Hart, November 1967) (Jizhong, 2009) (Sun, 1984), where an initial approximation to the voltage solution is made in order to be applied in the complex power equation ($(P_k + jQ_A) = E_k \sum_{m=1}^{N} Y_{km}^{*} E_m^{*}$). A system of equations describing the network's system changes (Jacobian,ΔP_k *and* ΔQ_k) is created. The voltages are calculated by Gaussian elimination and back-substitution. This transforms the complex power column into a column of voltage angles and magnitudes which is the desired result. Finally the change in complex power is calculated to check if the correct solution is found. If the change is small enough it implies the solution has been found.

It is said the accuracy of the Newton Power Flow Method is limited *only* by the round-off error of the direct solution, otherwise the solution is exact. It does take a lot of system memory to compute but one can use reduction methods. It is said by the author (Tinney & Hart, November 1967) the Newton Method does not have the ability to compute with negative transfer reactance such as those found in 3-windings transformers. While this method is good, improvements are foreseen. Sun (Sun, 1984) does an easy simplification by decoupling the matrix and, therefore, reducing its size and memory usage.

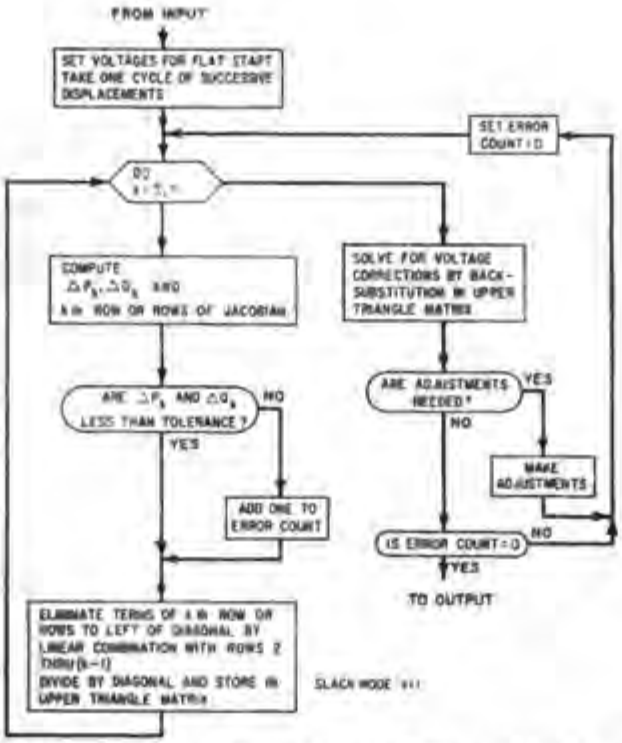

Figure 4: Flow chart for the Newton Method algorithm (Tinney & Hart, November 1967)

Tinney and Hart's paper on the Newton's method (Tinney & Hart, November 1967), says there is no method for the absolute optimum except by checking every single possibility at every single node. Considering the size and complexity of modern power networks this would not be possible before the system changes occur. The paper describes three methods for approximating optimal power flow for networks: the simplest method is ranking each node according to the amount of branches connected to the node, while it does not take into account the elimination steps. It is simple to program and quick to execute; the next method simulates the elimination process, the nodes are numbered so the node with the least connected branches are removed; the most complicated, and therefore least used (Tinney & Hart, November 1967), is where at each step the node introducing the least new equivalent branches are emitted. This is done by simulating the change at every possible step as well as its solution.

1.3. Gradient Method

A later method of optimising power flow in any power network is described further in (Dommel & Tinney, 1968). This method applies the above explained theory but then measures the behaviour at each system change (transformer tap settings, nodal voltages etc.). The basic theory is that the gradient of the function is applied and the control variables are changed to obtain a negative gradient (moving to lesser amount). Once the negative gradient has reached a small enough value (approaching zero), the optimum has been found.

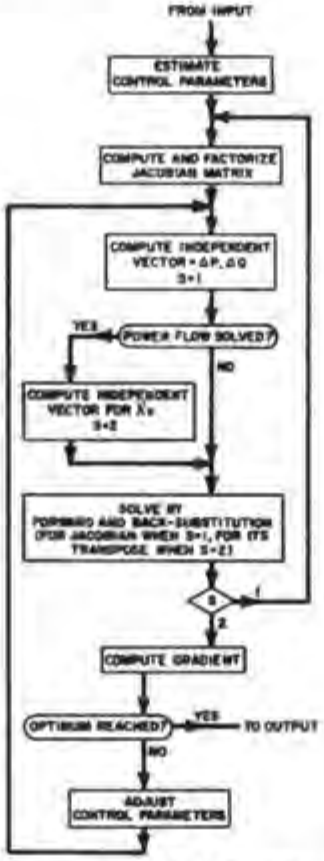

Figure 5: Flow chart for the Gradient Method algorithm (Dommel & Tinney, 1968)

The paper written by Dopazo, et al (Dopazo, et al., 1967), describes the economic allocation of real and reactive power generation using Lagrangian multipliers. They describe the dynamic of the power system and then use a gradient method to find the optimum. This method works on reducing transmission losses in the power network and provides line loading and voltages before generation changes have taken place. The gradient method is used again in (Hano, et al., 1969). This OPF gives two computational time periods for voltage and reactive power. It determines the sensitivity relationships between the control variables and using a direct technique, finds the minimum losses.

It is said by Dommel and Tinney (Dommel & Tinney, 1968) that this method of gradient optimal finding only works well if the set of linear equations describing the network is not too distorted by excessive penalty functions. To help with convergence, this method can be changed from first order to second order. This will, however, increase computation time.

1.4. Modified Interior Point OPF

This method puts its objective and cost functions in quadratic forms. This enables a few mathematical manipulations: the Taylor Expansion of the function has the attribute of terminating in second-order without truncation error; the Hessian of the function is constant and the higher order function is easily evaluated. The simple process of this method is to: obtain the bus voltages in rectangular co-ordinates; choose a starting point satisfying positive conditions; perform the Newton Method and find the Newton direction; compute and update the step length changes and; if the step length is sufficiently small stop, else reiterate.

This process has been said to be the modern and most-used OPF today (Jizhong, 2009), because this function is not predetermined and can be modified by the user at the operation control. Torres says this method is sufficient but only produces an approximation to the optimal (Torres & Quintana, 1998). It also does not require a feasible starting point, for it to converge (Wei, et al., 1995). The interior point method has been said to be the most efficient method (Momoh, et al., 1999) (Momoh, et al., 1999) (Jizhong, 2009) (Wei, et al., 1995).

1.5. OPF with Phase Shifter

Flexible AC Transmission System (FACTS) is a recently developed modern way to improve the efficiency of reactive power in systems. It uses variable series capacitors, phase shifters and unified power flow controllers which change the transmission line parameters by meeting certain requirements, (Liu & Song, 1999) similar to Akagi's(1984) method. These functions are performed to reduce transmission losses and better utilise the thermal capacity of the transmission lines. This will increase stability margins while maintaining supply to the loads. The development of power electronics and the increase in power system size has influenced the availability of these devices (Liu & Song, 1999).

Numerous optimisation methods are used to locate these FACTS devices so as to minimise cost. Reduction in real power of a particular stressed line, a reduction in the total power of the system and the real power flow performance index are all parameters which are of main focus when allocating FACTS devices (Singh & David, 2001). A reduction of one may result in an increase of another.

An optimal power flow method is described by using phase shifters to enhance network security. It speaks about locating capacitor or inductor banks in a well determined place in a power network to not only secure it but also provide a power saving attribute (Momoh, et al., 2001) (Jizhong, 2009) .

1.6. Particle Swarm Optimization for OPF

The Particle Swarm Optimisation (PSO) method recently discussed in the literature by Abido (Abido, 2002) has the advantage over the Gradient method because it can find both the local and the global minimums. It also has the benefit of not being dependent on using good starting variables; it will find the optimum no matter which is chosen (Abido, 2002). This method is best explained by thinking of particles flying through a hyperspace searching for conditions with two vectors associated to it, one for position and another for velocity. Each of the particles interact and when they come across each other they communicate, informing each other of the best locations found and, therefore, arriving at a new best (Jizhong, 2009).

1.7. SMART Grid

The power grid of the future is the SMART grid (Farhangi, 2010) (Amin & Massoud and Bruce F., 2005), where each of the nodes in the network can communicate with the central control brain of the network. This can be used to optimise power flow as well as provide a stronger more secure network. The central control can know what each node wants to do and, therefore, know the future variables of the network. This method is definitely the faster and best optimal method. However, it has only become possible from the advances in technology through time (Metke & Randy L., 2010) (Farhangi, 2010). A lot of work has to be done to implement this process in the modern grid. Each end node has to have new technology installed.

Existing Grid	Intelligent Grid
Electromechanical	Digital
One-Way Communication	Two-Way Communication
Centralized Generation	Distributed Generation
Hierarchical	Network
Few Sensors	Sensors Throughout
Blind	Self-Monitoring
Manual Restoration	Self-Healing
Failures and Blackouts	Adaptive and Islanding
Manual Check/Test	Remote Check/Test
Limited Control	Pervasive Control
Few Customer Choices	Many Customer Choices

Figure 6: Comparison between present and future intelligent grid (Farhangi, 2010)

2.4 Review of Thévenin Equivalent Parameter Computation Methods

A number of applications require the Thévenin parameters to operate. These operations vary from real and reactive power compensation to grid contingency and stability. The parameters were used to find the solution to best inject power so as to reduce losses (Gaunt & Malengret, 2013) (Larsen & Charlton, 1993) or used to find when the load impedance is approaching the Thévenin impedance seen from a node (Johannsson, 2011) (Pinzon, 2000). This results in the need to change transformer ratios or power flow. Johannsson's method requires the Thévenin parameters at every node in the network.

In my previous paper I show how an inverter device can compute the Thévenin Equivalent model parameters viewed at the PCC for any network, where the Thévenin Equivalent model represents the network's dynamic behaviour accurately. Another method of obtaining the Thévenin reactance and applying it to reactive power compensation, was patented by Larsen and Charlton (Larsen & Charlton, 1993). The method is interesting and requires an estimation of the parameters initially to achieve a reasonable result. It injects reactive power and applies the change of the voltage to compute the change in reactance. This is similar to the method used, however the method applied in my previous paper, made two injections. As to cancel the voltage drop over the unwanted component of impedance.

Each wire in a network looking at the PCC can be represented by a Thévenin Equivalent model, like the one in Figure 7 below. The desired outcome is that a inverter placed at the PCC is able to compute all three parameters R_{th}, X_{th} and V_{th}, for all wires.

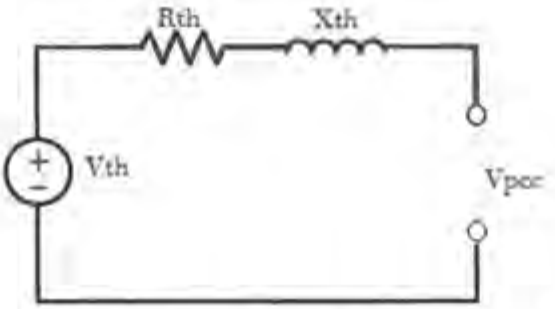

Figure 7: Diagram of a Thevenin Equivalent network

The parameter V_{th} is easily found, as the device knows V_{pcc} and if no current is injected at the PCC, there is no voltage drop over either the resistance or the reactance and therefore the voltage are equal as shown in Eq. 8.

$$V_{th} = V_{pcc} \text{ (if } I_{pcc} = 0) \qquad \text{Eq. 8}$$

The method of the finding the impedance of the network requires the assumption that within a short time period, none of the parameters change. At two different time instances the PCC injects current and the voltage at the PCC is measured.

At the first time instance, the current (by the inverter) at the PCC was *in-phase with* V_{pcc} and forced a voltage drop over both R_{th} and X_{th}. Giving V_-, the voltage at the PCC with an in-phase current.

$$|V_-| = |V_{pcc}| \text{ (if } I_{pcc} \; in-phase \; with \; V_{pcc}) \qquad \text{Eq. 9}$$

At the second time instance (within a short period), the injection (anti-phase) current by the same inverter, caused the voltage drop over R_{th} and X_{th} to be the other way (shown in Figure 8, on the right) and resulted in V_+ at the PCC as shown in Eq. 10.

$$|V_+| = |V_{pcc}| \text{ (if } I_{pcc} \; anti-phase \; with \; V_{pcc}) \qquad \text{Eq. 10}$$

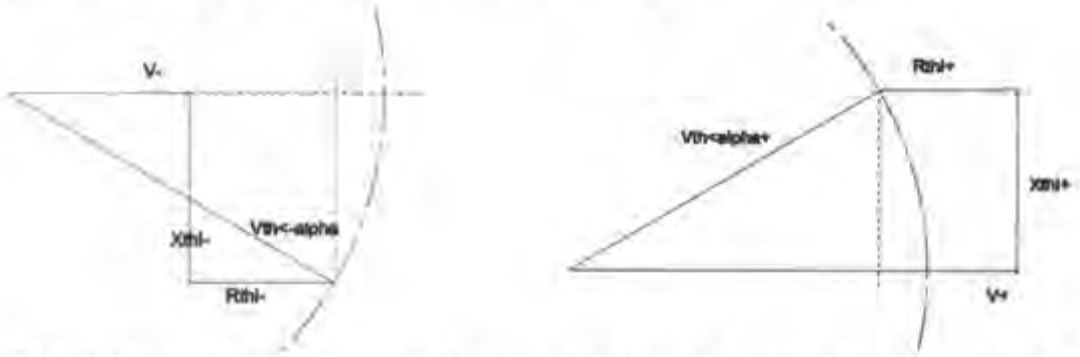

Figure 8: Diagram for the voltage vectors for a current in-phase (on the left) and for a current anti-phase (on the right) both with the same magnitude

This is useful as the voltage drops over X_{th} cancel leaving just twice the voltage drop over the resistance, as shown in Figure 8 above. This method only used the magnitudes of the voltage and current at the PCC to find the resistance as shown in Eq.11.

$$R_{th} = \frac{|V_+| - |V_-|}{2|I_{ppc}|} \quad \text{Eq. 11}$$

Again, by applying this same method, by injecting currents at ninety (and two-hundred and seventy) degrees out-of-phase from the voltages on the line, the inductance parameter can be found by any power device. The voltage drop over the R_{th} cancels and leaves twice the voltage drop over the reactance, resulting in Eq.12.

$$X_{th} = \frac{|V_{+\infty}| - |V_{-\infty}|}{2|I_{ppc}|} \quad \text{Eq. 12}$$

The stability estimation method patented by Johansson uses phasor measurement units (PMUs) to obtain the real-time voltages, the current phasors and the frequency (Johannsson, 2011). It applies one factorisation of the network admittance matrix from the present state of the power system. The advantage of this method is that there is no current injection required at each PMU to compute the Thévenin impedances. The major disadvantage is that all the systems' parameters are required to compute the impedances. On the other hand, the novel method which injects currents is able to compute the Thévenin parameters without the knowledge of the rest of the network. It applies the voltage changes at the node we are looking at.

The closest method, to compute the Thévenin impedance at any point in the network, to the novel method presented in my previous paper was patented by Pinzon (Pinzon, 2000), where he shows a method where two currents are used. The voltages while these two currents are being injected, are measured and used to calculate the impedance. However, this is an approximation as the phase of these measurements are unknown. Therefore only when these are relatively small are the results found to be accurate. In the case of injecting the currents at a known phase, the exact solution can be found as shown above.

2.5 Relevance to guiding questions

- The importance of using the term optimal current flow over power flow is shown, where optimal power flow has a lot to do with the cost of generation at specific locations and current flow is looking at removing all the components not contributing to energy at the load but still give power losses in transmission.
- The definition of reactive power has been looked at, where the definition including voltage imbalance and distortion is used.
- A few methods for computing the Thévenin parameters are available, but it seems from the literature the method developed in my previous paper is the best. However, this still needs to be looked at more and experiments need to be performed so as to provide proof.
- It is difficult to come to a conclusion saying this will work constructively or destructively with other compensator/power-balancing devices in the network.

- The dynamic behaviour of a typical network can be measured, with a few methods presented by Johansson (2011), Pinzon (2000), Larsen (1993), and myself (2013).These methods have previously been applied in compensators and contingency analysis.
- It is shown that Malengret and Gaunt have a method which applies parameters to find the desired current components so as to reduce resistive losses by removing the reactive current components. It is shown in my previous paper that this method can use the Thévenin parameters which can be calculated.

Chapter 3: Computation of Thévenin Resistance for Network Changes

An investigation, with the aim to prove a power electronic device computes the correct Thévenin Equivalent Resistance.

3.1 Introduction

The method to compute the grid parameters for the Thevenin Equivalent model is shown above and resulted in Eq.11 for the Thevenin Equivalent Resistance and Eq.12 for the Thevenin Equivalent Reactance.

This chapter is used to demonstrate an inverter connected anywhere on a grid, finding the Thevenin Equivalent Resistance for each line. The grid is large and is physically difficult to measure, so a resistance was switched into the grid and the found results were looked at.

Nodes in power networks can be represented by constant power, current or resistance sources. In the appendix it is shown how a power injection can be represented by a negative resistance and it is shown how the computed resistance is changed when a power injection is made into the network.

3.2 Method

The method used to show the method computes accurate resistance parameters is shown below:

3.2.1 The Code

A PowerStar, 3 module, 3 phase MLT Drives 18kVa inverter was used. The code presently on the inverter was adapted to record the voltage and current with a greater resolution. Previously the measurement parameters had no decimal place, for accurate results the parameters were changed to a single decimal place.

The code was made to toggle a variable which either increases the target amperes (positive power) or decreases the target amperes (negative power). At every second as the transient is reached, the voltage and current magnitudes were recorded into a variable dependent on the direction of power. Every 2 seconds, the formula above was used to calculate the resistance on each of the wires and was logged into Docklight (v1.3).

3.2.2 Experiment for Switchable Resistance

The PowerStar Inverter with the new code was connected in a three-phase topology as shown in Figure 9, where each of the phase wires had a switchable 0.2 ohm resistance present on it. Rswitchable1 for phase one, Rswitchable2 for phase two and Rswitchable3 for the third phase.

Both conductors (copper conductor, and the switchable resistance in parallel, equates to approximately zero resistance in series with the grid resistance) were applied when the switch was on and only the 0.2 ohm resistance was made available when the switch was turned-off. In other words when the switch was

on, the resistance should be the grid resistance and when the switch is off, the calculated resistance should be the grid resistance plus 0.2 ohms.
The resistance was switched onto a phase every minute while the Inverter logged (in DockLight v1.3) every 2 seconds, the calculated resistance values for each of the phase wires. This experiment was performed on each of the phases as to see if it in fact calculates the correct resistive values for every wire.

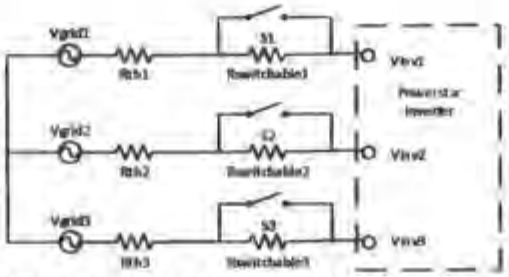

Figure 9: Powerstar inverter connected to three-phase grid

The added line resistance was also measured by finding the voltage drop over the added resistance, using a multimeter. It was compared to average over the minute time periods of the difference between the ON and OFF switch states.

ON State = grid resistance
OFF State = grid resistance + switchable resistance (0.2ohms)

Therefore, the difference between these are compared with the actual resistance
i.e.
ON – OFF = -switchable resistance, is compared with the found resistance from the measured voltage drop over the resistor.

3.2.3 *Experiment for Power Injection Toggle*

As shown in the appendix, a power injection can be represented by a negative resistance. This experiment is to obtain the change in the calculated Thévenin Resistance due to power injections into the network via another PowerStar Inverter.

Again the updated code was used to keep computing the resistance every 2 seconds while the other Inverter injected no power into the network. After which at a new time instant the power injected was changed to a significant magnitude of 4kW on phase 1.

The equivalent resistance was calculated as a resistance in parallel with the inverter. Then the series combination of the two resistances were used to compute the expected resistance.

3.2.4 *Analysis*

The logged values with the time stamps were imported into Microsoft spreadsheets. The expected values were calculated, compared and graphed.

3.3 Results and Discussion

The following results were found by the described method above:

3.3.1 Resistance Switched in on Line One:

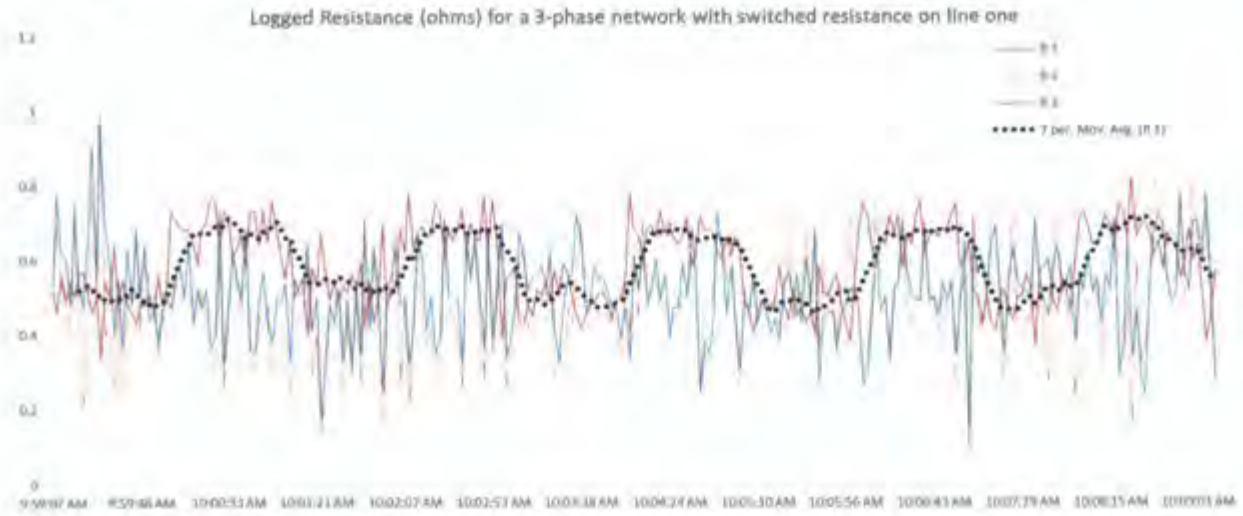

Figure 10: Output for the found line one resistances for the Inverter Computational method

Table 1: Expected and found results for switched in resistance on line one

Minute	Average	Change	Expected	Error (%)
-1	0.5008333			
0	0.6804545	0.17962	0.2	-10.19%
1	0.5404167	-0.14	-0.2	-29.98%
2	0.6745833	0.13417	0.2	-32.92%
3	0.4970833	-0.1775	-0.2	-11.25%
4	0.6645833	0.1675	0.2	-16.25%
5	0.4808333	-0.1838	-0.2	-8.13%
6	0.6786364	0.1978	0.2	-1.10%
7	0.5052	-0.1734	-0.2	-13.28%
8	0.6658333	0.16063	0.2	-19.68%

The graph for line one (red in Figure 10) shows at every minute the resistance for line one step up and down while the other two line resistances remain. The dotted black line shows the moving average for line one. It shows that the grid resistance (for line 1) changing from 0.5 ohms when it is just measuring the grid resistance to 0.7 ohms when it is measuring the grid resistance in series with the 0.2 added resistance.

The reason for this excellent output would be, line one's current was changed by the biggest magnitude (three amperes, double the magnitude of the other lines). Therefore the recorded voltages were changed by a significant amount. Another reason could be the lack of dynamic activity on this line. As while the transient is happening between positive and negative current nothing in the grid happens giving off good results.

From Table 1 above, where the average computed resistance over the time period is shown. The step changes from the expected are within a reasonable amount. The smallest error calculated on this wire was -1.98% and the largest found to be -32.92%. These include the dynamic behaviour of the grid, where the grid could have had a change (in line resistance on line one) in the minute I was reading. The graph in Figure 10 above, shows the step changes clearly and the moving average is expected with flat tops and steep slopes on the edges of each minute. The calculated resistances for this line are shown to be rather stable, implying the grid resistance for this wire is rather static.

3.3.2 Resistance Switched in on Line Two:

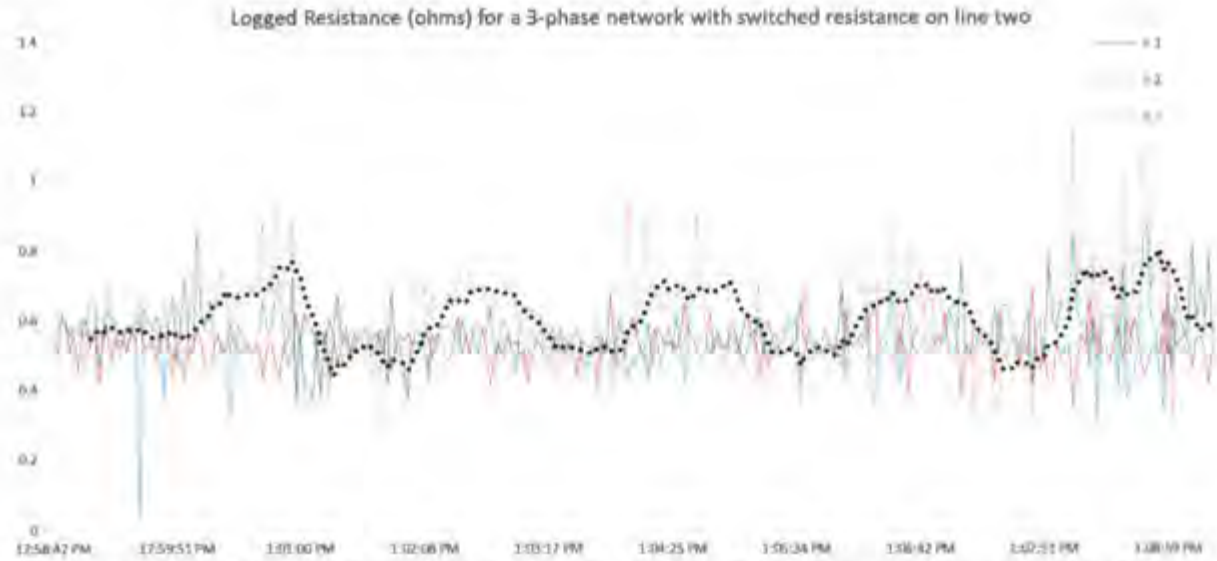

Figure 11: The graphed output for the found line 2 resistances for the Inverter Computational method

Table 2: The expected and found results for switched in resistance on line 2

Minute	Average	Change	Expected	Error(%)
-2	0.55286		0	
-1	0.55917	0.00631	0	
0	0.71375	0.15458	0.2	-22.71%
1	0.4768	-0.237	-0.2	18.48%
2	0.6696	0.1928	0.2	-3.60%
3	0.5192	-0.1504	-0.2	-24.80%
4	0.67769	0.15849	0.2	-20.75%
5	0.5068	-0.1709	-0.2	-14.55%
6	0.67375	0.16695	0.2	-16.53%
7	0.50875	-0.165	-0.2	-17.50%
8	0.7348	0.22605	0.2	13.03%
9	0.6	-0.1348	-0.2	-32.60%

The results for line two are not as static as the results for line one. It is difficult to see the step changes at times, for the computed resistances for line two in Figure 11 above. However the moving average does display this better, though still not as well as the experiment on phase one. This experiment did reveal a stable computation for the other two lines. This could suggest this line is highly active with a dynamic loads being switched on/off of it. Also the moving average (black dotted trace in Figure 11) shows a dip at 1:07pm, which would be a sudden change in the grid resistance.

Table 2 shows a good result where the smallest error is -3.6% and the largest being -32.6%, this large error would be a result of the dynamic behaviour of the grid resistance which the inverter is also measuring. Another observation to notice in minute 1 and 8 the error became positive for the first time, showing the error is a consequence of the grid's dynamic behaviour.

The results in the graphs seem to be messy. They calculated resistances seem to jump up and down, which seems to be a result of what the inverter is doing. When calculating the respective value on the other wires. However, the moving average gives a great idea of what is happening on the line.

3.3.3 Resistance Switched in on Line Three:

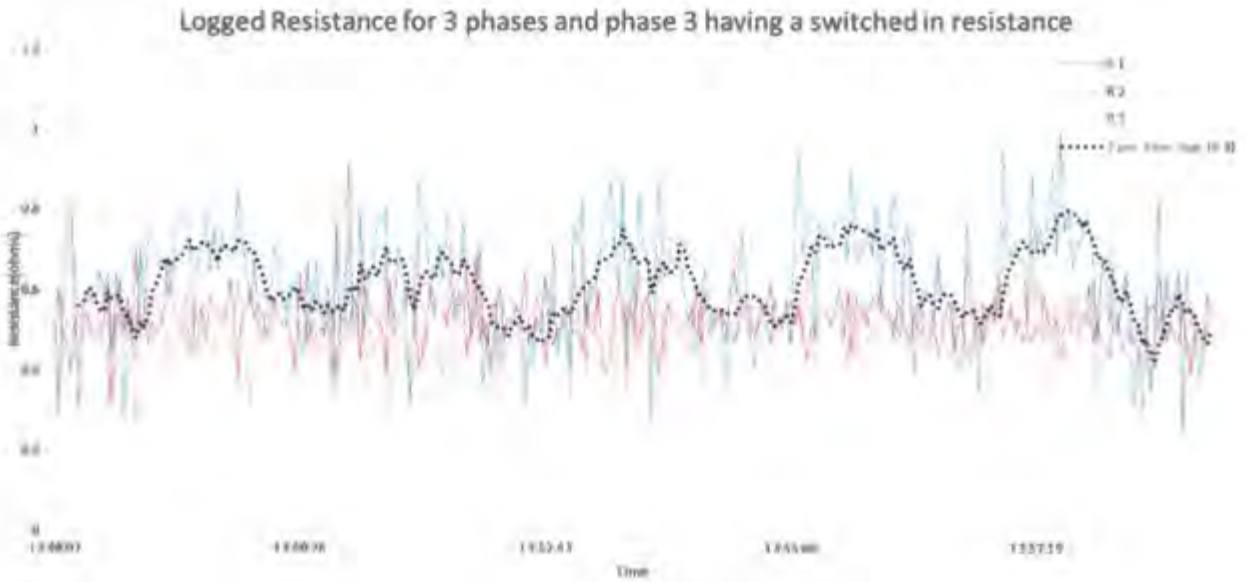

Figure 12: The graphed output for the found line 3 resistances for the Inverter Computational method

Table 3: The expected and found results for switched in resistance on line 3

Minute	Average	Change	Expected	Error (%)
-2	0.55227			
-1	0.69542	0.14314	0.2	-28.43%
0	0.5736	-0.1218	-0.2	-39.09%
1	0.64417	0.07057	0.2	-64.72%
2	0.5104	-0.1338	-0.2	-33.12%
3	0.67833	0.16793	0.2	-16.03%
4	0.54591	-0.1324	-0.2	-33.79%
5	0.73435	0.18844	0.2	-5.78%
6	0.5552	-0.1791	-0.2	-10.43%
7	0.7225	0.1673	0.2	-16.35%
8	0.51083	-0.2117	-0.2	5.83%

The results for the final wire are similar to line two. However the error goes all the way past 60% shown in Table 3 above. The expected reason for this is other activity on this wire's network, which could have influenced this and countered our step change as the change is much smaller than the expected. What are still shown in the graph are the step changes being much like the first case, rather flat with steep slopes on each minute edge.

The general resistance for the three wires was about half an ohm. In all three experiments the Thévenin Resistance for line one was the most stable and remained at half an ohm. Whilst the other two wires were highly oscillatory. It is expected these are actually false readings, as the network changes during the switch over between injection and extraction. By shortening the time period between injecting the positive and negative current, would fix this or by changing the current magnitude.

3.3.4 *Power Injection on Line One:*

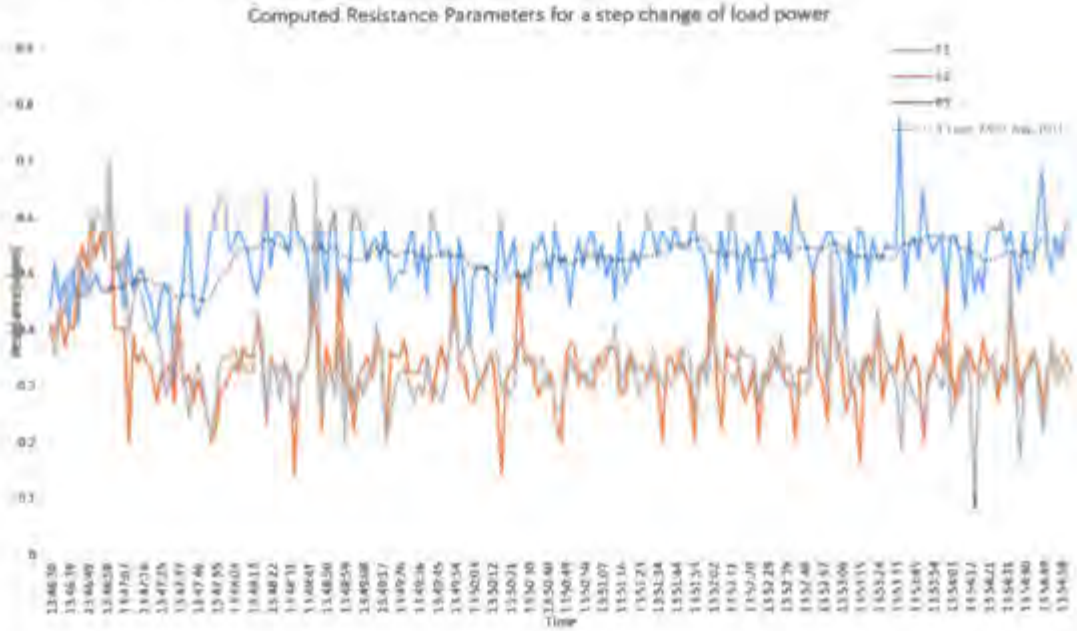

Figure 13: The graphed output for the found line 1 resistances for the Inverter Computational method for nearby power injections on the network

Table 4: The expected and found results for switched in power on line 1

Average (ohms)	Expected(ohms)	Error	Power (watts)	-4000
0.509868421			Voltage(Vrms)	230
0.536890756	0.53031381	1.24%	Rload(ohms)	-13.225

In the final set of results with power being the control, Figure 13 shows the parameters logged over both time periods remaining relatively stable (except for the initial time period, as inverter transients were still being met). This is expected as no controlled power was taken or injected onto those two phases. However, the phase in which power was taken off by a known amount did change. The moving average trend line displays this perfectly. Table 4 above shows an error of 1.24% from the calculated expected value. This error was unexpectedly excellent, which is noticeably better than the errors found in the switchable resistance experiments.

For all these experiments the general resistance found for each of the lines were expected. They were in the range of 0.1 to 1.1 ohms. The found resistance did become negative at stages. The expected reason for this was the network changed in between current injections and therefore the voltage changed. Therefore the assumption made about the grid not changing during the calculation became invalid. Making the formula not work.

This problem can easily be dealt with by ignoring any unreasonable values found. If we are calculating the values as often as every 2 seconds we can use the previous value when a bad result occurs but if the values persist then only use the found negative resistances. Another solution could be using an estimation method explained in the literature in parallel with this method to achieve the best results. However seen from all

three graphs the data remains relatively constant for the full duration of each of the experiments. This implies it is unnecessary to constantly be reading values every two seconds, a more realistic duration would be every two minutes.

3.4 Conclusion

In conclusion the Thévenin Resistance parameter computational method calculates the correct resistive parameters for both resistive and power changes in the grid. The error calculated goes from positive values to negative values implying a lot of the error is the unpredictable grid changes. This also implies we are in fact measuring the grid's dynamic behaviour which is exactly what we want. We can achieve an excellent representation of the resistance of the lines.

It was also found that the dynamics of the grid measured in these experiments, hold a relatively stable resistance on each of the wires, except for the large spikes experienced, which returned back to about half an ohm. Implying that we wouldn't want and it is not necessary for the Inverter to read the parameters so often.

Chapter 4: Thévenin Equivalent Model Power for Optimal Current Flow

This chapter demonstrates the power flow and optimisation for a network and its Thévenin equivalent model.

4.1 Introduction

Any network small or large can be represented by an equivalent Thévenin network. Previously it has been shown, the voltage and resistive characteristics perfectly match. What is undetermined is the way power flow is treated with regard to this representation. It has been shown the optimal injection ratios can be found using Current Compensation for any Thévenin Equivalent model. The location where the least resistive power is lost, is of interest for both the physical network model and its Thévenin Equivalent.

The physical network in Figure 14 below was used to demonstrate the differences and similarities between power flow for physical networks and its Thévenin Equivalent model. The network has a resistive load (R4) between the first two phases, which can represent a single leg of a three-phase load. R9 in Figure 14 would represent a typical single phase load.

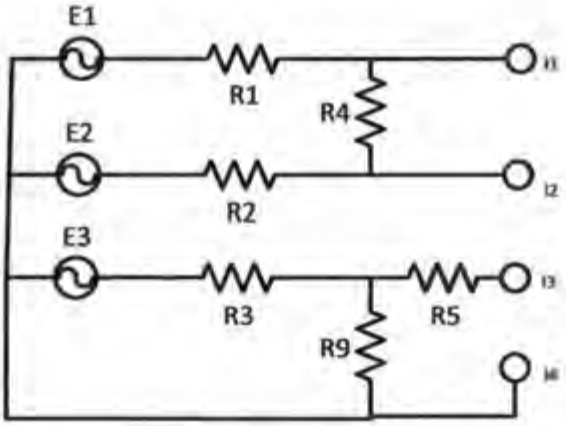

Figure 14: Physical network, with a phase-to-phase load and phase-to-neutral load

Thévenin Equivalent parameters for the first wire was calculated by looking at all the components connected between I1 and I4 (from Figure 14) and representing the network as Figure 15 below. Where V1 is the voltage source on the first wire (E1) and V2 is the voltage source on the second wire (E2). Ra is the resistance on the first wire (R1) and Rb is the series combination of R2 and R4.

The voltage difference between V1 and V2 in Figure 15 below was used with Ohm's law to find the current, shown in Eq.13 below. Using the current, the Thévenin Voltage was calculated by subtracting the voltage drop over Ra from the voltage V1, as shown below in Eq. 14.

$$I = \frac{V1 - V2}{Ra + Rb} \qquad \textbf{Eq. 13}$$

$$Vth = V1 - IRa \qquad \textbf{Eq. 14}$$

Note the signs in the above equation depend on the current direction. Therefore, the signs can be changed until both agree.

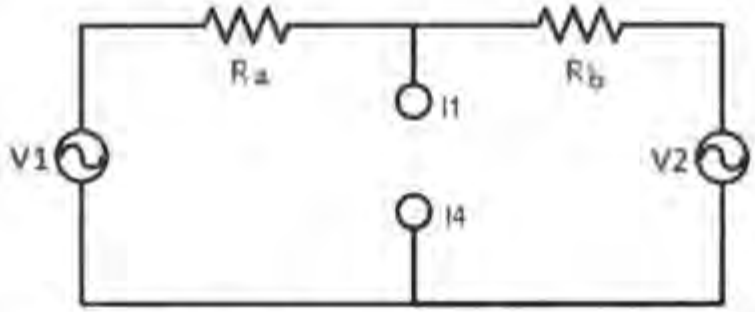

Figure 15: Schematic of Simplification to describe the Thévenin Equivalent process

The Thévenin Equivalent resistance was calculated by short circuiting all the voltage sources, then calculating the resistance between the two points (I1 and I4). This was done by applying the parallel resistance Eq. 15 shown below:

$$Rth = \frac{Ra \times Rb}{Ra + Rb} \qquad \textbf{Eq. 15}$$

The final concept required in this chapter was a sweep analysis, where the current was swept on one of the lines and the other two line currents were calculated using two constraints: the first was that all the current must add-up to zero (KCL) and the second was the conservation of power. This is shown again in the next chapter.

4.2 Investigation Design

Simplorer 7.0 was used to investigate the power for the physical network and its Thévenin Equivalent model. The physical network parameters were changed to match typical network conditions and what happens when things deviate from the general parameters.

The Thévenin network in Simplorer was programmed to calculate the Thévenin Equivalent parameters from the physical network. From this the power at the voltages sources and the power lost due to the

resistances, are calculated for both networks and compared. The points of interest (maximum power at the voltage sources and minimum losses over the lines) were zoomed into and compared in three different cases.

The three cases investigated were as follows from Figure 14:

- Line resistance (R1 = 0.2, R2 = 0.5 and R3 = 0.4 ohms), and load resistance (R4 = 100 and R5 = 200 ohms).
- Same line resistances and load resistance (R4 = 1 and R5 = 2 ohms).
- Line resistance (R1 = 0.02, R2 = 0.05 and R3 = 0.04 ohms), and load resistance (R4 = 0.5 and R5 = 0.1 ohms). Representing large loads.

The current sources (I1, I2 and I3) in Figure 14 above and the current sources for the Thévenin Equivalent models were made to inject a predetermined power of three hundred watts between all wires. A range was estimated and was swept for the currents on line one. The currents on lines two and three were therefore calculated from KCL (all the current add-up to zero) and the conservation of power.

4.3 Results and Discussion

The following results were found using Simplorer 7.0.

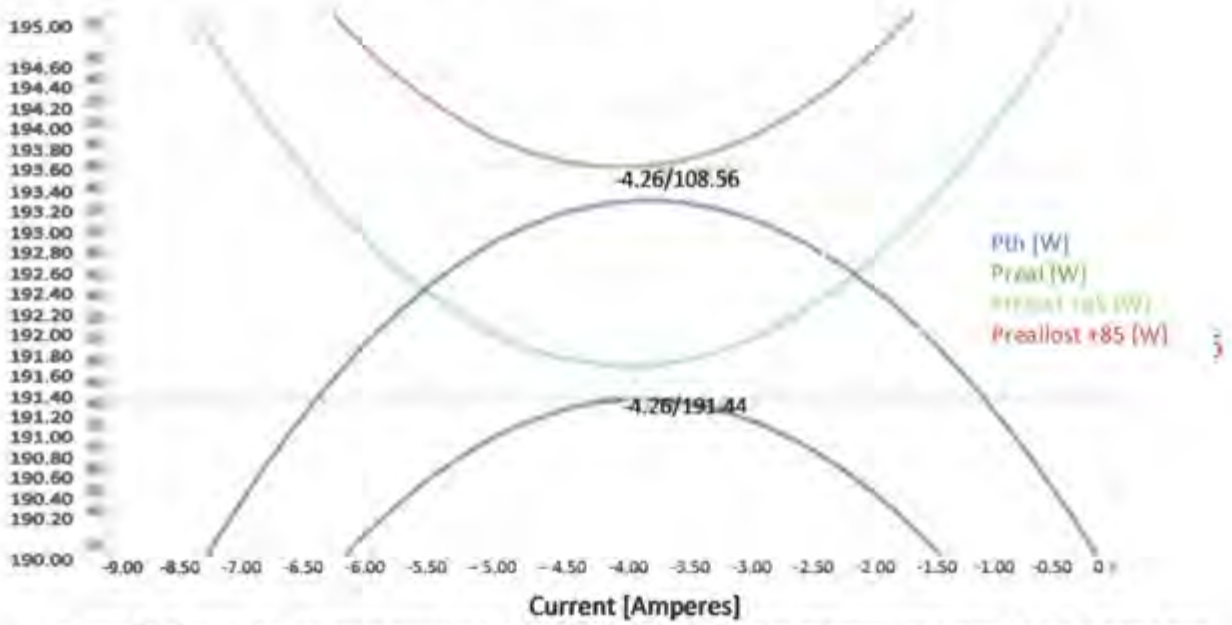

Figure 16: Power at the voltage sources and lost for both the Thévenin and physical networks, for the first case

The first case investigated in Figure 16 above shows the physical network is optimal at the same current on line one as the Thévenin Equivalent model, where the blue graph (Pth in Figure 16) is the power at the Thévenin Voltage and the green graph (Plost in Figure 16) is the power lost over the Thévenin Equivalent Resistance. The dark green graph (Preal in Figure 16) is the power reaching the voltage sources in the physical network and the red graph (Preallost in Figure 16) is the power lost over the physical resistances.

What is also important, is the current on line one found in the graph above is similar as the current found in the Excel spreadsheet in the appendix Table 14, where the currents were -4.63, 12.4 and -7.82 amperes on lines one, two and three respectively. The reason for the small deviation was the calculated Thévenin parameters (resistance and voltage) for the simulation were close but not exactly the same as the parameters used in the Current Compensation calculation. When they were made to be the same parameters, the solutions found by both methods were the same.

The graph in Figure 17 below again finds the same solution as the Current Compensation method and the simulation. The graph below used normal power theory in Microsoft Excel, using the exact same parameters as the Current Compensation table (Table 14 in the appendix). The process of how this table and graph came together is explained in the **next chapter.**

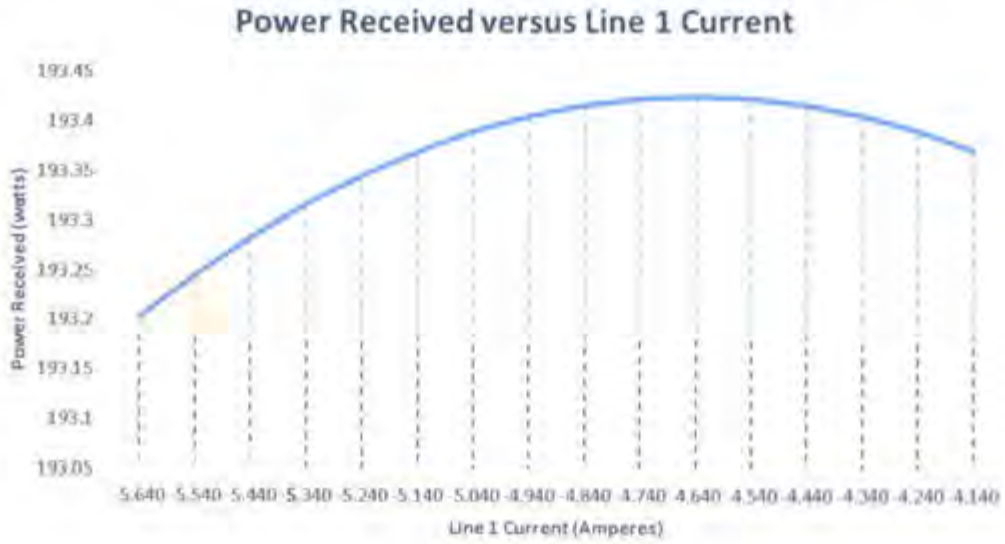

Figure 17: Current sweep analysis

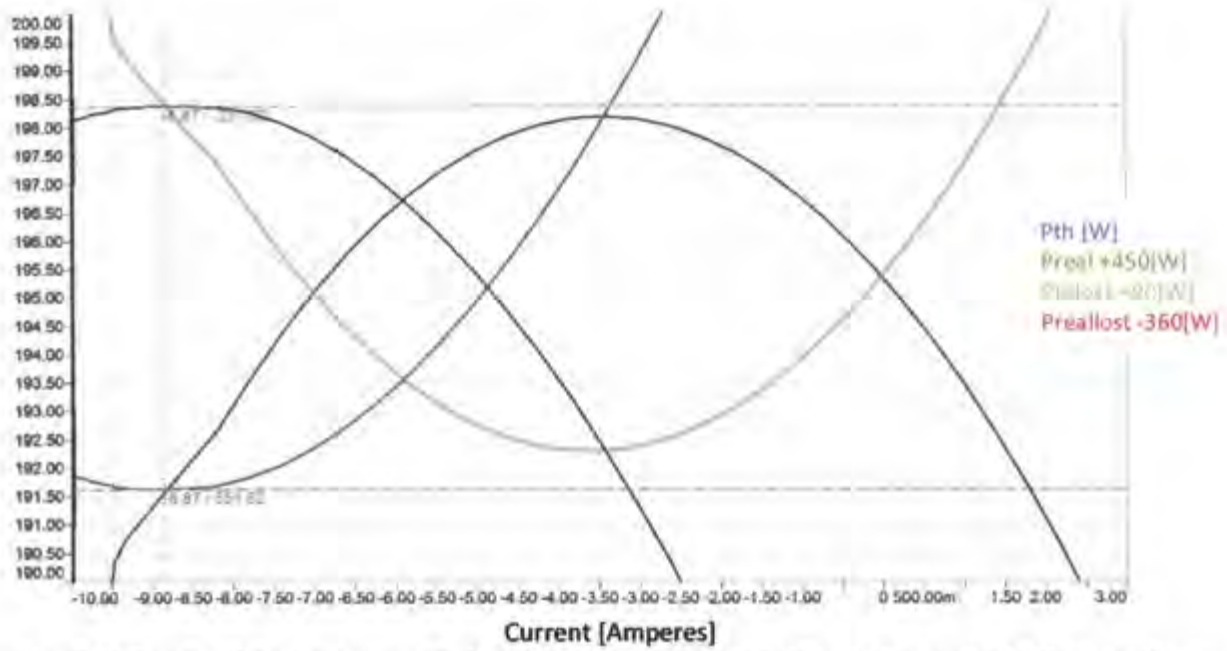

Figure 18: Power at the voltage sources and lost for both the Thévenin and physical networks, for the second case

When the second case was applied in the simulation, the points of interest were no longer aligned. A five ampere difference was found between the optimal for the Thévenin model and the physical network. The reason for this was that the size of the load resistances (R4 and R9 in Figure 14) was small relative to the line resistances (R1, R2 and R3 in Figure 14). Therefore when the Thévenin parameters were calculated, the equivalent resistance changed a lot of the actual parameters. When the load resistance is large it simplifies the current flow and most of the current goes through the line resistance anyway, as in the case above.

The total power on all the resistances in the physical network was found to be 551.62 watts which is different from the Thévenin model's lost power being only 103 watts. The physical network power before any injection is approximately equal to the difference between the power of the Thévenin model's power and the physical network power. This reinforces the fact that the network does change from our injection. All loads and nodes will see a change depending on the size of the power injection.

When applying the process, the resistances are well-represented seen from the node, however the present state and power flow of the rest of the network can never be known from the node we are at. The power flow of the system remains, only the power we are injecting is done so optimally. Hence the more power put through compensation, the greater the influence this process can have on whole networks.

In Figure 19 below, the powers for both networks, for a typical case are shown, where the line resistances are changed to around a hundredth of an ohm and the loads connected between the wires are absorbing most of the power. Here the points of interest align almost exactly, where the minimum power is lost in both the physical and Thévenin networks are found at the same magnitude of currents.

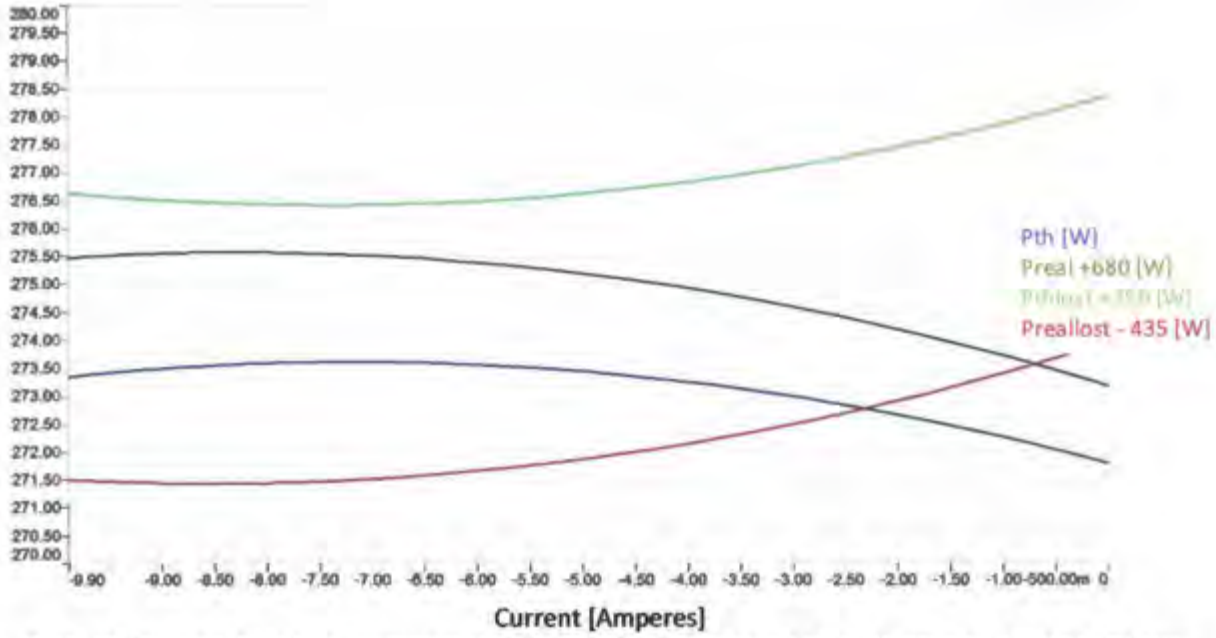

Figure 19: Power at the voltage sources and lost for both the Thévenin and physical networks, for the third case

4.4 Conclusion

In conclusion the Thévenin model perfectly represents the resistance and voltage dynamics of the network, seen from the node. However it doesn't have a model to see the power flow of the network. Only the power injected from the node is optimised and not the power flow of the whole system.

For typical grid parameters, the optimal power solution found for the injection in both the Thévenin model and its physical network are similar. Implying the same ratios make the Thévenin model optimal as well as the physical network.

More research needs to be done with regard to the impact this type of injection will have on the loads connected to the grid.

Chapter 5: Current Compensation Sweep Analysis

A chapter to prove the Current Compensation finds the optimal solution.

5.1 Introduction

In the previous chapter the correlation between a physical network and the Thévenin Equivalent model was shown. This chapter shows more cases of the Current Compensation method, finding the solution for a few different cases and comparing the solution to power theory. The power theory scans all the different possible permutations of current on each wire and computes the lost power.

If a specified amount of power at a node needs to be injected/extracted onto a network, the current ratios for all the wires will be according to their respective resistances and voltages. Assuming the Thévenin Equivalent parameters are computed in parallel, the Current Compensation method can be executed for an inverter, as all the parameters are known.

5.2 Investigation Design

The Current Compensation method was solved for the network below in Figure 20 and compared with the optimal currents found from the sweep for the same network. The Current Compensation method is shown in the literature above and Microsoft Excel was used to apply Eq.2 – Eq.7 to find the solution.

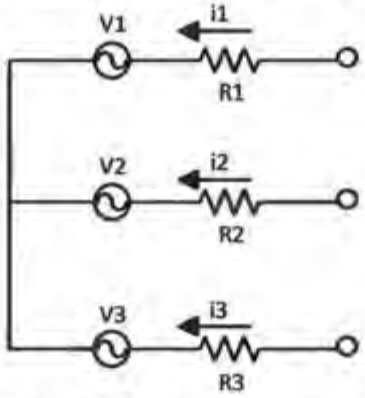

Figure 20: Power network for current compensation sweep

Also in Microsoft Excel a range of currents were swept, where the other two currents were calculated from KCL in Eq.16 and using power theory in Eq.17 below:

$$i_1 + i_2 + i_3 = 0 \qquad \textbf{Eq. 16}$$

$$P_{injected} = v_1 i_1 + v_2 i_2 + v_3 i_3 \qquad \textbf{Eq. 17}$$

Rearranging Eq. 16 and substituting into Eq.17, resulting in Eq.18 below:

$$i_2 = \frac{(v_3 - v_1) i_1 + P_{injected}}{(v_2 - v_3)} \qquad \textbf{Eq. 18}$$

From this the other two currents were calculated for each current on line one swept.

The power lost for every current on each line was computed in Excel and graphed. From the graph the currents on each line where the minimum power is lost is the power of interest. This was then compared with the current found from the Current Compensation method.

The following three cases were investigated:

1. 3-wire network, V1 = 0volts, V2 = 282volts, V3=-281volts, R1 = 0.2ohms, R2 =0.5ohms, R3= 0.4ohms
2. 3-wire network, V1 = 56volts, V2 = 282volts, V3=-281volts, R1 = 0.2ohms, R2 =0.5ohms, R3= 0.4ohms
3. 4-wire network, V1 = 56volts, V2 = 282volts, V3=-281volts, V4=12volts, R1 = 0.2ohms, R2 =0.5ohms, R3= 0.4ohms, R4=0.001ohms

5.3 Results

The following results were found from the method described above.

5.3.1 Case 1 (3-wire, Instantaneous AC voltages with a small amplitude imbalance and random line resistances):

Figure 21: Power received for current sweep on line 1 for a small amplitude imbalance and random resistances

For the case shown in the previous chapter where the parameters were all chosen at random, the three currents found by the Current Compensation method were -4.64, 12.47 and -7.83 amperes respectively for lines 1, 2 and 3. This case was used to show the correlation between the simulation of a physical network and its Thévenin Equivalent.

These three currents all add up to zero and therefore obey KCL and when transmitted on this network, 193.43 watts reaches the supply and the rest is lost due to the resistance. Shown in other permutation analyses, more power reaches the supply (less power lost), however KCL is not obeyed. Also shown in the appendix is a chapter where a software package doesn't obey KCL or take it into account.

Each value of current on a wire has different respective computable current values for the other two wires. These other two currents are calculated for a wide spread of values on each wire and find the same combination as the Current Compensation shown in the tables.

The first case in this chapter is an AC situation with a small amplitude imbalance and the voltage parameters are much larger, at around 280 volts. The voltage on line is a sinusoidal waveform at a time instant of (0 degrees) and the other two wires are the instant in time of 120 and 240 degrees away respectively. In this case the voltage on line one is small and therefore as expected, little current was being transmitted over it being only 0.03 amperes.

The second case is a situation where there is a phase imbalance of 10 degrees between the wires, which therefore increases the voltage on line one. The current solution found on line one becomes larger by more than double.

Again for both the first and second case, the sweeps found the exact same solution as the Current Compensation method. For the second case all three currents were swept (shown in Figure 22, Figure 23 and Figure 24 below) so as to prove the method's validity.

5.3.2 *Case 2 (3-wire AC voltages with amplitude and phase imbalance and random resistive parameters):*

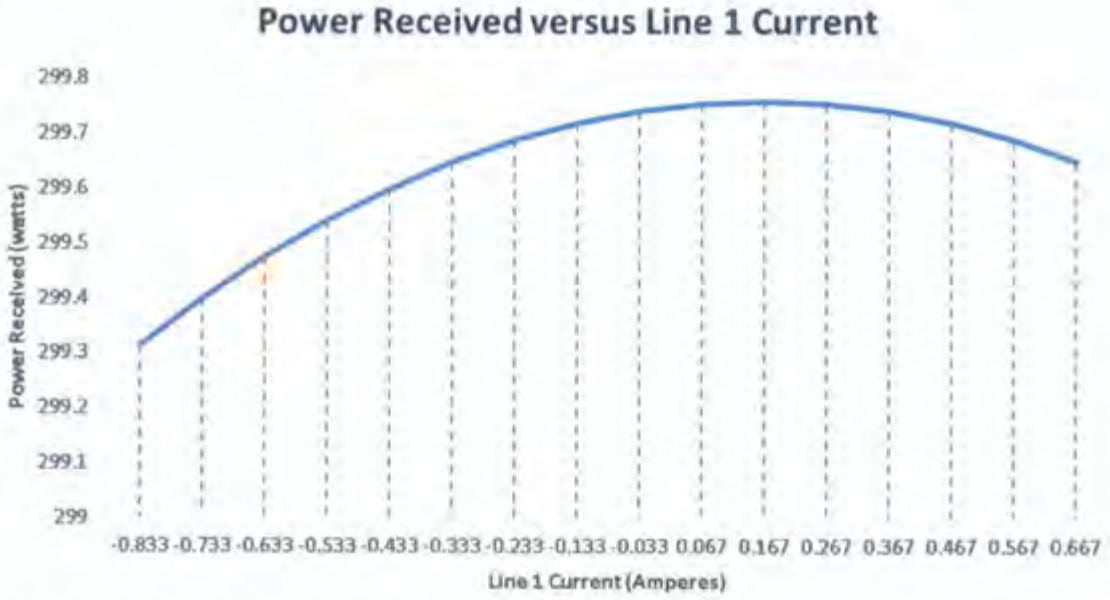

Figure 22: Power received for current sweep on line 1 for a small amplitude and phase imbalance and random line resistances

Figure 23: Power received for current sweep on line 2 for a small amplitude and phase imbalance and random line resistances

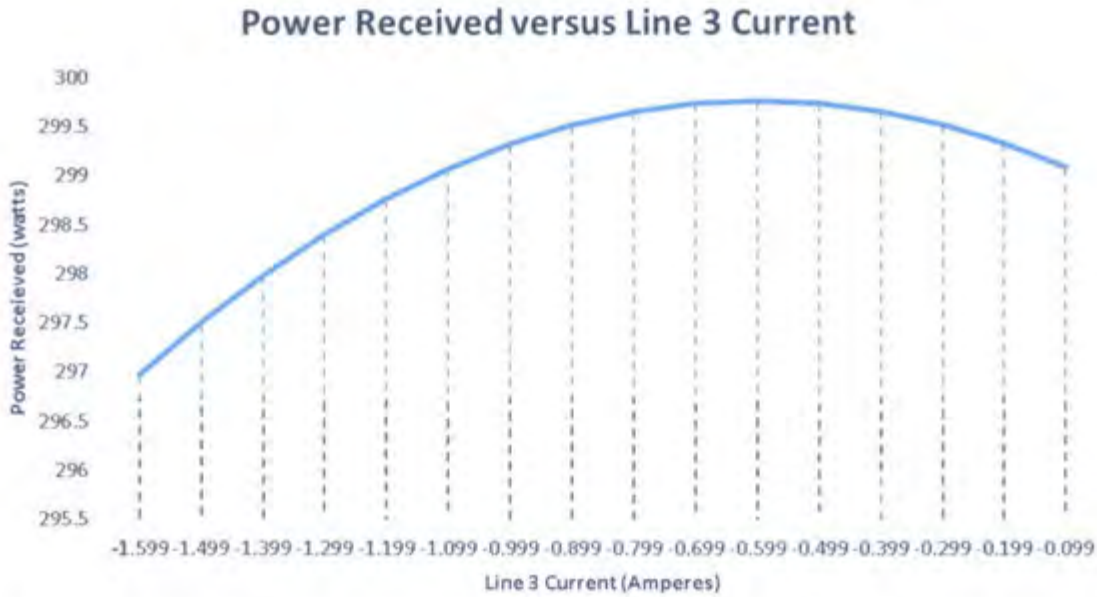

Figure 24: Power received for current sweep on line 3 for a small amplitude and phase imbalance and random line resistances

5.3.3 *Case 3 (4-wire AC voltages with amplitude and phase imbalance and random resistive parameters):*

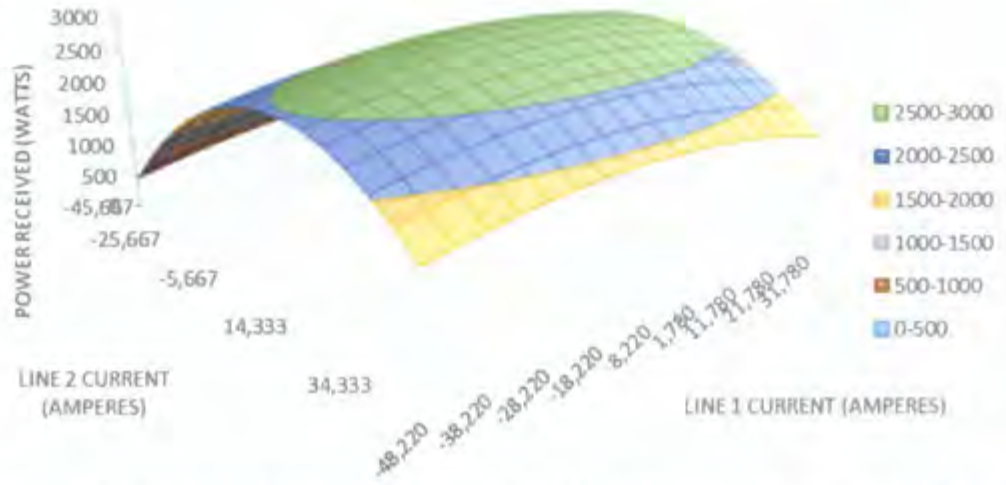

Figure 25: Power received for "zoomed in" current sweep on line 1 and 2 for a 4-wire system and for a small amplitude and phase imbalance and random line resistances

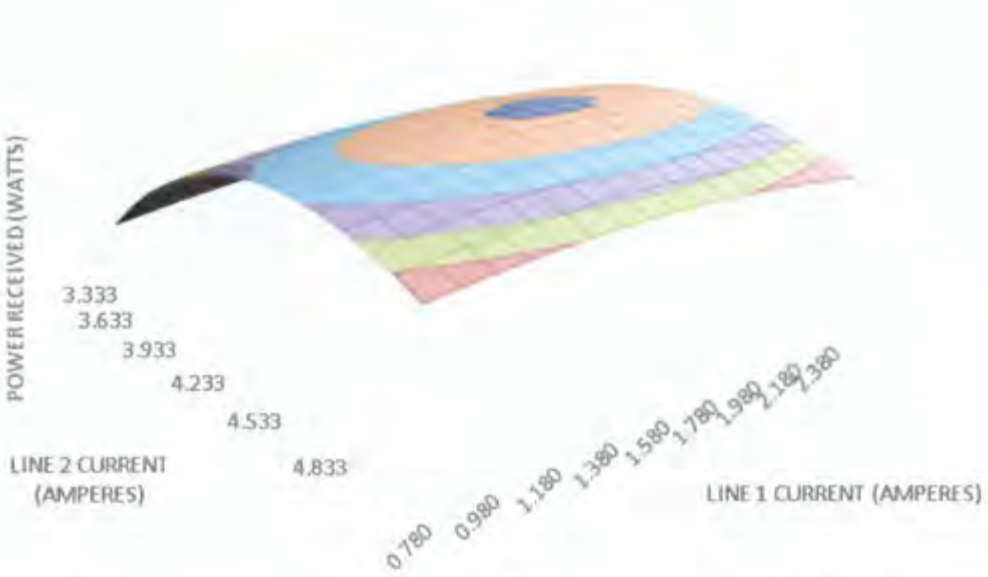

Figure 26: Power received for current sweep on line 1 and 2 for a 4-wire system and for a small amplitude and phase imbalance and random line resistances

Finally, the fourth case, where a neutral wire is included with a small dc voltage of 12 volts and a tiny resistance (*note: the line resistance cannot be zero, else applying the formula for the correct voltage reference we have to divide by zero. Zero resistance is equivalent to removing the wire*). As expected the solution is found where the largest currents are transmitted over lines two and three and the voltages are more than

five times larger than line one with the resistance only being about two times larger. Keep in mind that this method applied the weighted voltages which is a function of both voltage magnitude and resistance.

A 3-dimension graph is drawn up shown in Figure 26 above via the sweep of all the possible currents, where initially the "area" where the maximum current vector exists is found. After which this area is zoomed into and a second 3-dimension graph is drawn shown in Figure 25 above. This method found the same combination of currents on each of the wires for maximum power transfer and minimum resistive power loses as the solution found by the current compensation method shown in the table above. The found currents were 1.77, 4.33, -5.83 and -0.23 on lines one, two, three and four respectively.

5.4 Conclusion

A number of cases were analysed with both the Current Compensation method and the sweep method and both found the exact same solutions. From this we can conclude the method described by Michel Malengret finds the optimal current vector for any number of wires and any type of imbalance as expected for a Thévenin Equivalent model of a network.

Since from the previous chapter, it was concluded for typical network situations the Thévenin Equivalent point of interest matched with the physical network. It can be said this Current Compensation method applied can find a solution close to the optimal solution for the physical network.

Chapter 6: Weighted Voltage Vector Normal

This chapter demonstrates and explains the theory behind the normal of the *weighted* voltage vector.

6.1 Introduction

The concept of the weighted voltages was first described by Malengret and is mentioned in the literature above. Where the conductivity for power on a line is completely described by its weighted voltage. It does this by representing the voltage components for each line with a weighting of its line resistance. In terms of optimising current flow and reducing power lost due to transmission, less current (power) would be put onto the wires with low weighted voltage components and more current on the wires with high weighted voltage components.

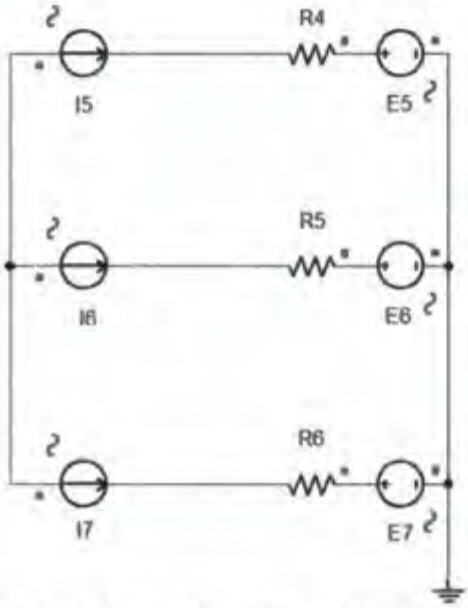

Figure 27: Schematic of a four-wire network with current compensation

The schematic above drawn in Simplorer was used to demonstrate how a node would inject/extract power into a network according to the weighted characteristic of the wires. The three current sources (I5-I7) in the schematic make up the current injection of the device on each wire.

The process of obtaining the line resistances in practical terms are assumed to be done in parallel. Implying the current sources have knowledge of the load resistances and voltages and are able to apply the MGWCC to find the optimal currents to be injected.

6.2 Investigation Design

Simplorer 7.0 was used to simulate the above network. The equation blocks in Simplorer were used to compute the weighted voltages, normal of the weighted voltage vector, k and the compensation currents on each of the wires. In the extern view of the 2d graphs the instantaneous currents and norm were displayed.

These results were looked at for a few different cases of line resistances on each of the wires and analysed:

- A single imbalance is the resistance on line two changing to eight ohms.
- A double imbalance indicates line two changing to eight ohms and line three changes to four ohms.

6.3 Results and Discussion

The following results were found using Simplorer 7.0 to simulate the method described above.

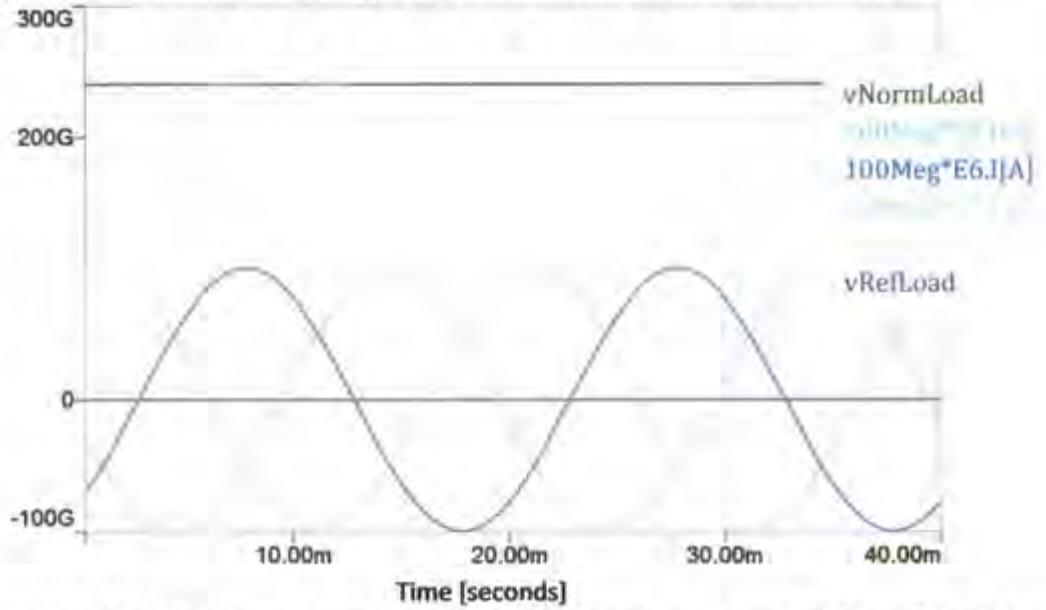

Figure 28: Graph of the load currents, voltage vector normal and reference for a network with equal line resistances

In Figure 28 above, all the resistances on the lines are the same and as expected since the voltages are balanced sinusoidal waveforms, the norm (green graph) in the figure above is constant. This is expected because three sinusoidal waveforms, phase shifted by a third of a period added together will make up a perfect constant being three times the rms of the waveforms. Using the MGWCC, the method will find, all equal average currents over a cycle, on each of the wires as expected for a system with equal characteristics as shown above in the dark blue, light blue and grey graphs. The purple graph is the reference error, this is zero as there is no error, correlating with Malengret's theory.

As an imbalance in the system occurs, the normal of the weighted voltages became an oscillating sinusoidal waveform, as shown in Figure 29 and Figure 30 below. The reason for this is because the weighted function of one or more of the waveforms has changed and is no longer balanced. Therefore at certain times when the potential of the heavily resistive wire is high, the system won't be as good relative to when the lightly resistive wire has high potential. Since the norm is made up, of the weighted voltages (takes into account the resistances of each respective wires), the norm therefore describes the ease of flow for current, in that respective wire. The blue graph in the figure below shows the current found for line two, where the resistance is eight times larger than the others. As expected the peak of the current for this line is smaller than the other lines as the power lost on this line is expected to be larger relative to the other wires.

A forth wire is made available and provides another path for current flow, where the MGWCC method finds the current to be injected on each wire, for optimal current flow, as shown in Figure 29 and Figure 30. Still looking at these graphs the currents found by this method are no longer sinusoidal. The oscillatory normal

of the voltage vector of the system with the voltages, result in a current solution, containing a second harmonic. As expected the graph below, show the found current waveforms from MGWCC to contain second harmonics, where the method perfectly allocates the power at every point depending on the voltage and resistance of the respective wire.

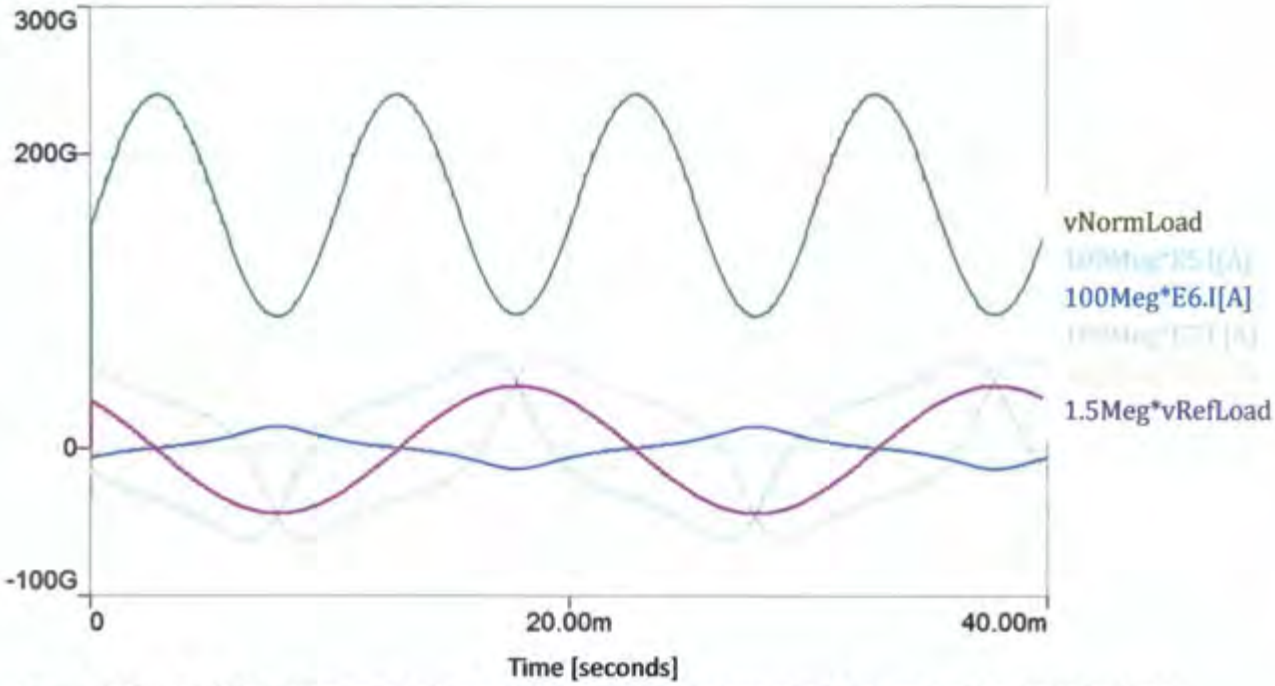

Figure 29: Graph of the load currents, voltage vector normal and reference for a network with a single load line resistance imbalance

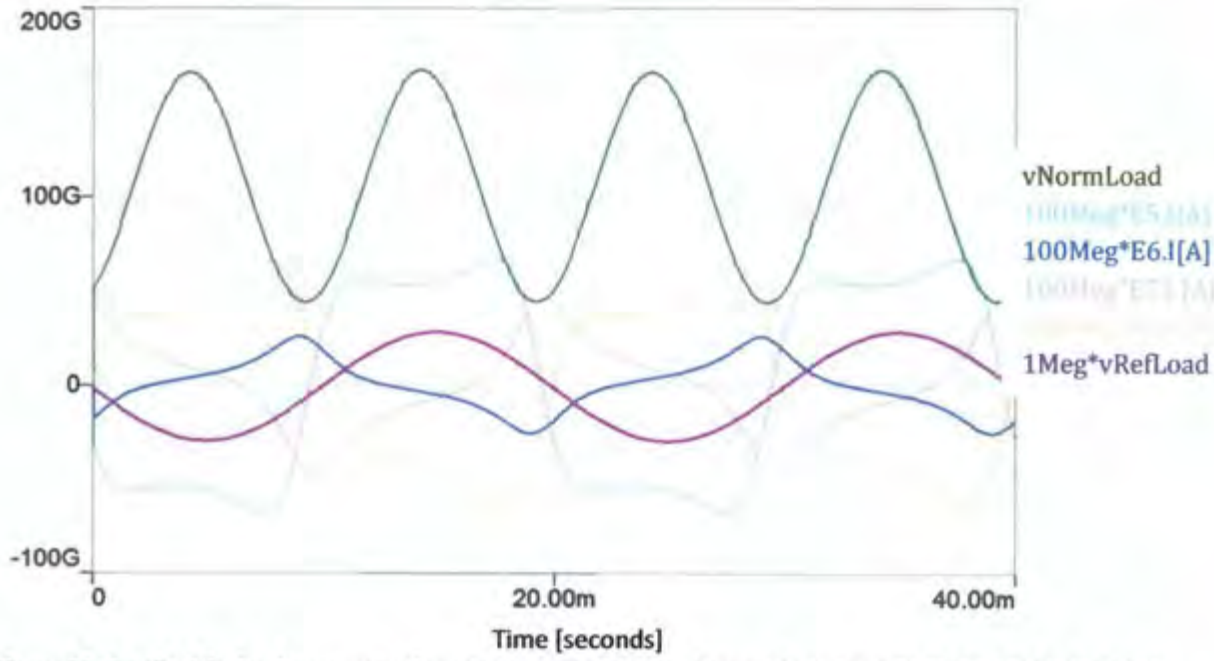

Figure 30: Graph of the load currents, voltage vector normal and reference for a network with a double load line resistance imbalance

In Figure 31 and Figure 32 below, the power lost is shown with the normal of the system and the voltage on line two.

In the first case, the normal of the system is at its highest at the same points, the power lost due to the whole system is at its minimum. Similarly the converse is true, at the same points when the norm is at its lowest, the power loss of the whole system is at its maximum. This shows the normal describes the system state.

For both these graphs the instantaneous voltage is of the line with the resistance imbalance. Showing when the voltage of the line with the heavy resistance is peaking, the power lost due to the whole system is at its highest. Since the voltages of the wires were left balanced, when one wires voltage, is peaking the other two wires are *not*.

In the second case, with the double imbalance, the norm of the system moves *out-of-phase* with the voltage of line two. This is expected as the state of the system (normal of the weighted voltage vector) moves towards line three. The normal of the system is lowest in-between, the peaks of lines two and three.

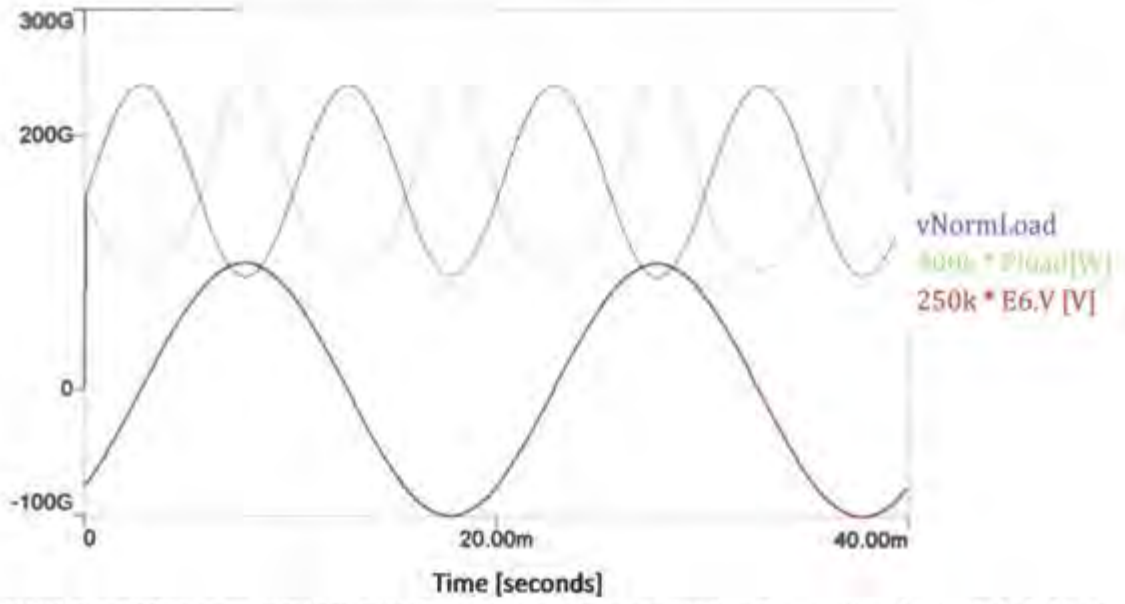

Figure 31: Voltage vector norm, total power lost and source voltage on line 2, with a source side, single imbalance

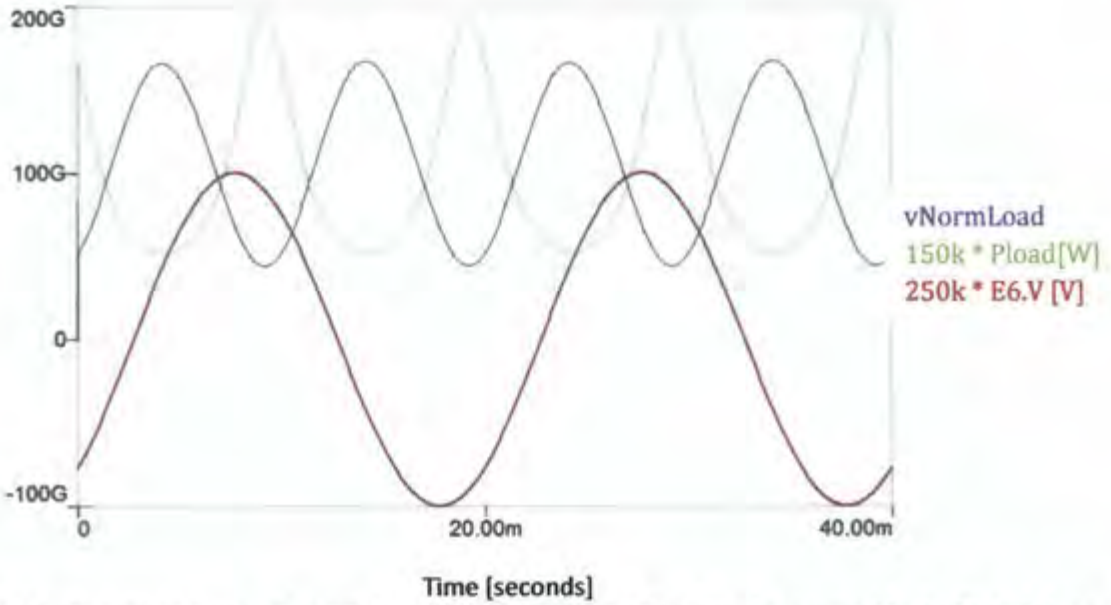

Figure 32: Voltage vector norm, total power lost and source voltage on line 2, with a source side, double imbalance

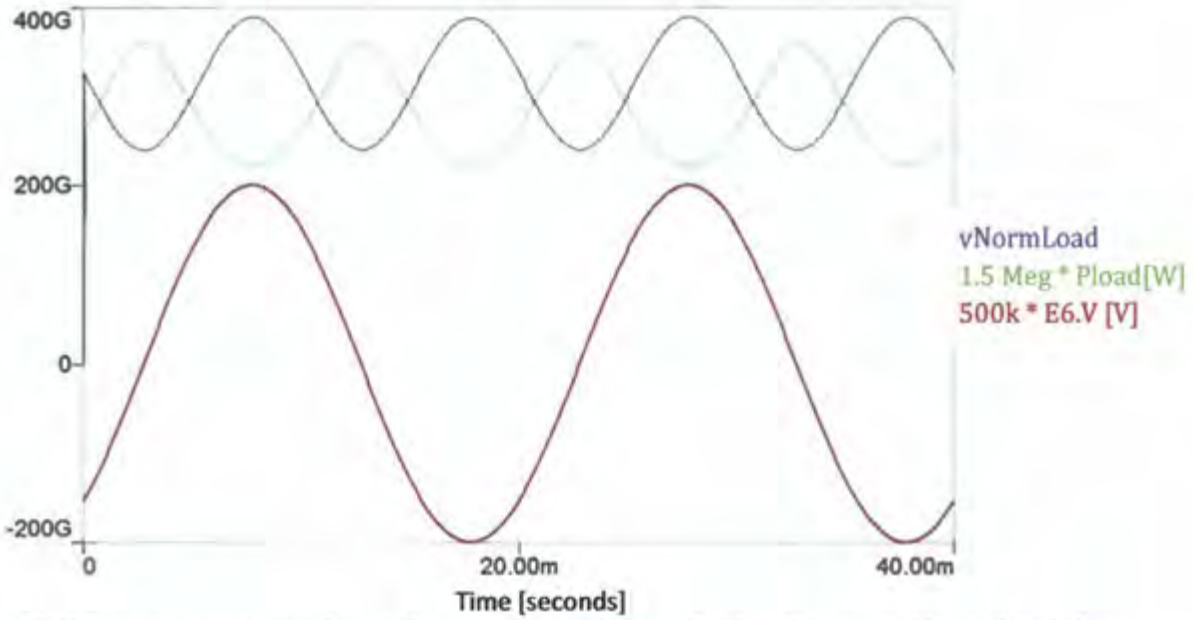

Figure 33: Voltage vector norm, total power lost and source voltage on line 2, with a source side, single imbalance (0.5ohms)

6.4 Conclusion

In conclusion, the weighted voltages and the normal of the weighted voltage vector, perfectly describes the systems state, by applying the voltage and resistive parameters for all the lines. In the instantaneous domain when a small imbalance is present, the found currents from MGWCC, are irregular and will contain harmonics, making it high undesirable.

Chapter 7: Instantaneous and Average Power over a Cycle

This chapter analyses the Malengret Gaunt Weighted Current Compensation method applied both instantaneously and averaged over a cycle.

7.1 Introduction

Up until now the Current Compensation method has been looked at in the instantaneous domain, finding the normal of the voltage vector at every instant of time and applying it to find the currents. It has been shown that at every point in time it finds the absolute optimal current flow solution in order to minimise resistive losses over the wires.

The literature states that using the average of the weighted voltage norm over a cycle, instead of the instantaneous norm, improves the system. The reduction of power loss comes from the control of total current output which is dependent on the system-state over the time cycle. Instances of higher weighted voltages (when the weighted norm is higher) result in more power being transmitted (finds higher total currents) and over periods of low voltages and higher resistance (when the weighted norm is lower), the compensator output finds smaller total currents. The average of power over the whole time cycle is unchanged but what must be noted is that small power storage is required for this in the form of capacitors or batteries. A method has been described to calculate the power at the Thévenin's side if the normal of the voltage vector and the injected power are both known. It needs to be seen whether this formula still holds for calculating the power on this side if the average of the voltage normal is applied.

To prove the validity of the MGWCC method, where in the average domain, it finds the perfect amount of total current to be transmitted at every time instant, a cycle is divided into two periods and every fraction of power on both sections is checked and the power at the source is found for all the possible fractions. The maximum is compared with the solution found from averaging the norm over the cycle.

In the literature, the power triangle concept was said to hold only when the components were applied in the weighted format. To prove this, orthogonality must be shown, where the square of the compensation currents plus the square of the change must equal the square of the previous currents before compensation. It must be shown that when the line resistances are *not* equal, orthogonality only applies when the weighted components are used.

7.2 Investigation Design

Initially two DC time instants were used, the voltages and/or resistances were made different and randomly chosen. Using Microsoft Excel the MGWCC method was applied, for every fraction of power for both time sections, after which the total power at the source was calculated and graphed, enabling a maximum ratio location to be found. The maximum found from the sweep was then compared with the power received by the source using the method in question (MGWCC).

A sinusoidal case was next demonstrated where three voltages signals were looked at every 30 degrees (equivalent to six, DC time samples). The norms were calculated for each 30 degree signal with the power

available being constant and compared with the power received when the average of the norm was used. A table was drawn up for the power received for each case including a normal case where the currents followed the voltages. The results were tabulated, showing the power at the source when each instantaneous norm was used and when the average of the norm of the cycle was used. The power injected by the node was also graphed for both the instantaneous and the average case.

Finally, Simplorer 7.0 was used to prove orthogonality. The previous chapter's network was used to find the active filter, supply and load currents and these currents were then squared and checked in both weighted and non-weighted domains.

7.3 Results and Discussion

Using Microsoft Excel, the following results were formulated from the method described above.

Table 5: Ratio of power found by applying the average

	Instantaneous		Average	
PowerIn	30	30	20.76923	9.230769
		ratio	**1.384615**	

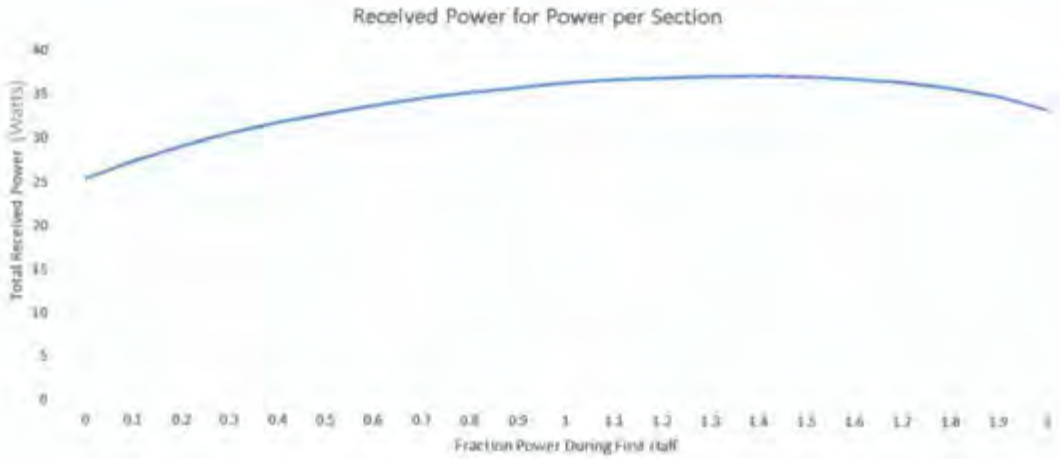

Figure 34: Graph sweeping the fraction of power for the first section

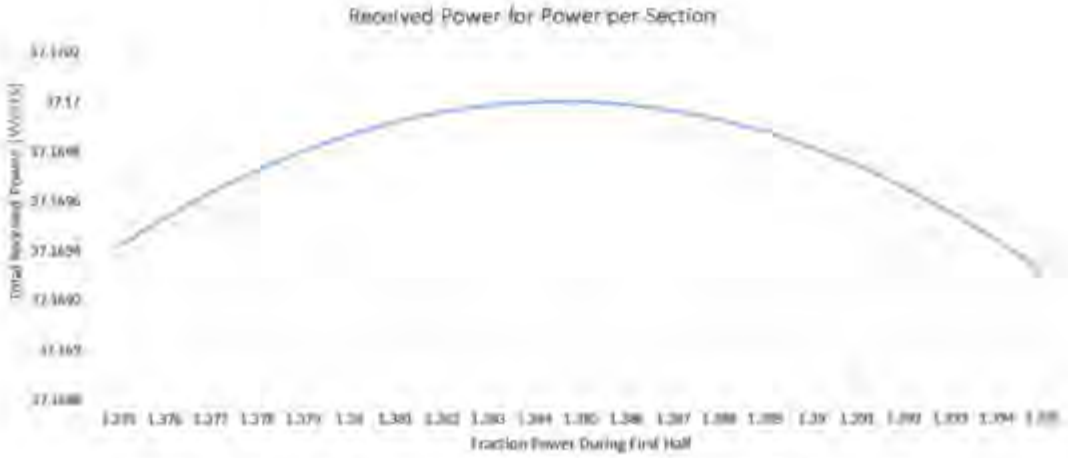

Figure 35: Zoomed-graph sweeping the fraction of power for the first section

In the first graph in Figure 34 above, which is sweeping over a large range, finds the maximum at around a ratio of 1.3. The next graph, in Figure 35 above, is a zoomed in sweep of the area found in the previous graph. The ratio found from this sweep is 1.384. This correlates well with the result found from averaging the normal voltage vector in Table 5 above. This proves that applying the average of the norm method with Current Compensation spreads the power over each zone perfectly and reduces the power lost by the largest amount.

In Figure 36, the power sent at each time instant follows the voltage norm perfectly. Also the blue line in the graph, which indicates the power sent for the average normal, is constantly changing above and below the red line (being the power sent for the instant case). However, the average over the whole cycle is still the 24 kilowatts available. When the norm is high, it takes the opportunity to send more power as the general (over the system) weighted voltage is higher and conversely when the norm is lower, it sends less power.

The weighted voltage normal takes into account the resistance of the wires and the magnitude of the combined voltages. If all the resistances are equal and the voltages are perfectly 120 electrical degrees apart, the combined normal will be greatest when the phase with the greatest magnitude is at its maximum. In the same way a wire with a quarter of the resistance it effectively has, doubles the voltage magnitude of the other wires. Thus when this wire's sinusoidal wave peaks, the overall normal describing the system will be at the maximum.

By using the average method over the whole time period, it was found 22654 watts arrived at the source, as indicated in Table 6. Again in Table 6 below, only 22600 watts was received when using the instantaneous norm for finding the currents. Using the typical method where the currents are proportional to the voltages, the power sent is greater than both other cases and less power is received than the average. The power lost in this case is a lot more than both the other two ways of applying the Current Compensation method.

Table 6: Power received for the instantaneous, average and normal methods.

Power	Instantaneou	Average	Normal
Injected	24000	24000	24133.74
Receive	22600.88263	22654.369	22654.37
Lost	1399.11737	1345.631	1485.631

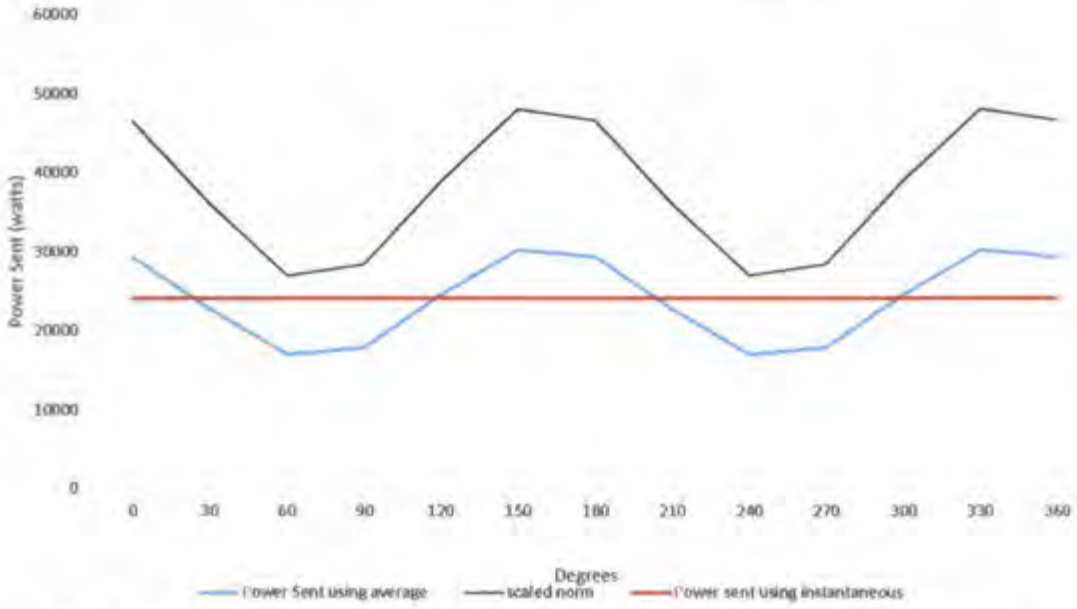

Figure 36: Power being sent when using the average norm and using the instantaneous norm

Figure 37: Non-weighted and weighted components of currents for equal resistance

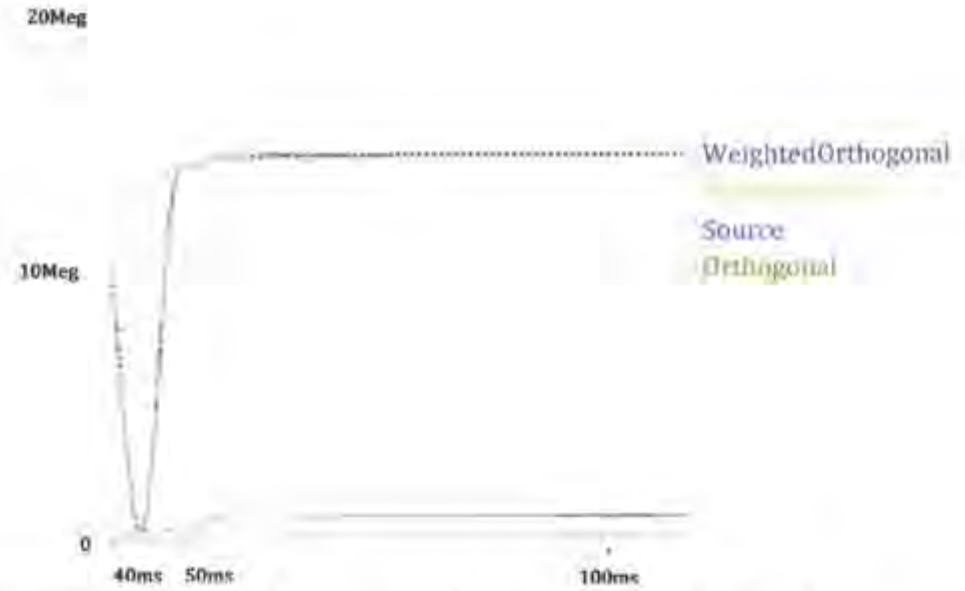

Figure 38: Non-weighted and weighted components of currents for unequal resistance

To prove that after compensation only the current component giving energy to the load is present, the square of the currents before compensation need to be equal to the sum of the compensation currents and the delta currents. As seen in the graph on the left all the components are equal, this is a case of when all the line resistances are equal. When the line resistances were changed, as in the case on the right, the unweighted components (green and light blue) don't match and orthogonally doesn't exist. On the other hand, the weighted components (orange and purple) are still equal and orthogonal even after a resistance change. This proves the system deals with the resistance components of the wires perfectly.

7.4 Conclusion

In conclusion, when storage is available, the average of the normal can be found over a period and this average can be used to find the currents, where the currents found by the average of the normal improve the system further.

It is difficult to comprehend that by applying the Current Compensation we have found the absolute optimal and then to say that applying it over an average is improving the system further. However, this statement is completely true if we are looking at a single instant in time. The instantaneous norm finds the absolute solution. Only when we are looking at a range of instants of time can we find periods where power flows with less losses. Therefore we transmit less power during the bad times and more power during the good times. This is demonstrated in the graph above where the power being transmitted follows the norm, thus describing the system perfectly.

Chapter 8: Active Filter

This chapter describes the active filter and the various ways it can be implemented.

8.1 Introduction

This is a device used in power networks to optimise power transmission. This is achieved by removing the non-active current components in each of the wires at the source. The process to obtain the Thévenin parameters (resistances, inductances, voltages and powers; at each location) is explained in previous chapters and is assumed to be understood and done in parallel with the MGWCC process by the device.

This device can be used in two different topologies: a) series and b) shunt active filters where each has its requirements, disadvantages and advantages.

In all cases we only consider a 3-phase, 3-wire transmission network. Since the Current Compensation method can be applied to any m-wire network (if the parameters are known), it can be assumed that if the process works for 3-wire cases it would work for m-wire cases in the same way (where m is any number greater than 2).

Initially, low power parameters are used to demonstrate each method as it is easier to see and understand the process. Later, typical transmission network parameters are used to show the magnitude of the improvement on a typical power network.

8.2 Series (Six-wire for3-phase), Active Filter

As mentioned already, this device interrupts the transmission lines and has two independent sides to it, as shown in the schematic below, which would typically be used in a mid-point situation. This doesn't require the assumption of treating any side of the network, as constant current sources and negligible line resistances. The process to obtain the Thévenin parameters (resistances, inductances, voltages and powers at each location) are assumed to be understood and done in parallel with the Current Compensation process.

It is hypothesised that this topology of active filter would be required to be larger as all the power has to be transmitted through it. The advantage is that it can be applied in the middle of any transmission network.

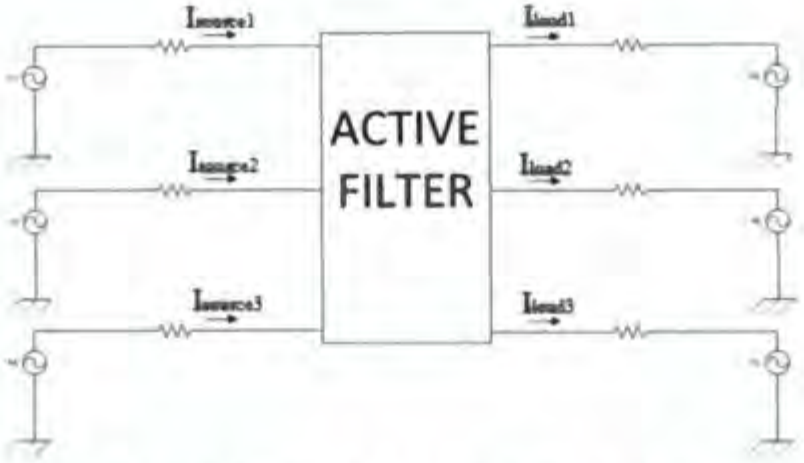

Figure 39: Schematic for the 6-wire, storage active filter

An example is shown below to demonstrate how it works. The parameters for each section of the network is displayed and found in a Microsoft Excel spreadsheet.

Table 7 below, the typical network parameters are shown, which are used throughout to show the differences and similarities between each method. The voltages are 100V, 20V, and -30V on lines 1, 2 and 3 respectively, these being deliberately chosen to have a significant voltage reference away from zero. The currents in the initial (without compensation) network, were well chosen with what would be typically on a network with these voltages at this time instant. From these, all the other parameters were calculated for the network in the table. The power at the load is 231 watts and the power being supplied by the source is 310 watts. The remaining 79 watts is the lost power, which is what we are reducing. In the series active filter case, the other two powers remain unchanged and all the saved power is gained at the device. However, it can be made to reduce the power required by the source so as to supply the same load. Also, in the same way, it can be made to supply the same amount of power and therefore increase the power received at the load.

Table 7: Initial system parameters for all three active filter demonstrations

	Source			Load				
	Vth	Rth	Power	Vth	Rth	Power	Current	Vin
Line1	100	2	200	94	1	188	2	96
Line2	20	1	20	16	3	16	1	19
Line3	-30	6	90	-9	1	27	-3	-12
Total			310			231	0	Plost
Vref	39			38,71428571				79

Knowing these parameters on both sides of the active filter, the Current Compensation method can be applied for both sides independently. In the appendix Table 18 below, the found currents for both sides are shown. The currents for the source side being 3.13A, -1.95A and -1.18A and the load side being 2.31A, 0.32, -2.00A for lines 1, 2 and 3 respectively. The lines having different voltages on either side reinforce the fact that the lines are not connected.

What must be noted here is that the power being supplied by the source is unchanged, remaining at 310 watts and the power reaching the load is also unchanged at 231 watts. The only power change is the power lost, which is now only 41.6 watts. Since the conservation of energy has to be maintained, we have to have the power coming up somewhere.

Using the voltages and currents at the compensator, Table 9 below shows the calculated power at the active filter, which as expected, is not zero but 37.43 watts. These two powers (active filter power and new lost power) add up to the initial 79 watts. The active filter power can now be used for a number of things like being put back into the network or being stored in batteries. This method has changed the amount of power being wasted in the form of heat on the transmission lines to 52.62% of what was being initially lost.

Table 8: Compensator parameters for a storage active filter

	Compensator			
	i	Power	Plost	Percent
Line1	-0,81615593	70,48413684	25,05044055	
Line2	1,635862579	-38,1072869	4,119223635	
Line3	-0,81970665	5,056250091	12,3972358	
Total	0	37,43310001	**41,5669**	**52,62%**

This implementation of the active filter shows a great reduction in power being wasted but because all the power goes through the inverter, the inverter has to be rated at high power for high power transmission lines. In this example it is not a problem, but when we are looking at transmission networks which typically transmit mega/gigawatts of power, this is a significant problem. Another issue is how to store the power saved as this requires batteries which are expensive and bulky. This implementation does enable a mid-point active filter to be applied.

8.3 Shunt Constant Load Power, Active Filter

Another type of proposed active filter is a "box" which is separate from the transmission lines, as shown in Figure 40. The transmission lines run as they were, only now the active filter injects currents (ic1, ic2 and ic3) to change (by Kirchhoff's Current Law) the source currents (is1, is2 and is3) and the (il1, il2 and il3) on each of the wires and therefore reducing the power lost.

The control behind this filter, looks to change the currents on the lines by changing the compensator currents (ic1, ic2 and ic3 in Figure 40). The desired line currents are found by the current compensation method.

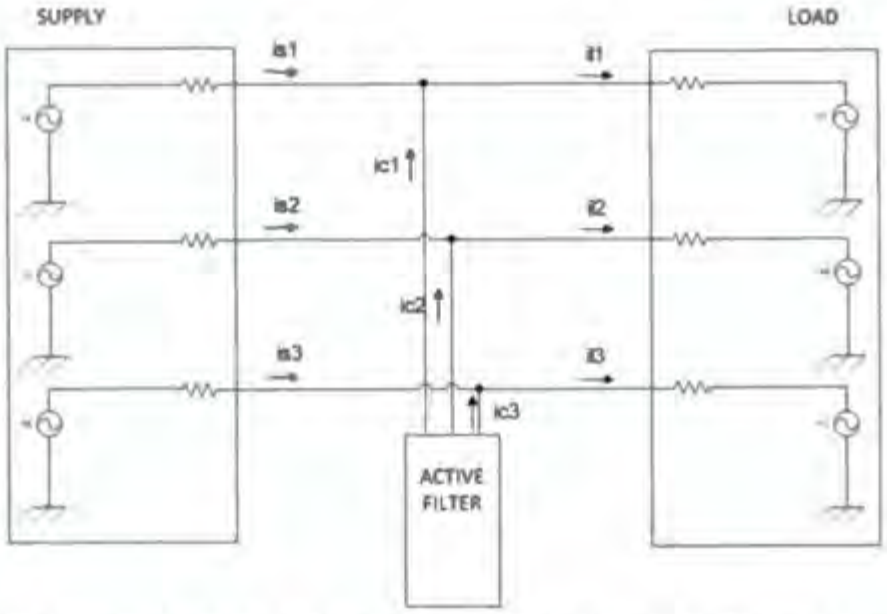

Figure 40: Schematic of how an active filter device will be typically applied in a transmission network

The same initial parameters were used as the case shown in Table 7, where 310 watts is being supplied and 231 watts is being taken by the load(s). However, by doing the active filter this way, the power at the device adds up to zero at all times. Ignoring the case of average power over a cycle to further save power, where a small storage is required in the form of capacitors (different to the storage required by the pre-mentioned active filter method). The power received at the load remains unchanged but the supply power changes to keep the conservation of energy.

In the appendix Table 19, the new power required to be supplied for the load with the rearranged currents is now 262.76 watts, which is significantly less than the 310 watts initially being supplied. Looking at the table below, we can see the currents at each of the lines in the active filter are 0.4A, -1.68A and 1.27A on lines 1, 2 and 3 respectively. This implies less current is required by the active filter, since it is only the difference between the currents on each side. The power lost in the whole network is only 31.75 watts (40.20%). This is a great result but not as great as the series case, but this is because less power is actually being transmitted. As expected, the change in power lost decreases the source power by the same amount and no power is generated at the device.

Table 9: Compensator parameters and results for the constant load power, active filter

	Compensator						
	i	**Power**	**Save**	**Percent**	**Vaf**	**Power**	**Plost**
Line1	0.407481394	39.24853892	-77.5707135		96.3198308	223.4457109	59.5066176
Line2	-1.67882334	-25.2610722	46.05539645		15.0468912	-4.78044138	-20.97215
Line3	1.271341949	-13.9874667	78.75551126		-11.0021279	22.02766697	-6.7746622
Total	0	-1.4211E-14	**47.240194**	**40.20%**	36.8238712	240.6929365	**31.75981**

In a previous chapter, a sweep of all the possible currents on the compensator was shown and it has therefore been proven that the Current Compensation method finds the exact solution in which the least power is lost. Since the first case uses this method exactly and independently on both sides of the filter, we

can conclude that the absolute optimal is found for both sides. However, when this method is applied to any single side, the voltages found need to be applied in the Current Compensation method on the other side. It has not yet been shown that when this happens the absolute minimum is found. A analysis is required as to validate this.

8.3.1 The Optimal Sweep

The 3-dimension graph below calculated the power lost with respect to all the different current combinations., The blue section in the middle, being the lowest values (optimal), indicates that we have not found the perfect solution because the lowest values run diagonally along the axes of currents on the line 1 of the load side and the current on line 2 of the compensator. This method finds the exact solution for the load side but not the source side. Where there are major resistances on the load side, the Current Compensation method finds a solution within fractions of a watt but when the source side is of major resistance and when transmitting 2.2 megawatts, the solution can lie up to 30 watts away.

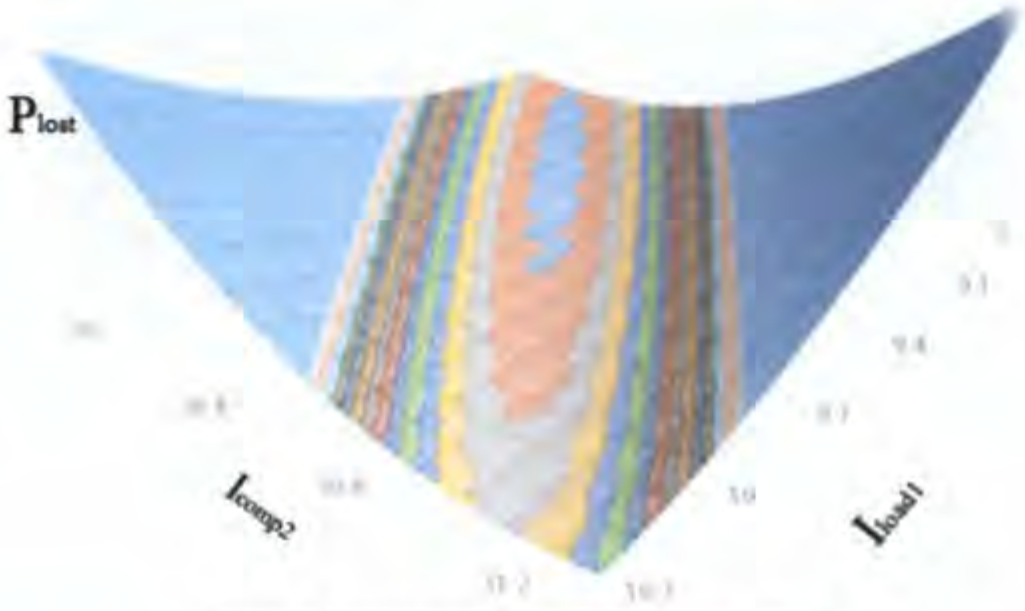

Figure 41: Current sweep for typical transmission network

The parameters shown in the appendix tables are of a typical transmission case where the power being transmitted is closer to what we usually have. The only difference is that in this case the source side lines have larger resistances, these being 20, 1 and 60 ohms on lines 1, 2 and 3 respectively. The voltages are also closer to what we find in High Voltage (HV) distribution networks, these being in the 22 kilovolt range. The tables all show what an active filter in this situation will do and how the active filter has -3.83×10^{-9} watts, which is actually zero. Some of the simplifications were made by Microsoft Excel and the same approximation was made for the current. It is found that we are reducing the power wasted and lost to 131kW, which is an improvement from 243kW (11.05%) of the total power being transmitted.

Usually the compensator would not be required to inject or change the currents by such a large number, but in this situation the source resistances were changed by such large amounts to demonstrate, that we do not find the absolute optimal.

Table 10: Active filter parameters for a typical transmission network

	Compensator						
	i	Power	Save	Percent	Vaf	Power	Plost
Line1	-47.2923464	-413906.04	883438.5387		8752.07241	105658.6259	-388951.42
Line2	32.40671283	648874.491	-1312355.6		20022.842	857818.7391	656372.298
Line3	14.88563352	-234968.451	672010.8206		-15784.9144	866819.4091	-135814.64
Total	-2.1316E-13	-3.8417E-09	**243093.76**	**11.05%**	18935.0285	1830296.774	**131606.2**

As shown in Table 11 below, looking at the location which was found by the sweep, the power lost due to the load side is, as expected, increased since we know we found the exact solution to the load side. The load side currents were computed using an exact solution, but there exists a solution which reduces the power lost on the source side, and as seen in the table the power lost due to the source side is decreased by more than the power lost increased on the load side, resulting in a total system improvement when changing the location of the solution. This happens because we are looking at the system as a whole and not only at the load side. By moving away from the solution of the load side by just a little bit, a better overall solution is found by decreasing the lost power on the source side by a lot.

Table 11: Changes in power lost on each section of the network

Source	Load	System
126583.2	5008.831063	131592
26.29588	-12.05690809	**14.239**

8.4 Shunt Constant Source Power, Active Filter

The final way an active filter can be applied is in the same way as applied in the constant load method described above, but now only starting on the source side. This active filter is also separated from the transmission network and doesn't transmit all the power through it but only injects currents (ic1, ic2 and ic3), to change the currents to optimise the network.

Again the same initial parameters were used. In the appendix Table 22, the parameters for the network after compensation are shown. What is noticed is that the currents on the source side are 3.13A, -1.95A and -1.18A and on the load side 2.44A, -0.16A and -2.29A on lines 1, 2 and 3 respectively. This implies that the currents provided by the compensator, must be the difference between these currents, from Kirchhoff's Current Law. The full 310 watts is still being supplied by the source and the power at the active filter is also still zero, implying the load power must increase if we are going to have a decrease in power lost. This is shown in the table below. By having the load power increase from 210 watts to 267 watts, a difference of almost 36 watts, the lost power is changed by the exact same amount of watts. This is a change of 54.63% of power lost, which is the best result out of the three. However, in many situations the increased power at the load could become a problem and is therefore undesirable.

Table 12: Compensator parameters for constant supply, active filter

	Compensator			
	i	Power	Added Power	Percent
Line1	0.691355861	64.79942044	35.15420718	
Line2	-1.79752524	-39.462088	-19.498686	
Line3	1.106169377	-25.3373324	20.1836025	
Total	0	0	35.839124	54.63%

In this case, there is still zero power at the active filter and the same amount of power is still being supplied, but now due to the active filter rearranging the current, more power is reaching the load. This could cause damage or have to be stored for later use. In typical networks, communication exists between the loads and the generators therefore the supply will decrease after a while. This might approach the same result as the constant load active filter.

Chapter 9: Current Compensation for Power Devices

This chapter demonstrates the impact of applying Current Compensation software inside a power device connected to a dynamic power system.

9.1 Introduction

Any power system can be represented by Thévenin Equivalent models for each of the wires and these parameters are dynamic, as the system changes these parameters change. As loads and sources are switched into the network, the Thévenin Equivalent Resistance and Voltage parameters for the lines change. These changes can be calculated constantly at a node by current injection and measuring the voltage change at the node.

When knowing these parameters, the Current Compensation method can be applied at a node and therefore take/inject power optimally. Current Compensation can be applied instantaneously where the currents on each of the wires are calculated at every time instant. Provided that small energy is available in the form of capacitors inside the Inverter device, the Current Compensation method can be applied over a period. It has been proven the resistive losses due to the lines is reduced further if this method is applied.

The three-wire network in the schematic is used to simulate the different methods. For this example the power device can be thought of as any power device, load or source. We are now going to consider a large battery bank. In Figure 42 below the current sources I5, I6, I7 are the battery bank. The voltage sources E5, E6, E7 and resistor R4, R5, R6, are the Thévenin Equivalent model parameters for the grid seen by the power device. It is assumed that at the battery bank node, the power device is calculating these parameters in parallel with the injection of power and these parameters are therefore always known.

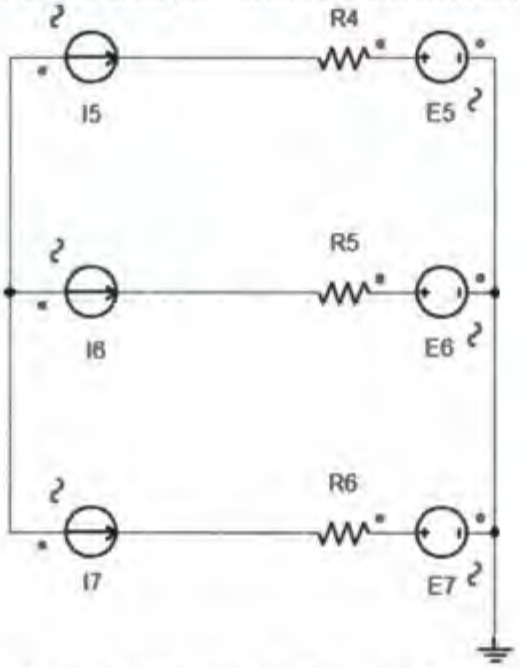

Figure 42: Schematic for a power device connected to a power system.

It must be remembered that the state of the system is measured by each wires' weighted voltages. The weighted voltages are a function of its voltage measured from the correct reference, and its resistance from Eq.2 and Eq. 3 in the literature. The weighted voltage norm of the system (Eq. 4), has the weighted voltages from each of the wires, which perfectly describes the present state of the system.

9.2 Investigation Design

The schematic in Figure 42 above was used in Simplorer 7.0 to simulate this process working both instantaneously and using average power with power storage. The equation blocks were used to calculate the compensation currents for both, where the current sources were made to apply this calculated current. For the first eighty milliseconds, the current sources applied the instantaneous currents, then for the next eighty milliseconds, the current sources applied the average calculated currents. The power, current and voltage waveforms were shown in the display portals in Simplorer.

9.3 Results and Discussion

The following results and discussion was found using Simplorer.

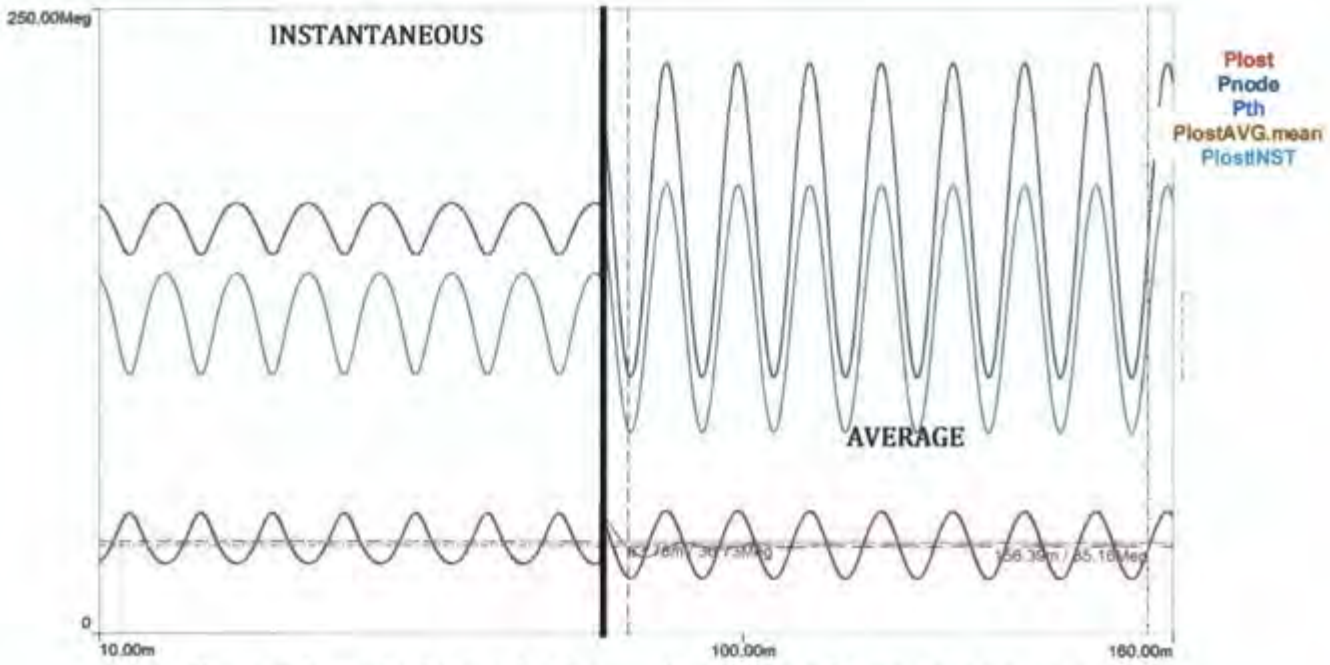

Figure 43: Transmitted, lost and grid powers for both types of Current Compensation

For the first half of the waveform above, the power device is taking power using instantaneous Current Compensation. The average lost power is 36.73 megawatts. It is important to note that the waveforms are a lot less oscillatory but are distorted. They contain harmonics which will be looked at again when the actual currents are found.

For the second half of the simulation, the currents were found using the average of the weighted voltage vector normal. To do this we require some energy storage or to be able to take/inject power more

dynamically, basically to take more power when the state of the system is good and take less power when the state of the system is bad. By applying current compensation in the average format, we reduce the resistive losses by a further 1.6 megawatts to 35.16 megawatts.

However, both the node power and the grid power are highly oscillatory, still sinusoidal and not containing harmonics.

Looking at the voltage waveforms below it can see that during the instantaneous simulation, the voltage drops over the resistances are distorting the voltages seen at the power device. As explained in a previous chapter, a second harmonic is introduced. However, on the other hand, during the average Current Compensation simulation the voltages are perfectly sinusoidal.

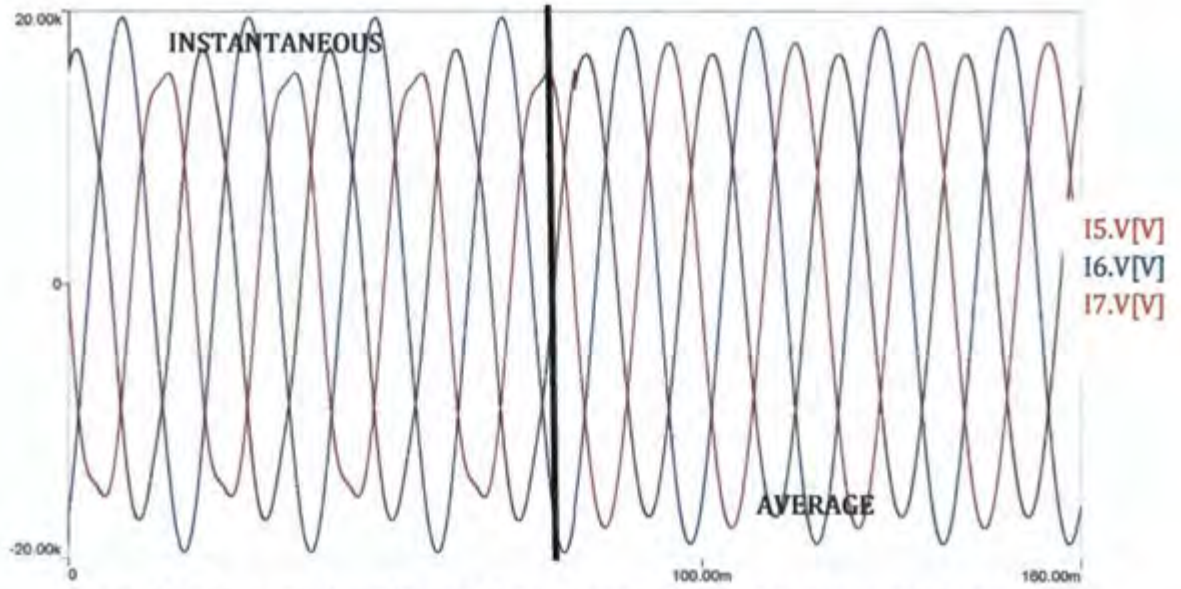

Figure 44: Voltage waveforms for each of the wires and for both types of compensation methods

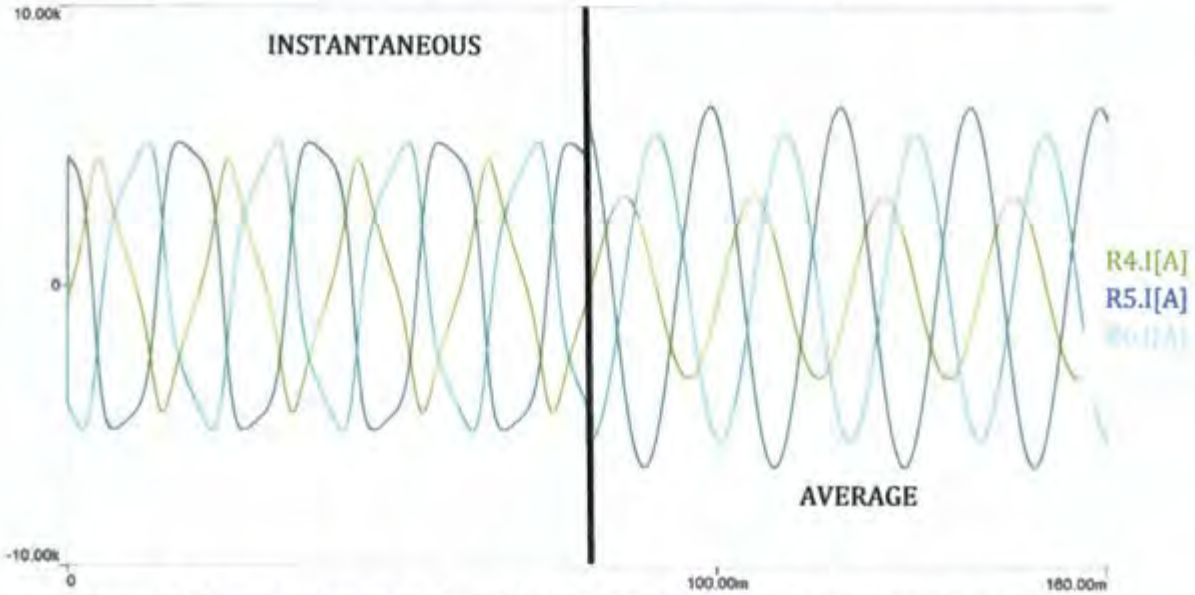

Figure 45: Current waveforms for each of the wires and for both types of compensation methods

In the instantaneous domain the norm is a waveform at double the frequency of the currents and voltages because the norm is a function of power. Therefore, as expected and shown in Figure 45 above, during the first half when the Current Compensation currents are found, they contain second harmonics and are distorted. However, in the average domain the norm is constant and therefore the found Compensation Currents are sinusoidal.

9.4 Conclusion

Provided we have energy storage performing the Current Compensation in the average format, the benefits of clean currents without harmonics and greater optimisation are seen. Performing Current Compensation without energy storage might become undesirable because of the amount of second harmonics introduced into the currents. This would become relevant in high power systems.

Also, in a device such as a battery bank, taking more power at certain instances and less in others wouldn't be a problem at all. Big grids would also be unaffected by this. However, more practical live experiments need to be done.

Chapter 10: Current Compensation Active Filter

This chapter demonstrates the idea of a device changing the currents and therefore reducing the resistive losses for a high power node.

10.1 Introduction

Reducing power losses through Current Compensation is easily seen in a hydro-storage power station. For this example we are going to consider the Palmiet Hydro-storage dam, a twin turbine combining to a capacity of four hundred megawatts. Hydro power stations have the ability to generate their full capacity when required. They have three stages: during the day when the peak is high they generate power by using the high potential of the water; conversely, during the night they act as a load using electrical power to move the water back up into the higher dam; and lastly as a reactive power compensator as its third mode.

In Figure 46 below, a schematic is shown of the Palmiet power station and the Thévenin Equivalent parameters for each of the wires seen by the station node. The current sources I5, I6, I7 represent the Palmiet power station. The current sources I1, I2, I3, and I4 represent the active filter device which is placed, in physical terms, within close proximity to the power station. Because the device is close to the power station, the dynamic nature of the resistive wires between the active filter and the power station can be assumed to remain constant and negligible. The Resistors R4, R5, R6 and R7 and the voltage source E5, E6, E7 and E8 in the schematic Figure 46, are the Thévenin Equivalent model's parameters for the grid.

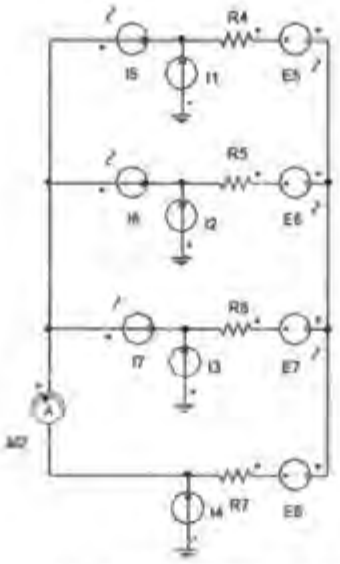

Figure 46: Schematic of Palmiet power station and the Thevenin Equivalent of the grid

Without compensation the generation control devices inside the power station will control the currents with equal magnitudes, depending on the voltages of the system. It is assumed that the active filter device which injects the compensation currents knows the Thévenin Equivalent model resistances and voltages. It can therefore calculate the optimal currents for the same power transfer from its PCC but reduce the

resistive losses on the grid. By reducing the power losses, the power required by the grid can be reduced to supply the same size load. Conversely, when the power station is generating power, by reducing the resistive losses more power reaches the grid.

Kirchhoff's Current Law (KCL) states that all the currents at a point add up to zero. Therefore, if the optimal current is calculated at the active filter, the current injected at the active filter is easily found. It would cancel all the current from the power station node and then inject the found optimal compensation current. This would result in the compensation current on the grid side of the active filter device, from KCL in Eq. 19, shown below:

$$i_g + i_s + i_{af} = 0 \qquad \textbf{Eq. 19}$$

Where, i_g is the current we want to be on the grid side of the device to minimise the resistive power losses, the power station current(i_s), is chosen by the power station devices and is dependent on the voltages. The active filter current (i_{af}), cancels out the power station current and then adds the found optimal current on each respective line. For this to work, the assumption of the currents coming from the one side has to be made constant current sources, as to have an effect only on the load side's currents.

If the desired current on the grid side is simply the found compensation currents and the supply current remains. Eq. 20 below finds the current for the active filter to achieve this:

$$i_g = i_{comp} \;\&\; i_s = i_{constant}$$
$$\therefore i_{af} = i_{comp} - i_{constant} \quad \textbf{Eq. 20}$$

In the instantaneous domain, no power is generated/absorbed at the active filter device since the compensation currents are found using the power required at the station. However, when we want to use the average of the voltage vector norm, a small amount of storage will be required. This is so that we can store power (transmit less) when the overall state of the network is bad and conversely inject extra power when the state of the network is good.

10.2 Investigation Design

Simplorer 7.0 was used, where the schematic above in Figure 46 in conjunction with a few equation blocks were used to simulate current compensation with a hydro storage dam. The current sources I1, I2, and I3 were coded to inject currents dependent on the voltages with a constant average real power of 200 megawatts. Using the equation blocks the compensation currents were calculated and using the equations above the instantaneous voltage vector normal was calculated. The Simplorer TR_probe was used to compute the average of the norm and the compensation currents were then easily calculated by finding the optimal power, using the method explained in the literature, Eq. 6 and Eq.7.

Where the power at the power station is P and $\|v\|$ is the norm of the voltage vector.

The active filter device was programmed to inject zero current for eighty milliseconds, and then for the remainder of the time simulation, the device injected currents to optimise the network.

This process was done because of imbalances in line resistances and voltages for both motor and generator modes.

10.3 Results and Discussion

The following results and discussion were formulated from the method described above.

10.3.1 Motor mode, 3-wire, line 2 resistance imbalance

The first situation simulated was a case when the power station was pumping the water up into the dam during the night. The Thévenin Equivalent voltages are all equal in magnitude and 120 degrees apart. However, the resistance of line two, is four times the resistance (1ohm) of the other lines resistance (0.25 ohms). The larger resistance on one of the lines would create a voltage imbalance at the power station node and as shown in Figure 47 below, the node power graph is sinusoidal as the currents are all equal in magnitude and 120 degrees apart. What is noted is that the node power, being the power at the station, is flatter but still sinusoidal after compensation. The reason for this is because the active filter device pulled more current on the lighter resistive wires and therefore less on the heavy resistive wire. This in turn forced a smaller voltage drop over the imbalanced wire as is shown in Figure 49 below. The voltage drop over the resistor in line two has decreased and therefore the voltage at the active filter on line two is higher, resulting in a more balanced system.

Also shown in Figure 49 is that the currents are all equal while the active filter is injecting zero current. For the time period of compensation, it is seen the current on line two is reduced. This is expected as this is the line with the highest resistance, resulting in a lower overall power loss due to the lines.

The average power at the active filter (grey dotted graph in Figure 47 below) remains zero, and the average power of the station remains constant. Therefore the reduction in lost power results in a decrease in the required power from the grid, as shown in the graph the blue dotted line is below the average supply power before compensation.

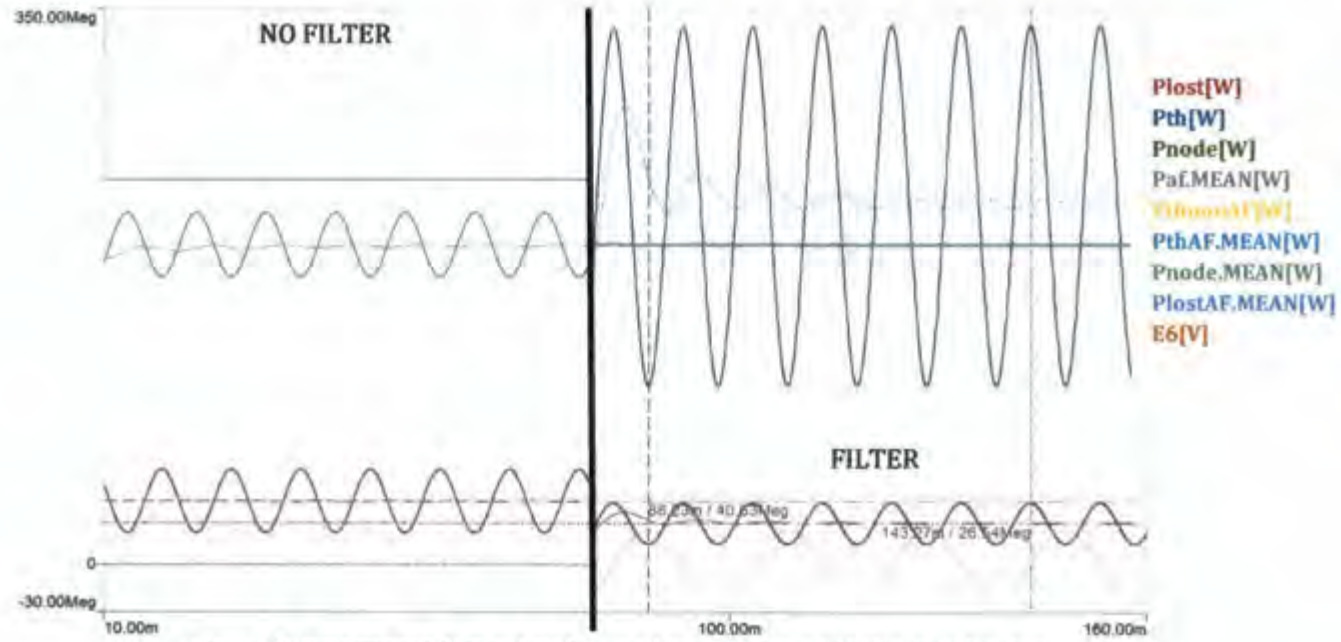

Figure 47: Transmitted, lost and grid power for a resistance imbalance on line two

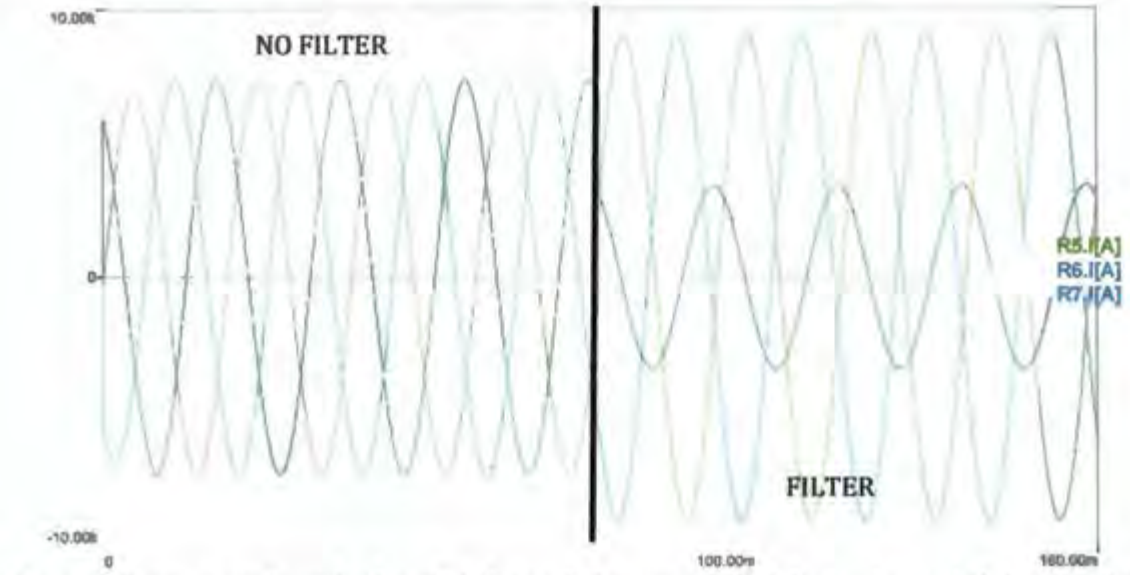

Figure 48: Current waveforms for the grid, before and after compensation for a resistance imbalance on line two

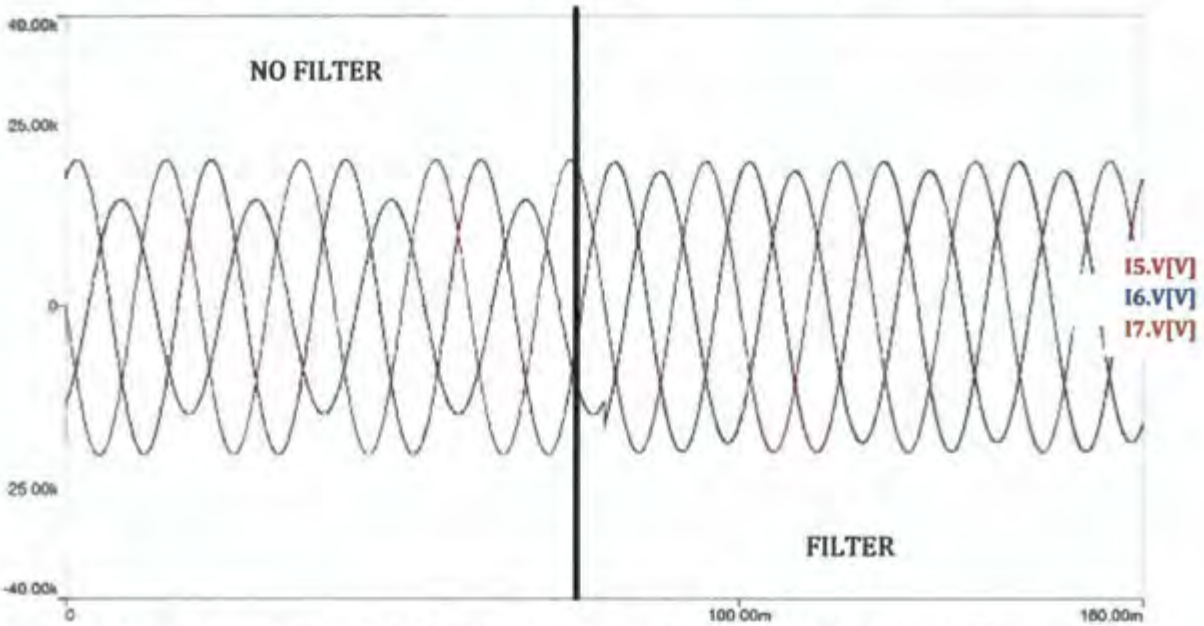

Figure 49: Voltage waveforms for the grid, before and after compensation for a resistance imbalance on line two

10.3.2 Motor mode, 3-wire, line 2, voltage imbalance

The next situation is when the lines all have equal resistances, however the Thévenin Equivalent voltages are imbalanced ($E_5 = E_7 = 28kV, E_6 = 10kV$). As expected, the imbalanced voltages result in the node power to be highly imbalanced as again the currents are all equal, as shown in Figure 50 below.

The equivalent resistances for each of the wires are half an ohm each, resulting in a massive average power loss of 53.18 megawatts (26.6%) of the two hundred megawatts reaching the station. This is more than four times more than a general transmission system where six percent of the total power is lost. However the huge power loss is used to demonstrate the change, and later more typical values are shown. After

compensation this average loss is decreased to less than 45.67 megawatts, this being a reduction of more than fourteen percent.

What must be noted is that the power being taken from the grid (blue graph in Figure 50) is highly oscillatory. This is because the active filter device which is said to have storage, is taking more power when the grid's state is at its highest and taking less power when the state is at its lowest. This is shown by looking at the voltage of the lowest potential (line 2). When this voltage is at its highest, the other two wires are at their respective lowest and therefore the state of the system is bad. This results in the active filter taking less power from the grid and supplying the hydro dam with the power it had previously stored. Conversely, when the potential of line two is at its lowest the voltage of the other two lines is high and therefore the state of the system is at its best. As shown in the graph below, the active filter demands the most power from the grid and stores it at times when the state is at its best.

Unlike the previous case, the active filter couldn't balance the voltages as dramatically, where even after compensation. This is show in Figure 52 below, where the voltage imbalance, had hardly been influenced even after compensation. In practise voltages imbalances will exist, however not to this extend.

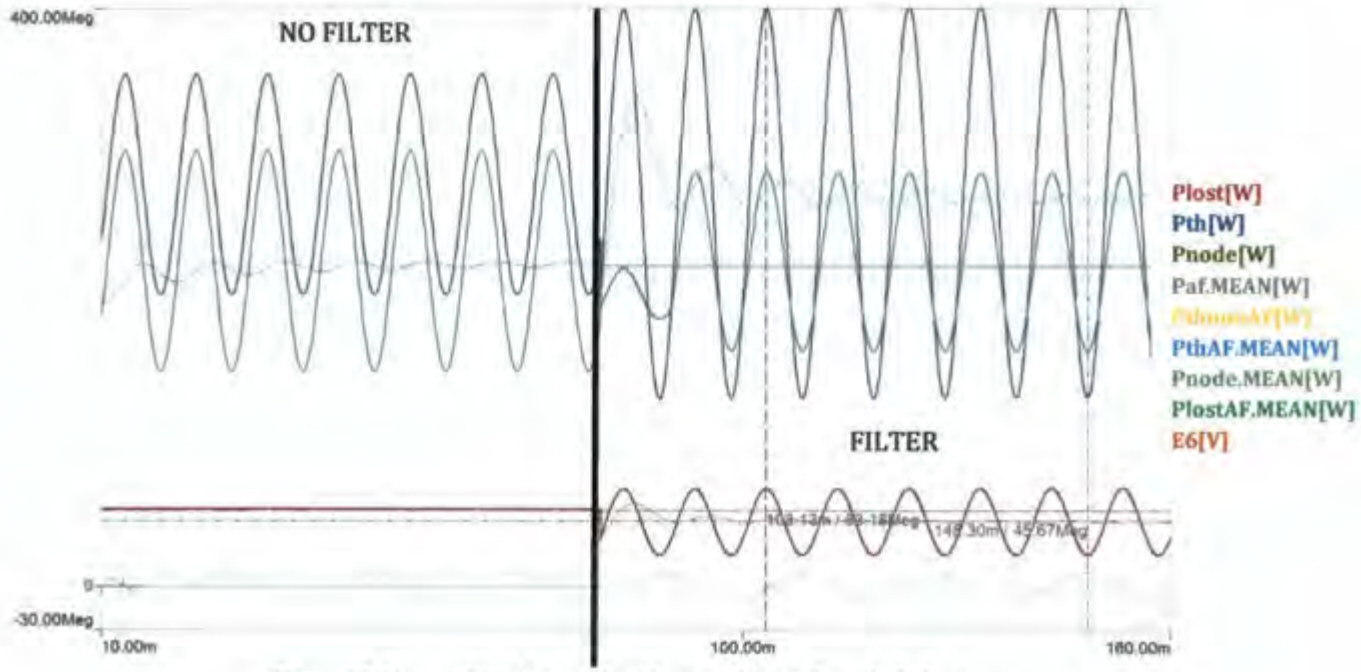

Figure 50: Transmitted, lost and grid power for a voltage imbalance

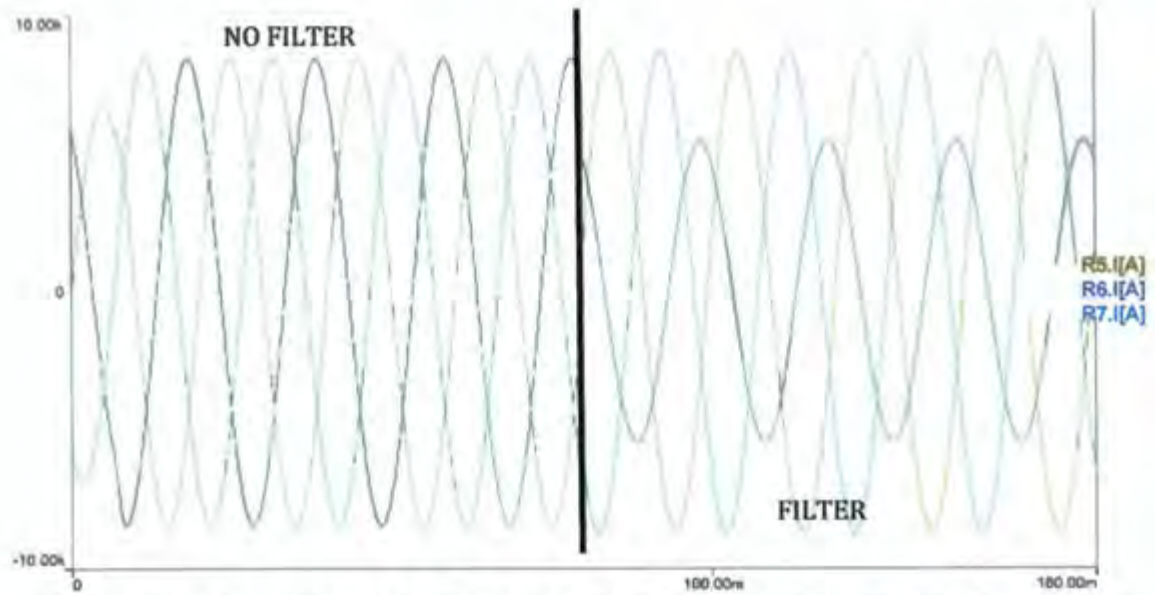

Figure 51: Current waveforms for the grid, before and after compensation for a line two, voltage imbalance

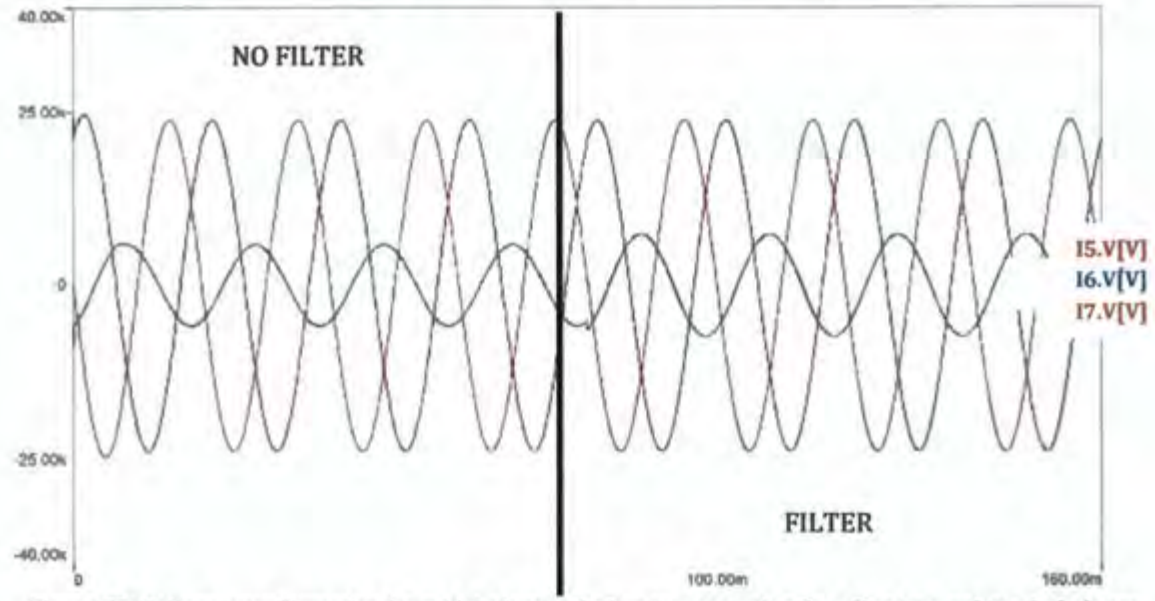

Figure 52: Voltage waveforms for the grid, before and after compensation for a line two, voltage imbalance

10.3.3 Generator mode, 3-wire, typical case

A typical generator mode operation was simulated, where before compensation a more realistic percent (nearly five percent) of power was lost. All the parameters for the grid were randomly chosen so as to depict a typical situation. The line resistances were 0.05, 0.08 and 0.2 ohms and the voltage magnitudes were 24, 22, 20 kV, respectively on lines 1, 2 and 3. Shown in Figure 53 below, the power losses decreased to 8.07 megawatts from its initial 9.91 megawatts after filtering. The process of filtering has therefore decreased the losses by almost nineteen percent. This result is larger compared to when the system parameters were smaller relative to the power transmitted.

If the general losses of most power systems are about six percent and we improve this by an estimated fifteen (estimated from both cases) percent, we could say we change the system losses from six percent to

just over five percent (5.1%). If we are transmitting at full capacity, from our example this being four hundred megawatts, we could save a total of almost one percent, this being four megawatts of power using current compensation. If we are in generator mode, an extra four megawatts of power would be available to be used. Also if we were in motor mode, we would require four megawatts less from the grid to move the water up to the dam.

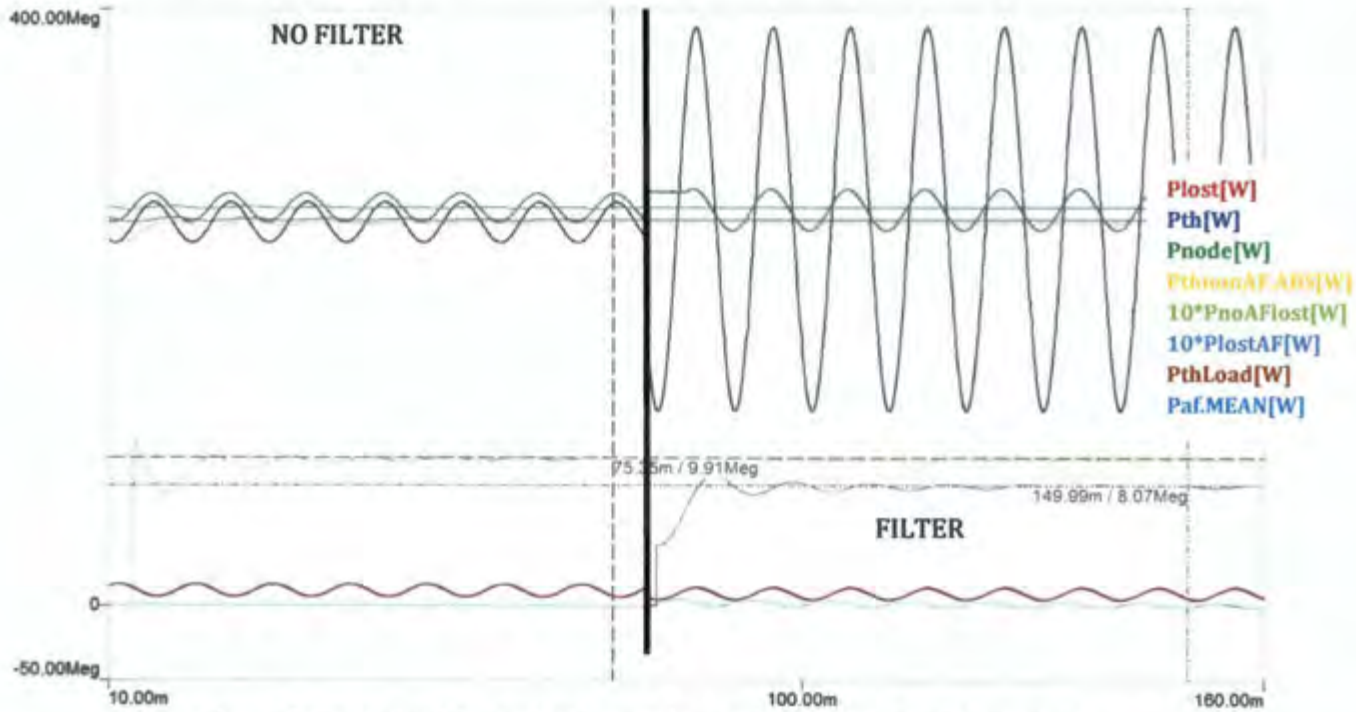

Figure 53: Transmitted, lost and grid power for a typical generator mode operation

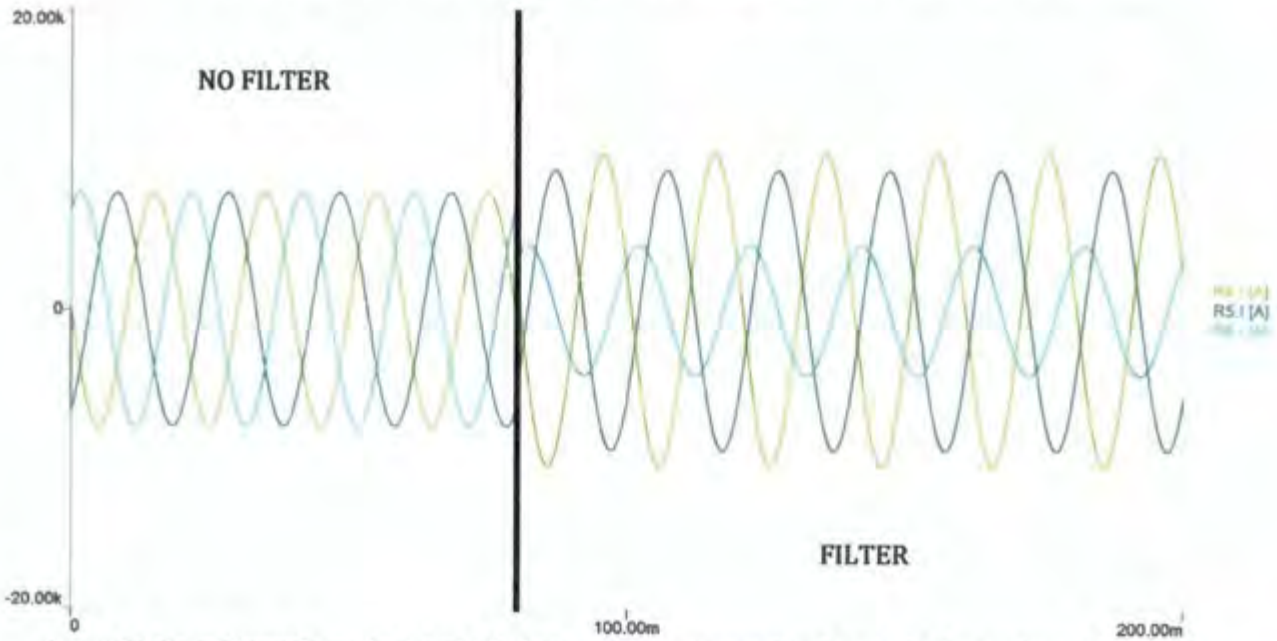

Figure 54: Current waveforms for the grid, before and after compensation for a typical generator mode operation

As seen in the graph above, the three currents over the wires are all perfectly allocated to reduce the power lost. The proof of this is in a previous chapter where each of the possible combinations of currents is checked. The minimum power lost correlates with the currents found by the Current Compensation method. What is noted is that the currents don't contain harmonic distortion and are clean regular waveforms. If no storage was available at the device this wouldn't be so.

10.3.4 Generator mode, 4-wire, typical case

A fourth wire, generally available in power systems, is known as the neutral wire. The final case, where the parameters represent the Palmiet power station, is shown below. Before compensation, 20.48 megawatts of power (5.12%) was lost when four hundred megawatts was being transmitted. The voltages parameters were chosen for a typical High Voltage transmission setup, where the voltages were all around 137kV. Previously, all the cases had the Thévenin voltages all perfectly separated by 120 degrees. However, in this case, small phase shifts were found on lines two and three. The parameters for the example below are:

$$E_5 = 137 < 0kV, E_6 = 136 < 125kV, E_7 = 130 < 243kV, E_8 = 1kV\ (dc)$$
$$\&$$
$$R_4 = 1ohm, R_5 = 1ohm, R_6 = 10ohms, R_7 = 1ohm$$

In the graph below the lost power is decreased to 10.71 megawatts (2.6% of the transmitted power). This is equivalent to a 47.7% reduction in power lost. The benefits of this is seen at the grid which is now receiving an additional 10 megawatts for the same generation at Palmiet.

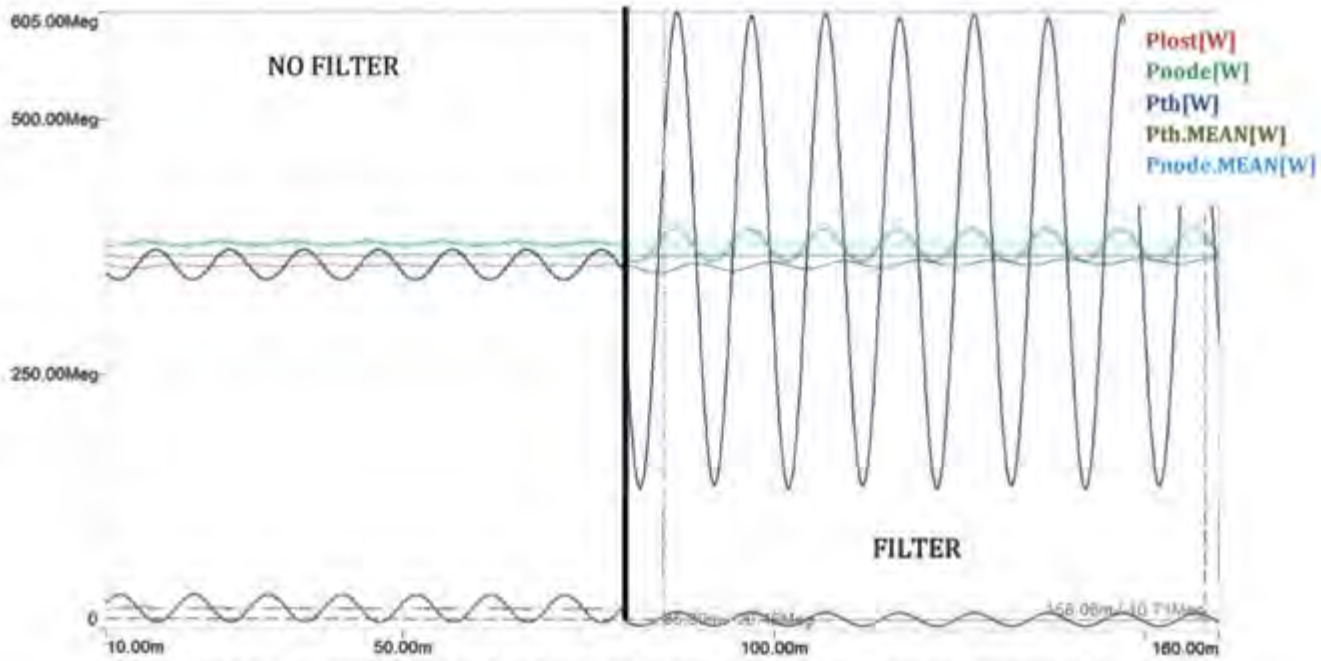

Figure 55: Transmitted, lost and grid power for a typical, 4-wire generator mode operation

Looking at the voltage waveforms in Figure 56 below, you can see the dc voltage present on line four in black. After compensation this voltage becomes a sinusoidal waveform with a dc component. This implies a current was put onto this wire so as to put a voltage drop over the resistance on this line. This makes sense

as we now have a fourth wire to provide current flow and therefore the compensator would look to put current on this path depending on its potential and resistance.

The waveform for the reference of the potentials of all the four wires together is also shown below in the blue graph. This is the actual null-point for the system and is used to obtain the weighted voltages with regard to the correct reference.

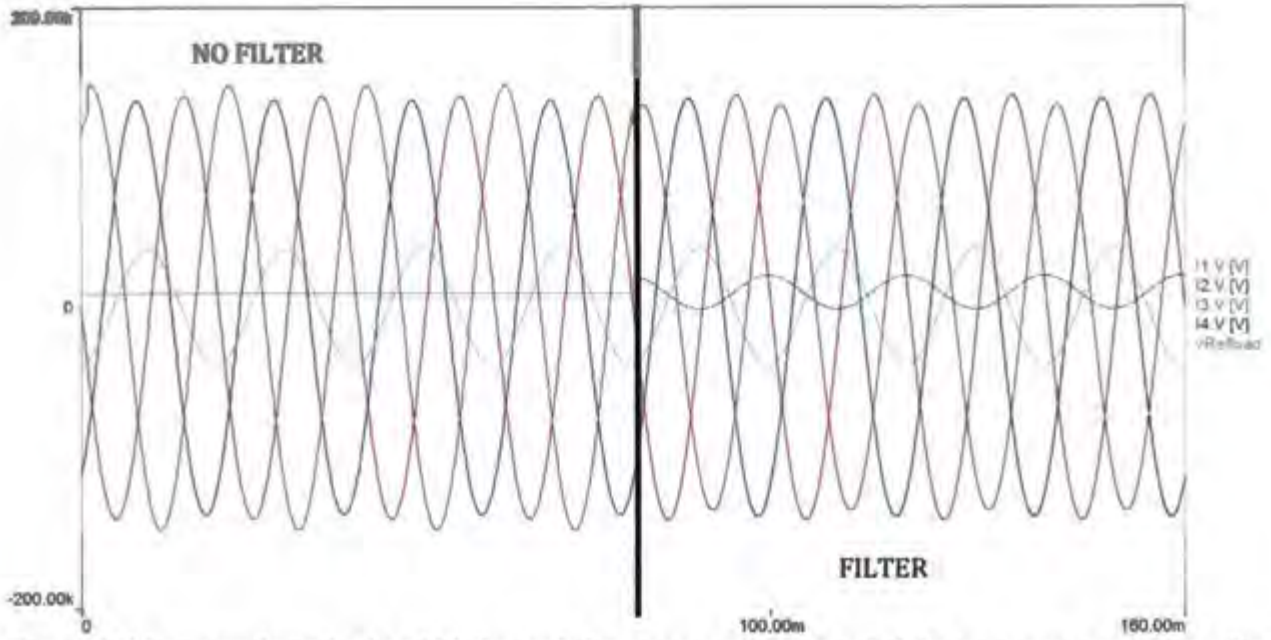

Figure 56: Voltage waveforms for the grid, before and after compensation for a typical, 4-wire generator mode operation

This case included all the possible variations of imbalance where wires had different voltage magnitudes, phase shifts, and resistive attributes, all of which would be found in transmission networks. The active filter device was still able to find the optimal solution to minimise the power lost over the resistances.

10.4 Conclusion

In conclusion, an active filter device connected separately from the injection node does reduce resistive losses on any network. This optimises the network with regard to decreasing the required power needed to pump the same amount of water up into storage, also increasing the power reaching the other nodes while generating the same amount of power.

Chapter 11: Conclusions

11.1 Summary of the chapters

Chapter 1: Introduction - introduced the reader to the work being explained. The research questions were found and a hypothesis was formed.

Chapter 2: Literature Review - demonstrated and defined what optimal power is by looking at literature. Carried on to focus on the history of the work of others on this topic. It showed how the methods for optimal power flow have been created and developed over the years. Provided what guiding questions were and were not answered.

Chapter 3: Computation of Thévenin Resistance for Network Changes - demonstrated an experiment, where a Power Inverter is coded to calculate the Thévenin Equivalent Resistance of a physical grid. The accuracy of this process was investigated, by performing known network changes and comparing it with the Inverter's computed parameters.

Chapter 4: Thévenin Equivalent Model Power for Optimal Power Flow - developed the theory of Superposition with regard to power and explained it in this chapter. It explained the power is only optimised with regard to the power we have available and doesn't change the flow of power already flowing.

Chapter 5: Current Compensation Sweep Analysis - proved optimal current ratios were found for the Current Compensation method by Malengret and Gaunt with unequal resistances by using the weighted parameters.

Chapter 6: Weighted Voltage Vector Normal - was used to explain to the reader what was meant by the normal of the voltage vector. The power of weighting the voltages with resistance was shown and it symbolises the state of the system perfectly. It has been proven, that orthogonality still applies in the power triangle, only when the weighted components of the system are used, even when unequal line resistances exist.

Chapter 7: Instantaneous vs Average Power over a Cycle - investigates a better solution when applying the Malengret and Gaunt Current Compensation method in the average domain instead of instantaneously. This requires energy storage at the node.

Chapter 8: Active Filter - introduced the concept of MGCC method applied in three different topologies in transmission networks.

Chapter 9: Current Compensation for Power Devices - showed the magnitude of the MGCC method being applied inside a power device injecting/taking power in a power network.

Chapter 10: Current Compensation Active Filter - showed the magnitude of an Active Filter device working in typical networks.

Chapter 11: Conclusion – summarizes and concludes the dissertation. Bringing the key contributions together and mentions future work to be done around this topic.

11.2 Key contributions

In summary this dissertation makes the following contributions:

1. Demonstrates that the Thévenin model's current flow is different to the actual current flow of the physical network. It doesn't consider the whole current flow of the network, only the current at the node where the model was derived.
2. Proves the Current Compensation method developed by Michel Malengret and Trevor Gaunt, by finding the absolute optimal in a permutation analysis. Where there only exists one solution that completely removed the reactive current component.
3. Shows and explains how an Inverter can inject currents, to find the Thévenin parameters by recording the voltage changes.
4. Explains three different topologies on how a compensation device can be applied into a transmission network. The positive and negatives of each topology are shown and a final topology is created.
5. Demonstrates the impact an Inverter with this installed on it would have on a power network, as well as the impact an active filter device installed separately from the grid would make.
6. It proves orthogonality. It shows that after compensation we have found the absolute optimum, by proving the components are orthogonal.

11.3 Conclusion

Previous ways of measuring a system's parameters do not compare with the current injection method presented in my paper. These methods estimate the parameters but do not find an accurate solution. The Malengret and Gaunt's Current Compensation method finds the parameters easily and accurately. Chapter five shows that a simple inverter can easily compute the system parameters for any network. It was found that it could calculate it every second, but that this would be undesirable, and computing the system parameters every two minutes would be feasible for the application of Current Compensation. It proves that the method detects changes in the grid and enables any device at any point to compute the Thévenin Equivalent Resistance. Multiple methods can be used in parallel, this method could be used as the primary method of computing the network parameters and any of the other methods could be applied as a secondary method. There is no constraint to the Malengret and Gaunt's Current Compensation method, as it could be used in conjunction with a number of other methods, using the Thévenin Equivalent Resistance and Inductance.

It was also found that by applying this Weighted Current Compensation method in modern transmission networks, significant reduction in resistive losses will be achieved. A typical setup of an active filter device can reduce the losses on a network by up to six percent. This implies that if one hundred megawatts is being injected/extracted, applying the MGCC method could typically save six megawatts. This may not sound like a lot, but in the case of Palmiet, where four hundred megawatts is generally being injected/extracted, twenty-four megawatts would be saved. This method could also be applied at both sides of a HVDC/frequency (from 50Hz to 60Hz in Japan) conversion device, converting gigawatts of power. Applying the method to a converter of this nature could save up to five percent per side (ten percent in total), and that just for the price of implementing this in the converter's software. The implementation of this method in already installed devices would be simple and not require any major hardware additions. It was also found that the power being optimised was only what was being transmitted and not that of the whole network.

In some simulations power and voltage balancing was found, but more research and investigation is required in order to check the validity of this. It was found that the voltage imbalance in networks causes the greatest adverse effect on the power flow and that having a resistance imbalance is equivalent of half a voltage imbalance. As expected the resistance is inversely proportional to the square of the voltage on that line.

In conclusion a device can be made to compensate the currents in any network and completely remove the reactive current components.

11.4 Future Work

Up until now, the only work that has been done on a physical inverter is to enable it to compute the Thévenin Equivalent parameters. An inverter programmed with this software, operating inside a micro-grid where the power at each node can be measured, still needs to be done. This will validate that the lost power is reduced and this method operates as expected. What will also be interesting is running a device with this software on, in parallel with a power balancing device, and see if they operate constructively or destructively towards voltage balancing.

References

1. Abido, M. A., 2002. Optimal design of power-system stabilizers using particle swarm optimization.. *Energy Conversion,* 17.3(IEEE Transactions), pp. 406-413.

2. Akagi, H., Kanazawa , Y. & Nabae , A., 1983. Generalized theory of the instantaneous reactive power in three-phase circuits. *Proc. IEEJ International Power Electronics Conf.*, Volume IPEC-Tokyo, pp. 1375-1386.

3. Akagi, H., Kanazawa, Y. & Nabae, A., 1984. Instantaneous reactive power compensators comprising switching devices without energy storage components. *IEEE Trans. Industry Applications,* IA-20(3), p. 625–630.

4. Akagi, H., Ogasawara , S. & Kim, H., Oct 1999. The theory of instantaneous power in three-phase four-wire systems: a comprehensive approach. *IEEE-IAS conference record,* Volume 1, pp. 431-439.

5. Alsac, O. e. a., 1990. Further developments in LP-based optimal power flow. *Power Systems, IEEE Transactions on 5.3,* pp. 697-711.

6. Amin, S. & Massoud and Bruce F., W., 2005. Toward a smart grid: power delivery for the 21st century. *Power and Energy Magazine, IEEE 3.5,* pp. 34-41.

7. Czarnecki, L., June 1989. Reactive and unbalanced currents compensation in three-phase asymmetrical circuits under non-sinusoidal conditions. *IEEE Trans. Inst. Meas.,* 38(3), pp. 839-841.

8. Czarnecki, L., March 1987. Minimisation of Reactive Power under Non-sinusoidal Conditions. *IEEE Trans, Inst. Meas.,* No.1(3), pp. 18-22.

9. Dash, P. K., Panigrahi, B. K. & Panda, G., 2003. Power Quality Analysis Using S-Transform. *Power Delivery,* 18(2), pp. 406-408.

10. Deeb, Nedal & Shahidehpour., S. M., 1990. Linear reactive power optimization in a large power network using the decomposition approach. *Power Systems, IEEE Transactions on 5.2 ,* pp. 428-438..

11. Depenbrock , M., Staudt, V. & Wrede, H., July 2004. Concerning "Instantaneous Power Compensation in three-phase systems by using p-q-r Theory. *IEEE Trans. on Power Electronics,* 19(4), pp. 1151-1152.

12. Dommel, H. W. & Tinney, W. F., 1968. Optimal power flow solutions. *power apparatus and systems, IEEE transactions on, (10),* pp. 1866-1876.

13. Dopazo, J. F., Klittin, O. A. & Stagg, G. W., 1967. An Optimization Technique for Real and Reactive Power Allocation. *Proceedings of the IEEE, VOL. 55, NO. 11,* pp. 1877-1885.

14. Farhangi, H., 2010. The path of the smart grid.. *Power and Energy Magazine,* Issue IEEE 8.1, pp. 18-28.

15. Filipski, P., 1980. A new approach to reactive current and reactive power measurement in non-sinusoidal systems. *IEEE Trans. Inst. Meas,* Volume 29, p. 423–426.

16. Gaunt, C. & Malengret, M., 2013. True power factor metering for m-wire systems with distortion, unbalance and direct current components. *Electric Power Systems Research 95*, pp. 140-147.

17. Geidl, Martin & Andersson, G., 2007. Optimal power flow of multiple energy carriers. *Power Systems*, 1(IEEE Transactions on 22), pp. 145-155.

18. Grigby & Leonard, L., 2012. *Power System stability and Control Vol. 5.* s.l.:CRC press.

19. Hano, I., Tamura, Y., Narita, S. & Matsumoto, K., 1969. Real time control of system voltage and reactive power. *Power Apparatus and Systems, IEEE Transactions on, (10)*, pp. 1544-1559.

20. Jizhong, Z., 2009. *Optimization of power system operation.* s.l.:John Wiley & Sons.

21. Johannsson, H., 2011. *Assessment of power systems*, WO 2012/163979 A2: International application published under the patent cooperation treaty (PCT).

22. Kirschen, D. S. & Hans, P. V. M., 1988. MW/voltage control in a linear programming based optimal power flow. *Power Systems*, 3.2(IEEE Transactions), pp. 481-489.

23. Kothari, D. P., 2012. *Power system optimization.* s.l., Computational Intelligence and Signal Processing (CISP),.

24. Lai, L. L., Ma, J. T., Yokoyama, R. & Zhao, M., 1997. Improved genetic algorithms for optimal power flow under both normal and contingent operation states.. *International Journal of Electrical Power & Energy Systems, 19(5), .*, pp. 287-292.

25. Larsen, E. V. & Charlton, N., 1993. *Method and apparatus for static*, US005570007A: US Patent.

26. Lee, K., Park, Y. & Ortiz, J., 1985. A united approach to optimal real and reactive power dispatch. *IEEE Transactions on Power Apparatus and Systems,*, pp. 1147-1154.

27. Lee, K. Y. Y. M., Park & Ortiz, J. L., 1984. Fuel-cost minimisation for both real-and reactive-power dispatches. *Generation, Transmission and Distribution*, 131(IEE Proceedings), p. 3.

28. Liang, Z.-X. & Duncan Glover, J., 1992. A zoom feature for a dynamic programming solution to economic dispatch including transmission losses. *Power Systems, IEEE Transactions on 7.2*, pp. 544-550.

29. Liu, J. & Song, Y., 1999. Comparison studies of unified power flow controller with static var compensators and phase shifted. *Electric Machines and Power Systems*, Volume 27, pp. 237-251.

30. Malengret, M. & Gaunt., C. T., 2008. Decomposition of currents in three-and four-wire systems. Instrumentation and Measurement. *IEEE Transactions on 57.5*, pp. 963-972.

31. Malengret, M. & Gaunt., C. T., 2008. *Definition of Apparent Power in 3-phase 4-wire Non-sinusoidal Power Systems. Diss.*. Cape Town: University of Cape Town.

32. Malengret, M. & Gaunt., C. T., 2012. General theory of average power for multi-phase systems with distortion, unbalance and direct current components.. *Electric Power Systems Research 84.1*, pp. 224-230.

33. Malengret, M. & Gaunt, T., 2012. Why we use the term non-active power,and how it can be measured under non-ideal conditions. *IEEE PEP Power Africa,* pp. 16-20.

34. Malengret, M. & Gaunt, T., 2012. Why we use the term non-active power,and how it can be measured under non-ideal conditions. *IEEE PEP Power Africa,* pp. 16-20.

35. Mamandur, K. R. C. & Chenoweth, R. D., 1981. Optimal control of reactive power flow for improvements in voltage profiles and for real power loss minimization. *IEEE Transactions on Power Apparatus and Systems, Vol. PAS-I1O, No. 7,* pp. 3185-3194.

36. Mesut, B. E. & Wu, F. F., 1989. Network reconfiguration in distribution systems for loss reduction and load balancing. *Power Delivery,* IEEE Transactions 4(2), pp. 1401-1407..

37. Metke, A. R. & Randy L., E., 2010. Security technology for smart grid networks. *Smart Grid,* Issue IEEE Transactions on 1.1, pp. 99-107.

38. Momoh, J. A., 2009. Smart grid design for efficient and flexible power networks operation and control. *Power Systems Conference and Exposition, 2009.,* PSCE'09.(IEEE/PES. IEEE).

39. Momoh, J. A., El-Hawary, E. & Adapa, R., 1999. A review of selected optimal power flow literature to 1993. Part I: Nonlinear and quadratic programming approaches. *Power Systems,* 14.1(IEEE transactions on power systems), pp. 96-104.

40. Momoh, J. A., El-Hawary, M. E. & Adapa, R., 1999. A review of selected optimal power flow literature to 1993. Part II: Newton, linear programming and interior point methods. *Power Systems* , 14.1(IEEE Transactions), pp. 105-111.

41. Momoh, J. A., Zhu, J. Z., Boswell, G. D. & Hoffman, S., 2001. Power system security enhancement by OPF with phase shifter. *Power Systems,* Issue IEEE Transactions on 16.2, pp. 287-293.

42. Noroozian, M., 1997. Use of UPFC for optimal power flow control. *Power Delivery, IEEE Transactions on 12.4,* pp. 1629-1634..

43. Pan & Zhiguo, 2005. Voltage balancing control of diode-clamped multilevel rectifier/inverter systems. *Industry Applications, IEEE Transactions on 41.6,* pp. 1698-1706..

44. Pinzon, C., 2000. *Method and device for assessing the stability of an electric power transmission network* , EP 1211 775 A1 : European Patent Office.

45. Riffonneau, Y., Bacha, S., Barruel, F. & Ploix, S., 2011. Optimal Power Flow Management for Grid Connected PV Systems with Batteries. *Sustainable Energy,* pp. 309-3012.

46. Singh, S. N. & David, A. K., 2001. Optimal location of FACTS devices for congestion management. *Electric Power Systems Research,* 58(2), pp. 71-79.

47. Sun, D. I., 1984. Optimal power flow by Newton approach. *power apparatus and systems,,* Issue ieee transactions on 10, pp. 2864-2880.

48. Tinney, W. F. & Hart, C. E., November 1967. Power flow solution by Newton's method. *IEEE Trans. Power Apparatus and Systems,*, Volume PAS-86,, pp. 1449-1460.

49. Torres, G. L. & Quintana, V. H., 1998. An interior-point method for nonlinear optimal power flow using voltage rectangular coordinates. *Power System*, 13.4(IEEE Transactions on), pp. 1211-1218.

50. Wei, H., Sasaki, H. & Yokoyama, R., 1995. *An application of interior point quadratic programming algorithm to power system optimization problems.* s.l., s.n.

51. Yuryevich, J. a. K. P. W., 1999. Evolutionary programming based optimal power flow algorithm. *Power Systems*, no.4(IEEE Transactions on 14), pp. 1245-1250.

I. Current Sources, Represented as Resistors

This appendix chapters demonstrates how positive and negative current sources can be represented as resistors.

Introduction

A node in a transmission network can be represented by a resistor, power source or a current source. A generator injecting power into a network is generally represented by a positive current/power source or a negative resistance. Conversely a load taking power from a network can be represented by negative current/power source or a positive resistance.

Investigation Design

The schematic below was used in Simplorer to demonstrate the similarities between the representations. Where the current source on the right is equal to the voltage over R3 divided by its ohmic value. R1 and R2 were made to be equal to R4 and R5 and the same for the voltage sources E1 and E2 were made equal to E3 and E4.

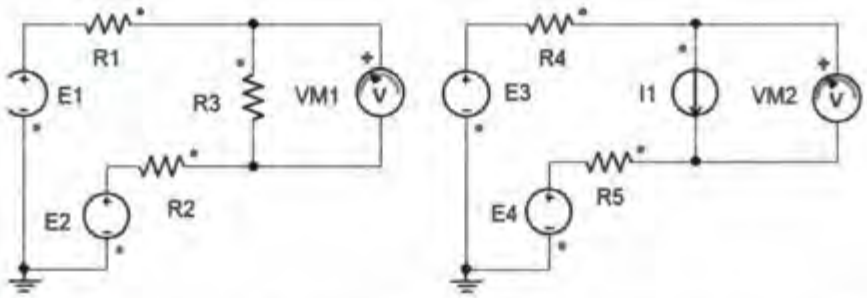

Figure 57: Schematic for the current source and resistance network equivalents

Six cases were used to investigate if the theory held for different directions of power as well as different network parameters.

The six cases were:

1. R3 = 100ohms, R1 = R4 = 0.4ohms. R2 = R5 = 0 ohms, E1 = E3 = 300V, E2 = E4 = 0V
2. R3 = -100ohms, R1 = R4 = 0.4ohms. R2 = R5 = 0 ohms, E1 = E3 = 300V, E2 = E4 = 0V
3. R3 = 100ohms, R1 = R4 = 6ohms. R2 = R5 = 10 ohms, E1 = E3 = 300V, E2 = E4 = 0V
4. R3 = -100ohms, R1 = R4 = 6ohms. R2 = R5 = 10 ohms, E1 = E3 = 300V, E2 = E4 = 0V
5. R3 = 6ohms, R1 = R4 = 6 ohms, R2 = R5 = 10 ohms, E1 = E3 = 230V, E2 = E4 = -70V
6. R3 = -6ohms, R1 = R4 = 6 ohms, R2 = R5 = 10 ohms, E1 = E3 = 230V, E2 = E4 = -70V

Results

In Table 13 below show the voltages, power, currents and resistances for both networks. In the first two cases the currents are almost equal to the negative, this is because the line resistance was made small. Here it is shown that the voltages are the same over both models.

The next two cases the voltages remain the same as the first two but the line resistances are made larger. The theory still holds for both cases. The currents, power and resistance all change sign together.

Table 13: Positive resistance and current simulation for a small relative line resistance

Case	VM1.V[V]	VM2.V[V]	P1[kW]	P2[kW]	R3.R[ohm]	I1.I[A]
1	298.8	298.8	892.84	892.84	100	2.99
2	301.2	301.2	-907.24	-907.24	-100	-3.01
3	258.62	258.62	0.67	0.67	100	2.59
4	357.14	357.14	-1.28	-1.28	-100	-3.57
5	81.82	81.82	1.12	1.12	6	13.64
6	-180	-180	-5.4	-5.4	-6	30

The final two cases both show the same voltages over both representations of the node. Also in case six the current is positive but the power and resistance is both negative, as the voltage over the node is negative.

II. Current Compensation Optimal Currents

Table 14: Current Compensation solution found

	Vth	Rth		v'	i'	Vin	i	PowerTh	PowerIn
Line1	-3	0.2		-3.76601	-2.07502	-3.92798	-4.63989	13.91966	18.22537
Line2	10	0.5		16.00294	8.817406	16.23485	12.4697	124.697	202.4436
Line3	-7	0.4		-8.98753	-4.95201	-10.1319	-7.82981	54.80866	79.33102
Power	300	||V'2^2||	351.0526	k	0.550987	Total	0	193.4253	300
Vref	-1.31579								
PowerTH	193.4253								

III. Current Sweep Parameter Tables

Table 15: Case one current sweep parameters

	Vth	Rth		v'	i'	Vin	i	PowerTh	PowerIn
Line1	0	0.2		32.71652	0.027591	0.012339	0.061696	0	0.000761
Line2	282.3243	0.5		419.9586	0.354169	282.5747	0.500871	141.4081	141.5335
Line3	-281.458	0.4		-421.891	-0.3558	-281.683	-0.56257	158.3391	158.4657
Power	300	||V'2^2||	355427.2	k	0.000843	Total	0	299.7472	300
Vref	-14.6313								
PowerTH	299.7472								

Table 16: Case two, current sweep parameters

	Vth	Rth		v'	i'	Vin	i	PowerTh	PowerIn
Line1	56.43566	0.2		92.49261	0.074686	56.46906	0.167002	9.42488	9.430458
Line2	282.3243	0.5		377.9522	0.305188	282.5401	0.431601	121.8513	121.9445
Line3	-281.458	0.4		-468.855	-0.37859	-281.698	-0.5986	168.4817	168.6251
Power	300	||V'2^2||	371227.8	k	0.000807	Total	0	299.758	300
Vref	15.07171								
PowerTH	299.758								

Table 17: Case three, current sweep parameters

	Vth	Rth		v'	i'	Vin	i	PowerTh	PowerIn
Line1	56,43566	0,2		99,29651	0,795873	56,79158	1,779626	100,4344	101,0678
Line2	282,3243	0,5		382,2554	3,063821	284,4907	4,332898	1223,282	1232,669
Line3	-281,458	0,4		-464,044	-3,71937	-283,811	-5,88083	1655,209	1669,043
Line 4	12	0,001		-0,91411	-0,00733	11,99977	-0,23169	-2,78028	-2,78022
Power	3000	||V'2^2||	371316,6	k	0,008015	Total	0,23169	2978,926	3002,78
Vref	12,02891								
PowerTH	2976,146								

IV. Active Filter Parameter Tables

Table 18: System parameters after a storage, 6-wire active filter

	Source					Load				
	v'	i'	i	Vaf	Power	v'	i'	i	Vaf	Power
Line1	43,13351365	4,434954969	3,135986733	93,72802653	293,929848	55,28571429	2,319830881	2,319830808	96,31983081	223,4457109
Line2	-19	-1,95356551	-1,95356551	21,95356551	-42,8877283	-13,114099	-0,5502776	-0,31770293	15,04689122	-4,780441384
Line3	-28,169132	-2,89632867	-1,18242123	-22,9054726	27,0839171	-47,7142857	-2,0021279	-2,00212788	-11,00212788	22,02766697
vref/Total			0	39	278,126036			0	36,82387119	**240,6929365**
norm	3015					5505,142857				
k	0,102819237					0,041960764				

Table 19: System parameters after a constant load power, active filter

	Load			Source					
	v'	i'	i	v'	i'	i	Vth	Power	v'
Line1	55,28571429	2,319830808	2,319830808	42,0699965	3,8570019	2,727312201	101,774455	277,5707135	45,92699841
Line2	-13,114099	-0,55027761	-0,31770293	-21,77698	-1,99652627	-1,99652627	13,0503649	-26,0553965	-23,77350624
Line3	-47,7142857	-2,00212788	-2,00212788	-19,5248824	-1,79005264	-0,73078593	-15,386843	11,24448874	-21,314935
vref/Total			0			0	36,8238712	**262,759806**	0,838557168
norm	5505,142857			2625,342493					
k	0,041960764			0,091680585					

Table 20: Initial parameters for a typical transmission network before active filter

	Source			Load				
	Vth	Rth	Power	Vth	Rth	Power	Current	Vin
Line1	10000	20	600000	8740	1	524400	60	8800
Line2	20000	1	200000	19980	1	199800	10	19990
Line3	-20000	60	1400000	-15730	1	1101100	-70	-15800
Total			2200000			**1825300**	0	
Vref	18906.25			4330				

Table 21: System parameters for typical network after compensation

	Load			Source					
	v'	i'	i	v'	i'	i	Vth	Power	v'
Line1	4410	12.0724122	12.07241222	-2276.978	-157.508334	-35.2199341	8047.67373	-283438.5	-2434.486534
Line2	15650	42.8420071	42.84200708	1087.8135	75.2487199	75.24871992	20098.0907	1512355.6	1163.062239
Line3	-20060	-54.9144193	-54.9144193	-4482.325	-310.061641	-40.0287858	-18186.642	727989.18	-4792.386997
vref/Total			0	-5671.49		-2.1316E-13	18935.0285	**1956906**	-6063.811292
norm	666774200			26459209					
k	0.002737508			0.0691743					

Table 22: System parameters for constant supply, active filter

	Load				Source		
	V	i'	i	Power	v'	i'	i
Line1	91.28339566	2.444630872	2.444630872	223.1542072	43.1335137	4.434954969	3.13598673
Line2	22.42168631	-0.27026967	-0.15604027	-3.49868595	-19	-1.95356551	-1.9535655
Line3	-20.616882	-2.2885906	-2.2885906	47.1836025	-28.169132	-2.89632867	-1.1824212
vref/Total			0	266.8391237			0
norm					3015		
k	0.040582007				0.10281924		